EARTHQUAKE ENGINEERING RESEARCH LABORATORY

SOME OBSERVATIONS ON THE RANDOM RESPONSE OF HYSTERETIC SYSTEMS

Thesis by

Leonidas G. Paparizos

REPORT NO. EERL 86-02

A Report on Research Partially Supported by
Grants from the National Science Foundation
and the Earthquake Research Affiliates Program
of the California Institute of Technology

Pasadena, California

1986

To my father
Joga Paparizos

Acknowledgements

The author would like to express his appreciation to Prof. W. D. Iwan for helpful discussions and continuous patience throughout the course of this research project.

The financial support received through the California Institute of Technology and the Fluor Corporation is greatefully acknowledged.

Special thanks to Janet Campagna, Pascale Dubois, Jose Fernandez, Harry Kytoma, Christodoulos Pilinis and Alex Serresiotis, for their support during the crucial moments of this dissertation and their friendship during my studies at Caltech.

Particular thanks to Sharon Girdner and her whole household for their patience and support. Finally, the author thanks his family for their support and their belief in education.

Abstract

In this thesis, the nature of hysteretic response behavior of structures subjected to strong seismic excitation, is examined. The earthquake ground motion is modeled as a stochastic process and the dependence of the response on system and excitation parameters, is examined. Consideration is given to the drift of structural systems and its dependence on the low frequency content of the earthquake spectrum. It is shown that commonly used stochastic excitation models, are not able to accurately represent the low frequency content of the excitation. For this reason, a stochastic model obtained by filtering a modulated white noise signal through a second order linear filter is used in this thesis.

A new approach is followed in the analysis of the elasto-plastic system. The problem is formulated in terms of the drift, defined as the sum of yield increments associated with inelastic response. The solution scheme is based on the properties of discrete Markov process models of the yield increment process, while the yield increment statistics are expressed in terms of the probability density of the velocity and elastic component of the displacent response. Using this approach, an approximate exponential and Rayleigh distribution for the yield increment and yield duration, respectively, are established. It is suggested that, for duration of stationary seismic excitation of practical significance, the drift can be considered as Brownian motion. Based on this observation, the approximate Gaussian distribution and the linearly divergent mean square value of the process, as well as an expression for the probability distribution of the peak drift response, are obtained. The validation of these properties is done by means of a Monte Carlo simulation study of the random response of an elasto-plastic system.

Based on this analysis, the first order probability density and first passage probabilities for the drift are calculated from the probability density of the

velocity and elastic component of the response, approximately obtained by generalized equivalent linearization. It is shown that the drift response statistics are strongly dependent on the normalized characteristic frequency and strength of the excitation, while a weaker dependence on the bandwidth of excitation is noted.

TABLE OF CONTENTS.

Figure Captions

Figure 2.1
Single degree-of-freedom (SDOF) model of a structural system.

Figure 2.2
Force deflection diagram for the hysteretic model described by equation 2.2. The model exhibits inconsistent behaviour under cyclic loading. $A = 1$, $\alpha = \beta = .5$, $n = 1$. (a) An example of stiffness strengthening under symetric cyclic loading. (b) An example of stiffness deterioration under cyclic loading.

Figure 2.3
Elasto-plastic model. (a) Restoring force diagram. (b) Idealized physical system.

Figure 2.4
The Distributed-Element model for hysteresis.

Figure 2.5
Power spectral density function of two stochastic seismic excitation models. (a) Kanai-Tajimi spectrum. (b) Normalized Kanai-Tajimi spectrum. (c) Proposed model for stochastic seismic excitation (eqn. 2.27).

Figure 2.6
Normalized envelope function for the proposed seismic excitation model.

Figure 3.1
The bilinear hysteretic model.

Figure 3.2
Covariance of Nonstationary Response. Bilinear hysteretic system subjected to filtered white noise excitation (eqn. 2.27), S_0=2.0, ζ_g=0.50, ω_g/ω_0=0.50, α_0=0.10 and ζ=0.05. (a) Displacement response. (b) Velocity response.

Figure 3.3
Covariance of Nonstationary Response. Bilinear hysteretic system subjected to filtered white noise excitation (eqno 2.27), S_0=2.0, ζ_g=0.50, ω_g/ω_0=1.0, α_0=0.10 and ζ=0.05. (a) Displacement response. (b) Velocity response.

Figure 3.4
Dependence of the Stationary RMS response levels on the strength of the excitation and α_0, for bandwidth of the excitation, ζ_g=0.50, and ω_g/ω_0=1.0 and ζ=0.05. (a) Displacement response. (b) Velocity response.

Figure 4.2
Nonstationary Covariance of the response of an elasto-plastic system. Equivalent linearization cannot predict the linearly divergent covariance of the displacement response, if the acceleration spectrum satisfies the condition $\Phi_{aa}(0)=0$. $S_0=0.40$, $\zeta_g=0.50$, $\omega_g/\omega_0=1.0$ and $\varsigma=0.01$. (a) Displacement response. (b) Velocity response.

Figure 4.3
Parametric investigation for the stationary RMS value of the velocity response. Bandwidth of the excitation (a) $\zeta_g=0.50$ (b) $\zeta_g=0.25$. Legend of the simulation data given in Figure 4.0.

Figure 4.4
Time history of the drift response.

Figure 4.5
The response states S_3, corresponding to elastic behaviour, and S_1 and S_2, corresponding to yielding in positive and negative direction, respectively.

Figure 4.6
Phase plane of the stochastic process $(x, \dot{x})$. The marked domain corresponds to trajectories for which upcrossing of the threshold $x = x_0$ occurs at times $\tau \in (t, t + dt)$.

Figure 4.7
Correlation factor, A, versus the ratio of transition probabilities p^+/p^-. Comparison between analytical and numerical simulation results.

Figure 4.8
Offset coefficient, ϵ_0', versus the ratio of transition probabilities p^+/p^-. Comparison between analytical and numerical simulation results.

Figure 4.9
Transient mean square value of the drift obtained by the simplified equation (4.90a). (a) $S_0=0.90$, $\omega_g/\omega_0=0.50$, $\zeta_g=0.25$. (b) $S_0=2.5$, $\omega_g/\omega_0=3.0$, $\zeta_g=0.25$.

Figure 4.10
Probability distribution of the drift response at time $t = 20T_0$ and for $S_0=0.40$, $\omega_g/\omega_0=1.0$, $\zeta_g=0.50$. Numerical simulation data obtained from 2500 samples of drift response.

Figure 4.11
Probability distribution of the normalized peak drift response at time t=$15T_0$ and $25T_0$, for $S_0=0.40$, $\omega_g/\omega_0=1.0$, $\zeta_g=0.50$. Numerical simulation data obtained from 2500 samples of drift response. The results suggest the Brownian motion nature of the drift of an elasto-plastic system.

Figure 5.17
Expected value of the normalized dissipated hysteretic energy per cycle. (a) ζ_g=0.50 (b) ζ_g=0.25. Legend of simulation data given in Figure 4.0.

Chapter 1. INTRODUCTION.

The safety of structures subjected to strong seismic excitation is of major concern for Civil Engineers, since the destructive effect of such an earthquake may have severe social and economic implications. Since the begining of this century large seismic events, such as the San Francisco earthquake of 1906 and the Tokyo earthquake of 1923, directed the attention of the scientific community toward the seriousness of the earthquake problem and the need for antiseismic structural design. In the last decades, intensive research has led to major improvements in antiseismic design and a better overall understanding of earthquake related problems. However, recent events, such as the Mexico City earthquake of 1985, suggest that structural safety problems are far from being solved and confirm that future research is required.

Most structures exhibit hysteretic response behaviour when subjected to strong seismic excitation. Thus, the analysis of such nonlinear systems is of major significance in the field of Earthquake Engineering. Due to the stochastic nature of earthquake excitation, the theory of random vibration is often used for this purpose. However, in general, analytical results on the response of nonlinear systems to stochastic excitation, as opposed to the case of a deterministic input, are far more difficult to obtain. The implication is that models of both structural systems and earthquake excitation should be simple, while maintaining their ability to capture the basic features of the physical problem.

Two basic methods, the now classical equivalent linearization and the yield increment approach, exemplified by the works of Caughey (43) and Karnopp and Scharton (39), respectively, have been followed in the analysis of the random response of hysteretic systems. Caughey, the first to examine the random response of a bilinear hysteretic system, obtained approximate results for the velocity and displacement response, for the case of white noise excitation, using

the Krylov-Bogoliubov method of equivalent linearization. It should be noted that this approximate method is based on the assumption of narrowbanded response behaviour and that Iwan and Lutes (44) showed that in the case of an elasto-plastic or nearly elasto-plastic system, the narrowbandness assumption is not applicable and leads to inaccurate response statistics. Thus, the applicability of this and similar techniques is restricted to the case of hysteretic systems which exhibit hardening behavior. This result is a consequence of the approximation technique which does not provide information regarding the nature of the hysteretic response behavior.

In contrast, the method proposed by Karnopp and Scharton is physically motivated. They formulate the problem in terms of the yield increment associated with inelastic response. The yield increment statistics were calculated from the stationary probability density function of an associated linear system. Although the method provides the basis for understanding hysteretic response behavior, computational difficulties which result from the complexity of the diffusion equation for the yield increment process, limit its applicability and they obtained no results regarding the drift statistics.

A significant factor in analyzing the random response of structural systems is the approximate modeling of earthquake excitation as a stochastic process. Housner (25) was the first to introduce a stochastic model when he defined the earthquake process as the sum of a large number of impulses which arrive at random times, i.e., a white noise process. Refinements to the model include stationary models (see Kanai (26), (27); Tajimi, (28)) and transient models (see Shinozuka and Sato (34); Jennings, Housner and Tsai (33); Saragoni and Hart (35)). Of particular significance is the work by Hanks and McGuire (61) and Boore (30) who propose approximate analytical model for the acceleration spectrum. The importance of their contribution, particulary with respect to

the ω-squared asymptotic expression for the low frequency of the earthquake acceleration spectrum, is more fully discussed in a later section.

The objective of the research conducted in this thesis is to continue the progress in the area discussed above by developing solution techniques which provide an understanding of the hysteretic response behavior for a general class of models, including the elasto-plastic system. For this purpose, particular attention is given to the nature of the drift response and its dependence on both system and excitation parameters.

The problem is formulated in Chapter 2 through a discussion of available models of hysteretic behavior and seismic excitation. Based on this investigation, it is determined that the multilinear hysteretic model is the appropriate one to be considered in the remainder of this research. Additionally, a stochastic seismic model, capable of defining the basic features of earthquake ground motion, is chosen for application in this analysis.

In Chapters 3 and 4 consideration is given to two classes of problems corresponding to hysteretic models exhibiting hardening behaviour and to the elasto-plastic system.

Approximate solutions for the second order response statistics of systems exhibiting hardening behavior are examined in Chapter 3. Following the formulation of Asano and Iwan (48), the hysteretic restoring force is expressed in terms of an additional state variable corresponding to the elastic component of the displacement response. A higher order equation of motion which is independent of the response history is then derived. Accurate estimates of the second order response statistics are obtained by the method of transient equivalent linearization.

Chapters 4 and 5 address the nature of the drift response behavior and thus represent the core of the contribution towards a better general understanding

of hysteretic behavior contained in this thesis. More specifically, in Chapter 4 the drift of an elasto-plastic system is expressed as the sum of yield increments associated with inelastic response. The approximate diffusion equation for the drift is obtained by considering simplified discrete Markov process models of the yield increment process. Through the analysis of these models, the drift properties are obtained. It is shown that for stationary seismic excitation of long duration the drift approaches Brownian motion behavior. This implies that the probabilistic structure of the drift process is defined by a single parameter.

Finally, in Chapter 5, an approximate solution scheme is derived for the calculation of the response statistics of an elasto-plastic system. The dependence of the response on system and excitation parameters is then examined.

Chapter 2. MATHEMATICAL FORMULATION OF THE PROBLEM.

The objective of this Chapter is to examine the analytical models related to the inelastic response of structural systems to strong earthquake excitation.

2.1 Equation of motion.

Although structural systems can be examined from a continuum point of view, the complicated geometry and the inhomogeneous material properties make such an approach extremely complex and ineffective. For this reason, by appropriate discretization of the equation of motion, the structure is commonly modeled as a finite-dimensional dynamic system. In the case of a linear equation of motion, further simplification of the problem is obtained by using modal analysis. Then, the system response can be accurately predicted by considering the contribution of first significant modes of oscillation. In many cases, even a single-degree-of-freedom (SDOF) analysis may provide useful information regarding the dynamics of the structural system. The SDOF analysis is often applied in nonlinear systems where analytical solutions for the multi-degree-of-freedom (MDOF) system are practically impossible to obtain.

Figure 2.1 gives an example of a simple structural system which is approximated as a SDOF. The equation of motion for the single-degree-of-freedom system is given by

$$m\ddot{x} + f(x, \dot{x}, t) = -m\ddot{a}(t), \tag{2.1}$$

where x, $\dot{x}$ are the relative displacement and velocity of the mass, $f(x, \dot{x}, t)$ is a general nonlinear restoring force and $\ddot{a}(t)$ represents the ground motion acceleration. Although the system governed by equation (2.1) represents a very simplified form of the actual structural system, it can be considered as a general basis for the investigation of the inelastic structural response to seismic excitation and can provide useful information regarding the features of the response

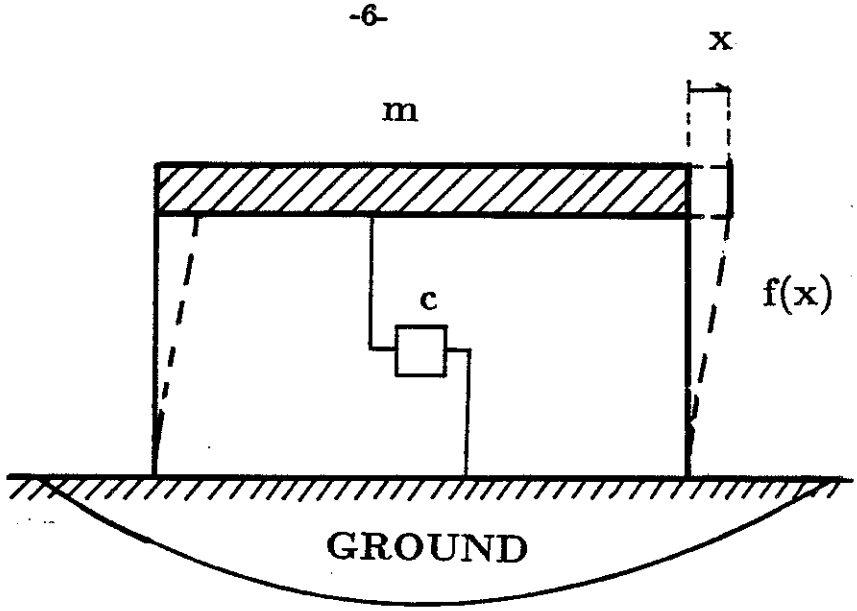

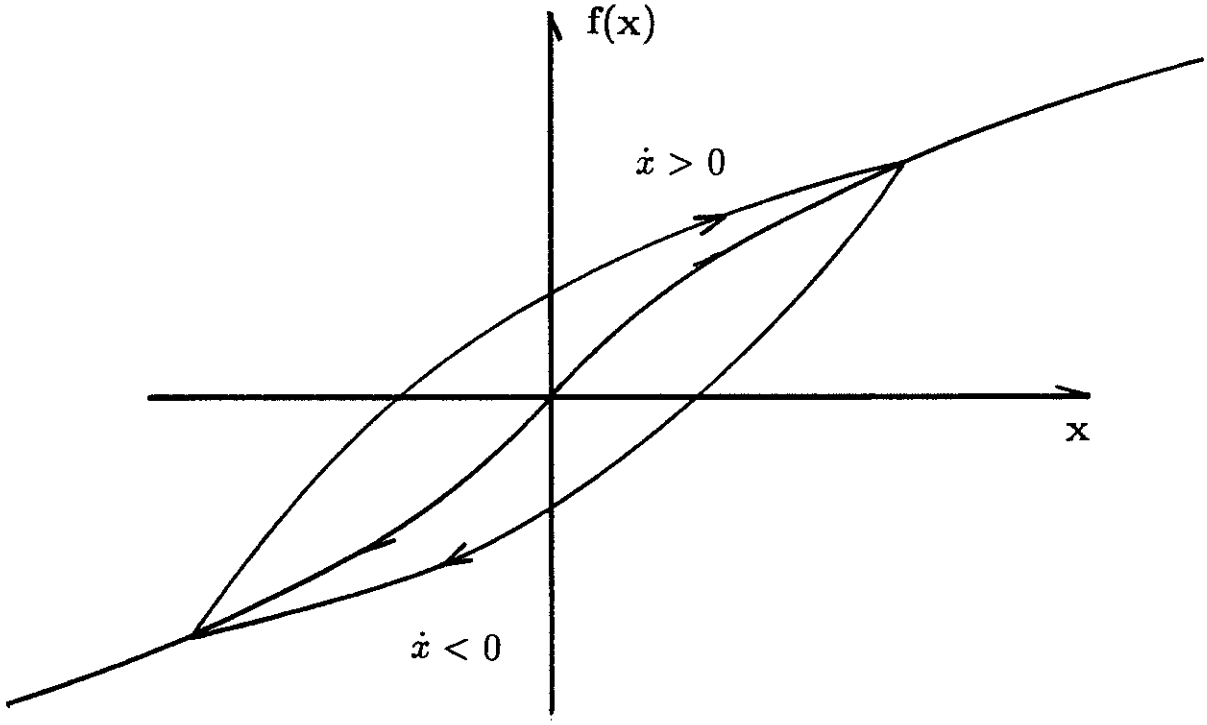

Figure 2.1
Single degree-of-freedom (SDOF) model of a structural system.

and dependence on system and excitation parameters. For this reason, the analysis presented in this thesis is based on the single-degree-of-freedom oscillator.

A detailed examination of models for the restoring force is presented in Section 2.2, while the modeling of the earthquake excitation as a stochastic process is discussed in Section 2.3.

2.2 Models for hysteretic behaviour.

2.2.1 Review.

The restoring force related to the inelastic constitutive material behaviour is, in general, of hysteretic form. The history dependence of the equation of motion makes the analysis of such systems extremely difficult. Because the study of history dependent systems becomes even more complex in the case of a stochastic excitation, in nonlinear random vibration analysis, models for hysteretic behaviour are frequently defined in terms of additional state variables.

A class of models based on this principle is the one initially introduced by Bouc (38) and later generalized by Wen (56). The hysteretic behaviour is modeled by defining a state variable $z(t)$, for which the following equation of motion is satisfied.

$$m\ddot{x} + g_0(x, \dot{x}) + z(t) = -m\ddot{a}(t), \tag{2.2a}$$

$$\dot{z} = -\alpha|\dot{x}|z^n - \beta\dot{x}|z^n| + A\dot{x} \qquad \text{for} \quad n \quad \text{odd}, \tag{2.2b}$$

or,

$$\dot{z} = -\alpha|\dot{x}|z^{n-1}|z| - \beta\dot{x}z^n + A\dot{x} \qquad \text{for} \quad n \quad \text{even}, \tag{2.2c}$$

where α, β, A, n-are model parameters and $g_0(x, \dot{x})$ is a general nonhysteretic component of the restoring force. This class of models has been generalized for different types of constitutive behaviour such as stiffness deterioration, pinching of hysteretic loops and two dimensional problems. A detailed review of all these

models has been done in a recent paper by Wen (58). The main weakness of the model is the lack of physical motivation and the inconsistent behaviour under cyclic loading, as is illustrated in Figure 2.2. The merit of the model lies in its simplicity and succesful application in different fields of structural engineering, such as random vibration and system identification.

2.2.2 The distributed element model for hysteresis.

The simplest form of hysteretic behaviour is elastic, perfectly plastic behaviour for which the restoring force-deflection diagram is plotted in Figure 2.3a. A physical system that exhibits such a constitutive relation is illustrated in Figure 2.3b. It consists of a linear spring, with stiffness K, in series with a Coulomb or slip damper with maximum allowable force Kx_y. This system can be considered an ideal elasto-plastic unit.

Following the approach used in Section 2.2.1, a state variable $y(t)$ can be defined as the elastic component of the deflection. Then, $y(t)$ will satisfy the following incremental equation

$$dy = \begin{cases} 0 & \text{if } |y| = x_y \text{ and } ydx > 0; \\ dx & \text{otherwise,} \end{cases} \tag{2.3}$$

where x_y represents the yielding level. Equation (2.3) specifies that the elongation of the spring element is restricted to $-x_y \leq y \leq x_y$.

Consider a system that exhibits such constitutive behaviour. Then, in the presence of additional viscous damping, the equation of motion will become

$$\ddot{x} + 2\varsigma_0\omega_0\dot{x} + \omega_0^2 y = -\ddot{a}(t), \tag{2.4a}$$

$$\dot{y} = \dot{x}g(y), \tag{2.4b}$$

where

$$g(y) = \begin{cases} 0 & \text{if } |y| = x_y \text{ and } y\dot{x} > 0; \\ 1 & \text{otherwise,} \end{cases} \tag{2.4c}$$

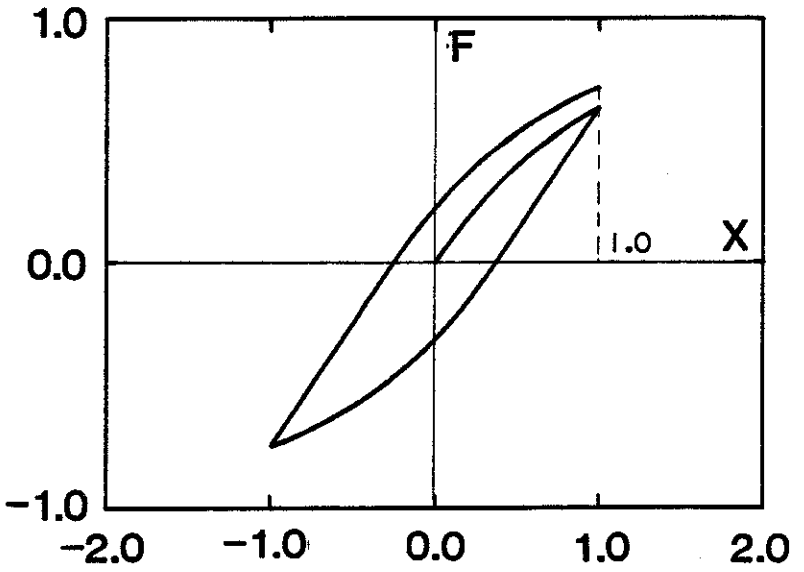

(a)

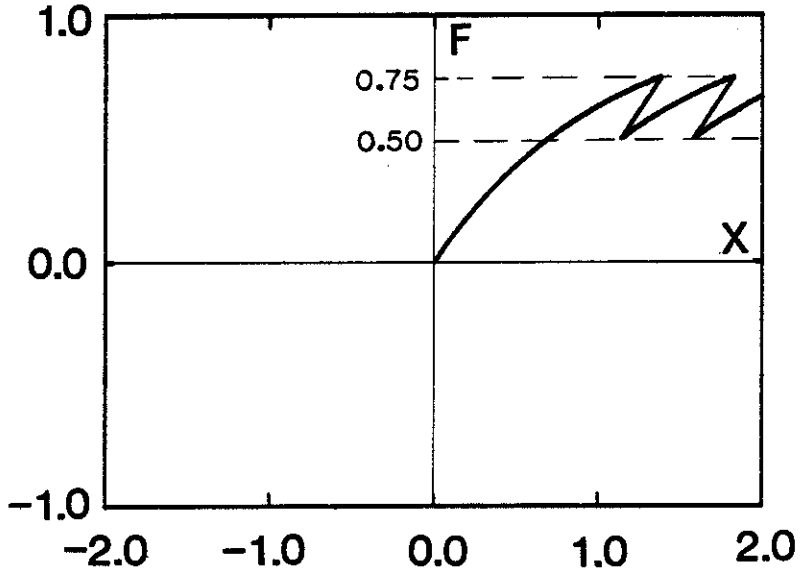

(b)

Figure 2.2
Force deflection diagram for the hysteretic model described by equation 2.2. The model exhibits inconsistent behaviour under cyclic loading. $A = 1$, $\alpha = \beta = .5$, $n = 1$. (a) An example of stiffness strengthening under symetric cyclic loading. (b) An example of stiffness deterioration under cyclic loading.

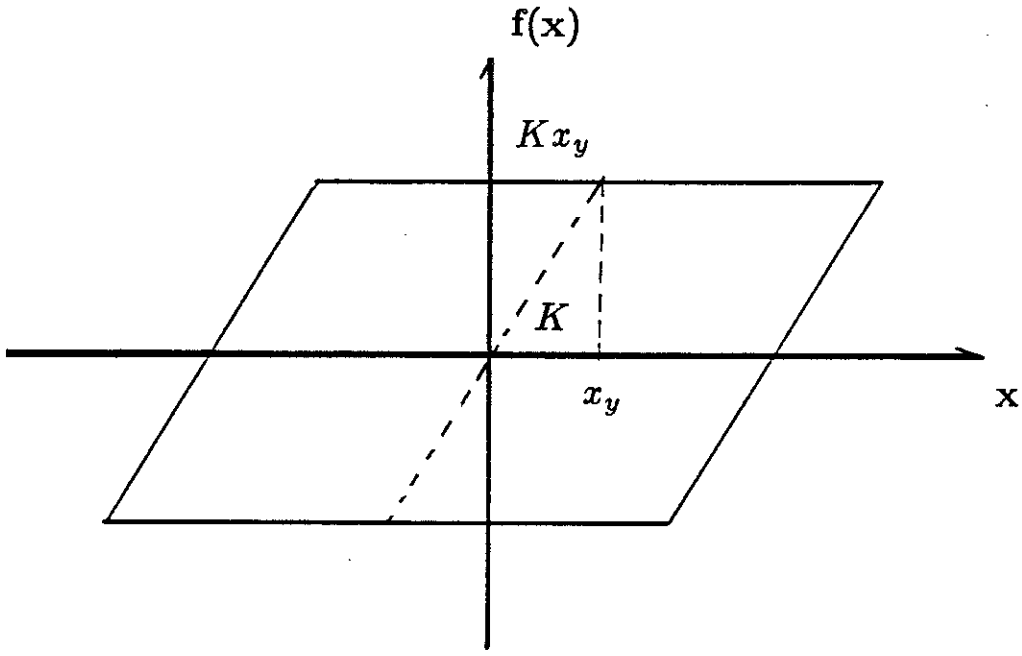

(a)

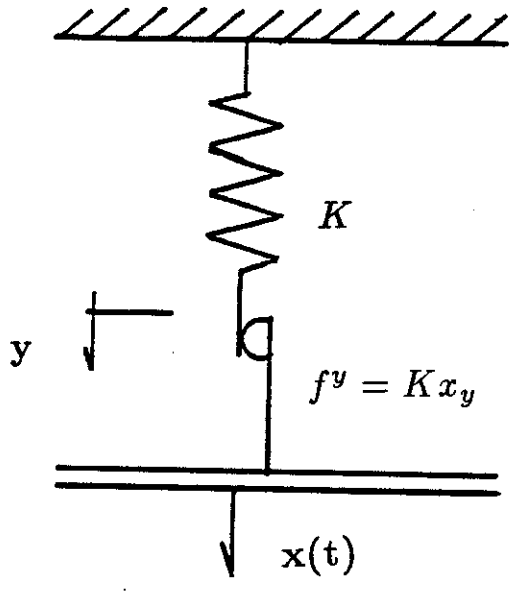

(b)

Figure 2.3
Elasto-plastic model. (a) Restoring force diagram. (b) Idealized physical system.

and

$$\omega_0^2 = \frac{k}{m} \tag{2.4d}$$

is the natural frequency of the linearized system corresponding to small displacements.

An alternative formulation for this model was used by Asano and Iwan (48), by defining a state variable ϕ , such that

$$y = g_1(\phi, \dot{x}, x_y). \tag{2.5}$$

The equation of motion may then be approximated by

$$\ddot{x} + 2\varsigma\omega_0\dot{x} + \omega_0^2 g_1(\phi, \dot{x}, x_y) = -\ddot{a}(t), \tag{2.6a}$$

$$\dot{\phi} = g_2(\phi, \dot{x}, x_y), \tag{2.6b}$$

where

$$g_1(\phi, \dot{x}, x_y) = \phi\{h(\phi + x_y) - h(\phi - x_y)\} + x_y\{h(\phi - x_y)h(\dot{x}) - h(-\phi - x_y)h(-\dot{x})\}, \tag{2.6c}$$

$$g_2(\phi, \dot{x}, x_y) = \dot{x}\{h(\phi + x_y) - h(\phi - x_y) + h(\phi - x_y)h(-\dot{x}) + h(-\phi - x_y)h(\dot{x})\}, \tag{2.6d}$$

where $h(...)$ is the unit step function and ϕ is defined on the whole real axis. For applications to probabilistic problems, the formulation used by Asano and Iwan has the advantage that the response variables are defined on a infinite domain. Approximate distributions, such as Gaussian or Hermite polynomial expansions, can be applied for this case, as it will be shown later in this thesis.

When analyzing the inelastic response of hysteretic systems, it is very important to consider the drift, or the plastic deformation of the structure. For the elastoplastic unit, the drift, z, is exactly the relative displacement of the slip damper element, or

$$z = x - y. \tag{2.7}$$

In contrast with the case of an elasto-plastic system, the drift of the hysteretic model described in Section 2.2.1 cannot be defined in terms of the response variables. From Figure 2.2b it can be also noted that the constitutive relation of the model described by equation (2.2) introduces artificial drift in the system response.

A more general class of hysteretic systems is the distributed hysteretic model introduced by Iwan (37). Consider such system, consisting of a linear spring with stiffness $m\alpha_0\omega_0^2$, a linear viscous damper and a distribution $mw(\xi)$ of normalized elasto-plastic elements with yielding level ξ, such that

$$\int_0^\infty w(\xi)d\xi = (1-\alpha_0)\omega_0^2. \tag{2.8}$$

The equation of motion for the system subjected to earthquake excitation will then be given by

$$\ddot{x} + 2\zeta\omega_0\dot{x} + \alpha_0\omega_0^2 x + \int_0^\infty w(\xi)g_1(\phi(\xi),\dot{x},\xi)d\xi = -\ddot{a}(t), \tag{2.9a}$$

where

$$\frac{\partial\phi(\xi,t)}{\partial t} = g_2(\phi(\xi,t),\dot{x},\xi). \tag{2.9b}$$

It was shown by Iwan that the continuous distributed model defined by equations (2.8) and (2.9) is capable of describing the hysteretic behaviour of a large class of structural systems. A special case of the continuous distributed model is the multilinear hysteretic model, illustrated in Figure 2.4. The system corresponds to a discrete distribution of elasto-plastic elements. For n such elements, equation (2.9) reduces to the following form

$$\ddot{x} + 2\zeta\omega_0\dot{x} + \alpha_0\omega_0^2 x + \omega_0^2\sum_{i=1}^{n}\alpha_i g_1(\phi_i,\dot{x},x_{y_i}) = -\ddot{a}(t), \tag{2.10a}$$

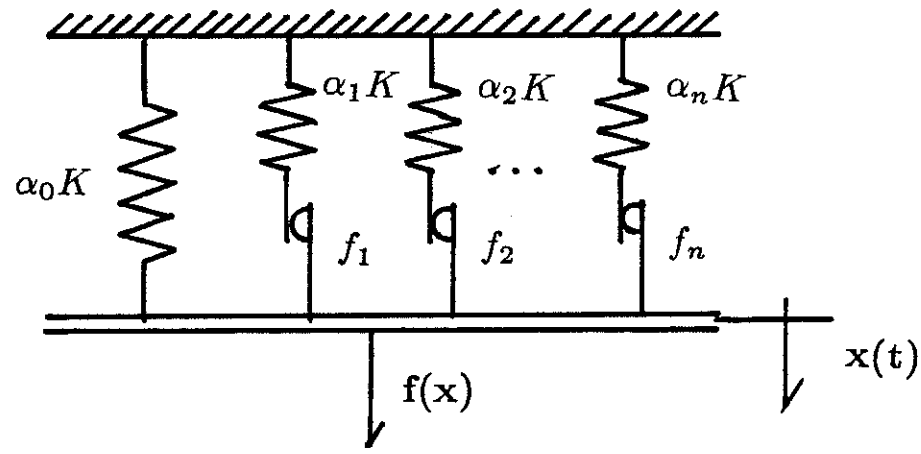

Figure 2.4
The Distributed-Element model for hysteresis.

where

$$\dot{\phi}_i = g_2(\phi_i, \dot{x}, x_{y_i}); \quad \text{for } i = 1, ..., n \tag{2.10b}$$

and

$$\sum_{i=1}^{n} \alpha_i = (1 - \alpha_0). \tag{2.10c}$$

Although from the physics of the problem the coefficients α_0, α_i $i = 1, ..., n$, are nonnegative quantities, the mathematical model derived can be also used for negative values of those parameters. In particular, the parameter α_0 gives the asymptotic behaviour for large deflections. Linear gravity effects can be modeled approximately by taking a negative value for the parameter α_0.

The analysis presented in this thesis is based on the multi-linear hysteretic system. In Chapter 3, the response of systems exhibiting hardening behaviour ($\alpha_0 > 0$, $\alpha_i > 0$ for $i = 1, ..., n$) and the dependence on excitation and system parameters is examined. Finally, the nature of the drift of structural systems subjected to seismic excitation, as well as its dependence on the frequency content of the excitation, are discussed in Chapters 4 and 5.

2.3 Stochastic modeling of strong earthquake ground motion.

2.3.1 Introduction.

A successful antiseismic study should be based on a knowledge of all potential earthquake excitations that could strike the site of a structure in consideration. Theoretically, the class of possible ground motions could be determined if information were available regarding the local conditions, material properties, neighbouring fault systems and the nature of expected fault rupture processes. The lack of such information and the complexity of the analytical problem that must be solved make this approach practically impossible to achieve. Alternatively, empirical methods can be applied in order to define appropriate models for the seismic excitation. It appears that deterministic models cannot be used for this purpose unless an analytical approach is applied to calculate the displacement field from a given fault mechanism. Defining the excitation as belonging to a general class of signals with prescribed time and frequency domain properties (duration, peak acceleration, total energy, energy distribution over the frequency range, etc.), appears as a more suitable approach. Stochastic models of the seismic excitation are an example of such an approach, and often have been used in examining the seismic response of structural systems.

The only limitation of the stochastic models is that the analytical methods for the analysis of nonlinear systems subjected to random excitation are far more complex than for the case of a deterministic input. For this reason, the mathematical description of the stochastic models should be relatively simple.

2.3.2 Stationary models.

Stationary stochastic models have often been used for the representation of the frequency content of long duration seismic ground motion. Consider an input earthquake acceleration, $\tilde{a}(t)$, of duration t_0. The Fourier amplitude spectrum of the excitation, $A(\omega)$, and the total energy, I_0, are defined as

$$A(\omega) = |\int_{-\infty}^{\infty} a(t) exp^{-i\omega t} dt| = |\int_{0}^{t_0} a(t) exp^{-i\omega t} dt| \tag{2.11}$$

and

$$I_0 = \int_0^{t_0} a^2(t) dt. \tag{2.12}$$

It can be proven by application of the Parseval's relation that

$$I_0 = \int_0^{t_0} a^2(t) dt = \int_{-\infty}^{\infty} a^2(t) dt = \frac{1}{2\pi} \int_{-\infty}^{\infty} A^2(\omega) d\omega. \tag{2.13}$$

From equation (2.13) it can be noticed that the Fourier amplitude spectra, $A(\omega)$, describes the distribution of the excitation energy over the frequency domain.

For a stationary stochastic model, the frequency content of the excitation is given by the power spectral density, $\Phi_{aa}(\omega)$. The relationship between $\Phi_{aa}(\omega)$ and $A(\omega)$ can be established in the case of a long duration strong ground motion acceleration, as follows. Recall, that for a weakly stationary random process, $a(t)$, the spectral density function, $\Phi_{aa}(\omega)$, is defined as

$$\Phi_{aa}(\omega) = \lim_{t_0 \to \infty} \frac{1}{2\pi t_0} E[|A^{t_0}(\omega, t_0)|^2], \tag{2.14a}$$

where $A^{t_0}(\omega, t_0)$ is the finite Fourier transform over a record of length t_0, or

$$A^{t_0}(\omega, t_0) = \int_0^{t_0} a(t) exp^{-i\omega t} dt. \tag{2.14b}$$

Equations (2.11) and (2.14) imply that

$$\Phi_{aa}(\omega) = \lim_{t_0 \to \infty} \frac{1}{2\pi t_0} E[A^2(\omega)], \tag{2.15}$$

which suggests that the spectral density function $\Phi_{aa}(\omega)$ is proportional to the mean square value of the excitation Fourier amplitude spectrum.

A stationary stochastic model of the seismic excitation is defined by specifying the spectral density function, $\Phi_{aa}(\omega)$. As can be seen from equation (2.15), $\Phi_{aa}(\omega)$ is given by the analytical amplitude spectrum, $A(\omega)$, of the actual earthquake ground motion. Boore (30), by analyzing the available records of seismic ground motion acceleration, obtained the following approximate expression for $A(\omega)$

$$A(\omega) = \frac{CM_0}{R} \frac{\omega^2}{1+(\omega/\omega_c)^2} [1+(\omega/\omega_m)^{2s}]^{-1/2} e^{-\omega R/2Q\beta}, \tag{2.16a}$$

where C, M_0, ω_c, ω_m, s, Q, β and R are model parameters. From equation (2.16a), the asymptotic behaviour for $A(\omega)$ is obtained as

$$A(\omega) \sim \omega^2 \quad \text{as } \omega \to 0 \tag{2.16b}$$

and

$$A(\omega) \sim e^{-\gamma\omega} \quad \text{as } \omega \to \infty. \tag{2.16c}$$

For applications to the nonlinear random response of structural systems, the stochastic excitation models should be mathematically tractable. Analytical results in the theory of random vibration can be obtained primarly for the case of Gaussian white noise excitation. For this reason, the models discussed in this section are obtained by appropriate filtering of a white noise excitation. Consider the excitation, $a(t)$, defined as

$$a(t) = M_{n_1}[x(t)], \tag{2.17a}$$

where $x(t)$ is the solution of the following equation

$$L_{n_2}[x(t)] = \xi(t), \tag{2.17b}$$

where $\xi(t)$, is a zero mean Gaussian white noise excitation with autocorrelation and spectral density function given by

$$E[\xi(t)] = 0, \tag{2.18a}$$

$$R_{\xi\xi}(\tau) = E[\xi(t)\xi(t+\tau)] = S_0\delta(\tau), \tag{2.18b}$$

and

$$\Phi_{\xi\xi}(\omega) = \frac{S_0}{2\pi}, \tag{2.18c}$$

and M_{n_1} and L_{n_2} are n_1 and n_2 order linear operators with $n_1 < n_2$.

The spectral density function of the process $a(t)$, $\Phi_{aa}(\omega)$ is then given by

$$\Phi_{aa}(\omega) = \frac{S_0}{2\pi}\frac{|H_L(\omega)|^2}{|H_M(\omega)|^2}, \tag{2.19}$$

where $H_L^{-1}(\omega)$ and $H_M^{-1}(\omega)$ are the transfer functions corresponding to the linear operators M_{n_1} and L_{n_2}, respectively. For nonlinear problems, the stationary stochastic model defined by equation (2.17) can be simply incorporated into the equation of motion and the problem is reduced to the case of white noise excitation. The rational filters are also physically motivated, and correspond to the modeling of the earth as a discrete dynamic system. For this reason, excitation models given by equation (2.17) are often used in the analysis of the random response of nonlinear structural systems.

An example of such a physically motivated formulation is the model defined by Kanai (26), (27) and Tajimi (28), often used in earthquake engineering. The excitation, $\tilde{a}(t)$, is given by

$$\tilde{a}(t) = \ddot{x}_g(t) + \xi(t) = -2\zeta_g\omega_g\dot{x}_g - \omega_g^2 x_g, \tag{2.20a}$$

where

$$\ddot{x}_g + 2\zeta_g\omega_g\dot{x}_g + \omega_g^2 x_g = -\xi(t) \tag{2.20b}$$

and ζ_g, ω_g are model parameters reflecting the local site conditions. The spectral density function for the Kanai-Tajimi filter is

$$\Phi_{K-T} = \frac{S_0}{2\pi} \frac{\omega_g^4 + 4\zeta_g^2\omega_g^2\omega^2}{(\omega_g^2 - \omega^2)^2 + 4\zeta_g^2\omega_g^2\omega^2}. \tag{2.21}$$

This is illustrated in Figure 2.5a for different values of the model parameter, ζ_g.

In Chapter 3 it will be shown that the drift of hysteretic structures is highly dependent on the low frequency content of the earthquake ground motion acceleration. The Kanai-Tajimi filter does not give a good representation for this frequency range. Recall that the asymptotic behaviour for $\omega \rightarrow 0$ is $\Phi_{aa}(\omega) \sim \omega^4$ (equation 2.16b), while in the case of the Kanai-Tajimi filter, $\Phi_{aa}(0) = \frac{S_0}{2\pi}$. It is suggested that the K-T model can not be used in the analysis of the hysteretic response behaviour. For this reason, an alternative model is introduced in Section 2.3.4.

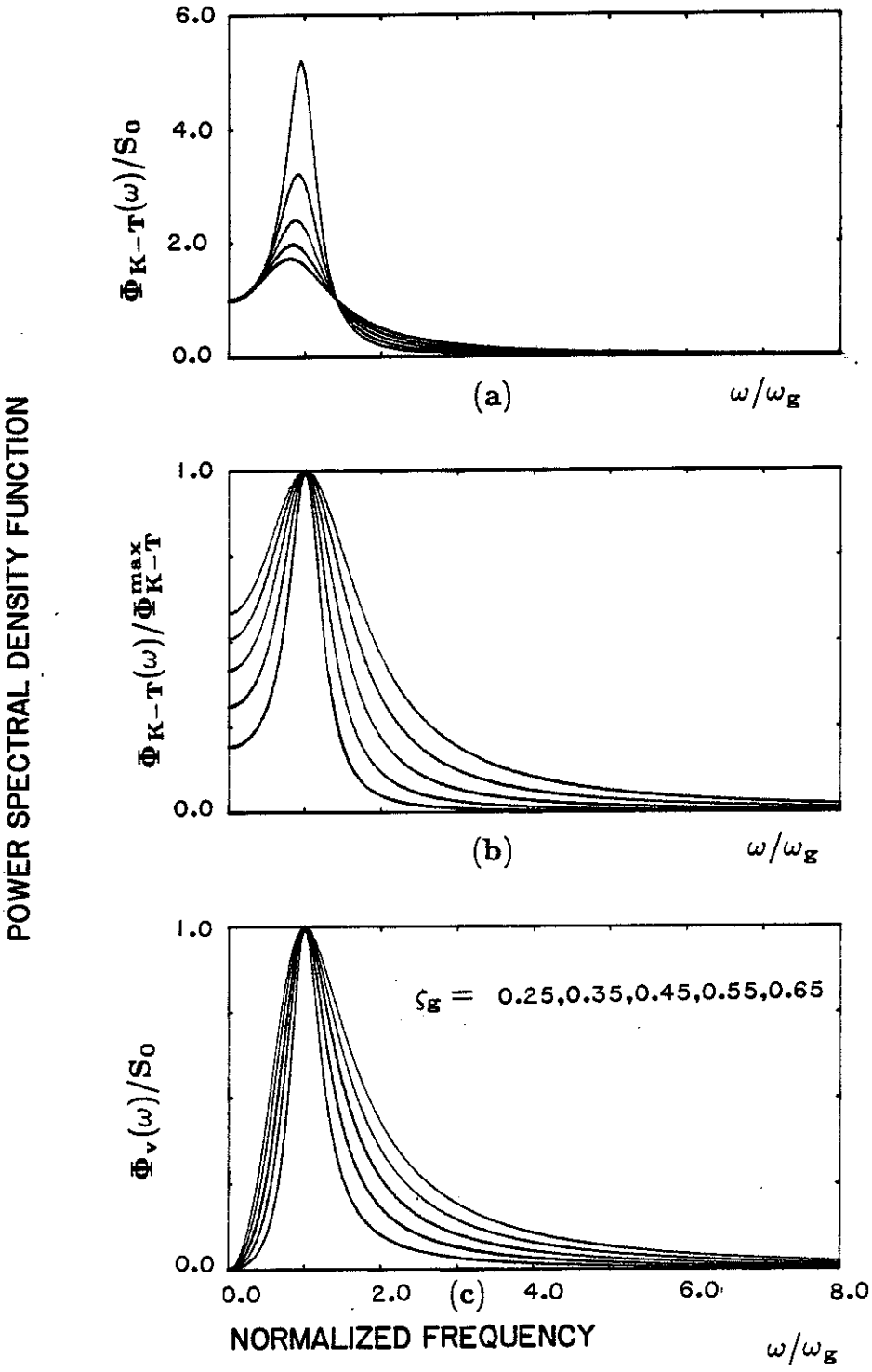

Figure 2.5
Power spectral density function of two stochastic seismic excitation models. (a) Kanai-Tajimi spectrum. (b) Normalized Kanai-Tajimi spectrum. (c) Proposed model for stochastic seismic excitation (eqn. 2.27).

2.3.3 Nonstationary models.

Stationary models can only be used for the case of long duration excitation, for which transient information is of no practical significance. In order to account for the transient nature of the seismic excitation, the time modulation of a stationary process may be considered. Define the process $a(t)$ as a time modulation of the zero mean stationary process $w(t)$ by applying a time window $\psi(t)$, or

$$a(t) = \psi(t)w(t). \tag{2.22}$$

In this case, the nonstationary mean square value or the envelope function for the process $a(t)$ is given by

$$E[a^2(t)] = \psi^2(t)\sigma_w^2, \tag{2.23}$$

where σ_w is the stationary RMS value of the process $w(t)$.

The envelope function of the excitation, defined by equation (2.23), provides the required information regarding the time domain properties of the process. Several empirical forms of modulation functions have been proposed in the literature. The intensity, duration and buildup time of the seismic excitation are expressed in terms of a few model parameters. The simplest form is defined by a boxcar type modulation, where

$$\psi_b(t) = \begin{cases} A, & \text{if } 0 \le t \le T_s; \\ 0, & \text{otherwise.} \end{cases} \tag{2.24}$$

Jennings, Housner and Tsai (33) defined a modulation function composed of a quadratic buildup phase, a constant phase and an exponentialy decaying tail. Shinozuka and Sato (34) proposed the form:

$$\psi_s(t) = A(e^{-\alpha t} - e^{-\beta t}) \qquad \beta > \alpha > 0. \tag{2.25}$$

Finally, Saragoni and Hart (35) suggested an envelope of the form:

$$\psi_n(t) = At^{\alpha}e^{-\beta t} \qquad \alpha, \beta > 0. \tag{2.26}$$

The effect of modulation on the frequency content cannot be given in a simple form. It should be noted that in the case of a short duration signal, the frequency decomposition of the modulation function can alter the desired frequency content possessed by the stationary process. It is understood that the effect will be less evident for the case of a long duration excitation.

The modulated stationary model cannot be applied for cases in which a significant change in the frequency content is noticed during the duration of the record. To represent such cases, Saragoni and Hart (35) introduced an excitation model defined by three distinct, modulated stationary processes accounting for the arrival of longitudinal, shear and surface waves. For the modulated filtered white noise (MFWN) models, the order in which filtering and modulation are applied lacks a physical interpretation. Indeed, modulation should be associated with source mechanisms, while the filtering is the result of the transition path.

A more physical model is the filter modulated white noise (FMWN) process, which is obtained by passing a deterministic modulated Gaussian white noise signal through a filter with prescribed transfer function. The observations made in the previous section regarding models for filters and modulation functions remain valid for the FMWN model. A comparison between the two methods was done by Smith (60). To summarize his conclusions, it can be proven that for a modulated stationary process, the envelope function is given by the square of the modulation function, while the frequency content of the filter is in general altered. In contrast, for a FMWN model the frequency of the filter is preserved, while the envelope function is in general altered. For a smoothly varying modulation and spectral density function, the two methods give approximately

identical results, as shown by Shinozuka and Sato (34) and Smith (60). This comparison suggests the difficulty that can be encountered in trying to define a time series of finite duration with a specified amplitude spectrum (Boore (30)).

2.3.4 Proposed model for stochastic seismic excitation.

Even though the number of available stochastic models for the earthquake excitation is quite large, only a few of them can be used for analytical investigation of the random response of hysteretic systems. As mentioned earlier, the only models that can be used systematically for this purpose are the ones obtained by passing a modulated white noise signal through a linear filter. For this reason, the white noise process and the Kanai-Tajimi filter are frequently used for the stochastic analysis of structural systems. In Section 2.3.2, it was shown that these models cannot be used in the analysis of hysteretic structural behaviour, due to the incorrect modeling of the low frequency content of the seismic ground motion acceleration.

For applications to the modeling of earthquakes that possess a characteristic frequency, the following model for the excitation $\ddot{a}(t)$, is proposed

$$-\ddot{a}(t) = 2\zeta_g \omega_g \dot{x}_g(t), \tag{2.27a}$$

where

$$\ddot{x}_g + 2\zeta_g \omega_g \dot{x}_g + \omega_g^2 x_g = e(t)\xi(t) \tag{2.27b}$$

and initial conditions

$$x_g(0) = \dot{x}_g(0) = 0. \tag{2.27c}$$

A boxcar type envelope function, $e(t)$, of duration T_s, is employed , where

$$e(t) = \begin{cases} 1 & \text{if } t \in (0, T_s); \\ 0 & \text{otherwise,} \end{cases} \tag{2.27d}$$

ω_g, ς_g are model parameters and $\xi(t)$ is a white noise process described by

$$E[\xi(t)] = 0 \tag{2.27e}$$

and

$$E[\xi(t)\xi(t+\tau)] = S_0\delta(\tau). \tag{2.27f}$$

A similar model was proposed by Kameda (29), but it has not been used very often for the stochastic analysis of hysteretic systems. This model belongs to the same family of models as the Kanai-Tajimi filter, in the sense that both are obtained by the use of a second-order linear filter.

By allowing $T_s \to \infty$, a stationary process is obtained for which the spectral density function $\Phi_v(\omega)$ is given by

$$\Phi_v(\omega) = \frac{S_0}{2\pi} \frac{4\varsigma_g^2\omega_g^2\omega^2}{(\omega^2 - \omega_g^2)^2 + 4\varsigma_g^2\omega_g^2\omega^2}. \tag{2.28}$$

A comparison between the spectral density of the present model and the Kanai-Tajimi model is given in Figure 2.5 for different values of the parameter ς_g. The acceleration spectrum in the case of the proposed model possesses an asymptotic which is linear in omega for $\omega \to 0$. This can be viewed as an improvement over the Kanai-Tajimi filter. At the same time, the model parameters have a precise physical interpretation; ω_g corresponds to the peak frequency of the process, ς_g is a measure of the bandwidth and S_0 accounts for the strength of the process.

The envelope function of the process, $\sigma_a^2(t)$, defined as

$$\sigma_a^2(t) = E[a^2(t)] = 4\varsigma_g^2\omega_g^2 E[\dot{x}_g^2(t)], \tag{2.29}$$

is illustrated in Figure 2.6 for different values of the bandwidth of excitation, ς_g, and for duration $T_s = 15T_g$. T_g represents the natural period of the linear filter. As $T_s \to \infty$, the envelope function reaches a stationary value, σ_{as}^2 given by

$$\sigma_{as}^2 = S_0\omega_g\varsigma_g. \tag{2.30}$$

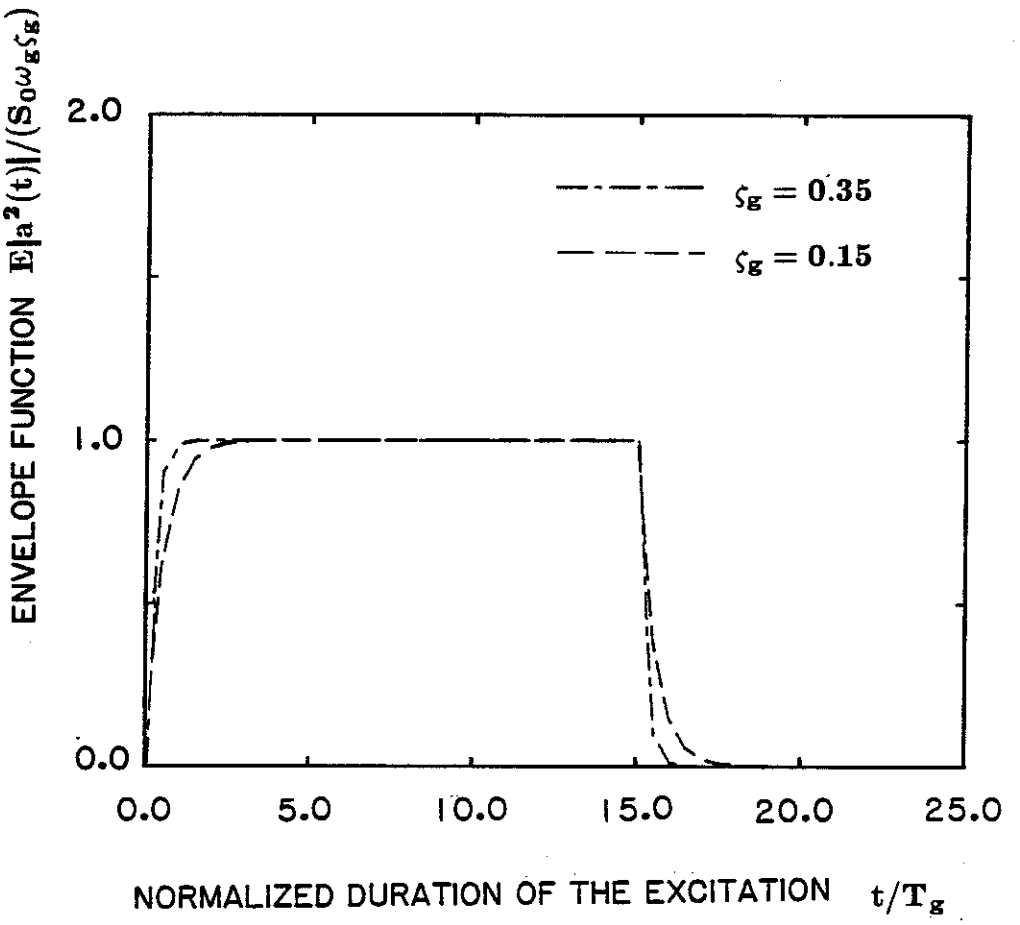

Figure 2.6
Normalized envelope function for the proposed seismic excitation model.

Practically speaking, this value is achieved after only a few periods of excitation, as noticed in Figure 2.6.

The boxcar type modulation function used in this model is a simplified representation of the central portion of the strong motion and accounts approximately for the shear wave contribution to the strong motion. As a FMWN model, the modulation function is altered by the filtering process, as shown in Figure 2.6. The buildup and tail components of the envelope function should not be considered as a realistic explanation of the actual phenomenon because they are described in terms of the same model parameters ς_g, ω_g. For an actual earthquake, these components contain information regarding the longitudinal and surface wave contributions to the record.

A stochastic seismic model for applications in the analysis of hysteretic structures is proposed in this section. Although of a very simple form, the proposed model is capable of defining the basic features of earthquake ground motion, such as duration, strength and frequency content. Because of the influence of the low frequency content of the excitation on drift response, the proposed model is prefered over the Kanai-Tajimi model. It is also selected over other more complex models, due to its applicability in the analysis of nonlinear random vibration problems. In the numerical examples illustrated in this thesis, the bandwidth of excitation is chosen equal to $\varsigma_g = 0.25$ and $\varsigma_g = 0.50$, corresponding to narrowbanded and broadbanded excitation, respectively. The duration is choosen equal to $T_s = 25T_0$, where T_0 is the natural period of the system. For actual structural systems, $T_s = 25T_0$, corresponds to a duration of approximately 5-75 sec.

Chapter 3. APPLICATION OF EQUIVALENT LINEARIZATION IN THE ANALYSIS OF HYSTERETIC SYSTEMS.

3.1 Introduction.

The objective of this Chapter is to identify the basic features of the random response of hysteretic structural systems subjected to stochastic seismic excitation. Approximate solutions for the second order response statistics of such systems have been introduced by Caughey (43), Kobori, Minai and Suzuki (46),(47), Asano and Iwan (48) and Wen (57). Caughey was the first to propose an approximate solution for the random response of a bilinear hysteretic system subjected to white noise excitation. The parameters of an equivalent linear system were calculated with the method of slowly varying parameters. As shown by Iwan and Lutes (44), the method produces very good results for the case of narrowbanded response, while for an elasto-plastic or nearly elasto-plastic system, the method underestimates the RMS value of the displacement response by up to 60 percent. Kobori, Minai and Suzuki (47) and Wen (56) formulated the hysteretic constitutive behaviour in terms of additional state variables. Following this procedure, a higher dimension and independent of response history equation of motion is obtained. With the use of generalized equivalent linearization, and for white noise excitation, Asano and Iwan (48) and Wen (57), obtained accurate estimates of the second order response statistics.

The discussion presented in this Chapter is based on the random response of multilinear hysteretic systems; the problem is solved approximately by transient equivalent linearization (Asano and Iwan). The formulation of the solution scheme and numerical results for transient and stationary response statistics are presented in Sections 3.3 and 3.4, respectively. A comparison between this approximate scheme and the equivalent linearization introduced by Caughey is

presented in Section 3.5.

In Section 3.5, it is shown that the nature of hysteretic response behaviour cannot be described only in terms of the RMS value of the process. For this reason, the drift and the frequency content of the displacement response are examined in Sections 3.6 and 3.7, respectively. In particular, the dependence of the displacement response frequency content upon the stochastic seismic excitation model is also discussed in Section 3.7.

3.2 Equation of motion.

The equation of motion for the nondeteriorating hysteretic system described in Section 2.2.2 is given by the following set of equations

$$\ddot{x} + 2\zeta\omega_0\dot{x} + \alpha_0\omega_0^2 x + \omega_0^2 \sum_{i=1}^{n} \alpha_i g_1(\phi_i, \dot{x}, x_{y_i}) = -\ddot{a}(t) \qquad (3.1a)$$

$$\dot{\phi}_i = g_2(\phi_i, \dot{x}, x_{y_i}) \qquad \forall i = 1, n, \qquad (3.1b)$$

where

$$\sum_{i=1}^{n} \alpha_i = 1 - \alpha_0, \qquad (3.1c)$$

and $g_1(...)$ and $g_2(...)$ are nonlinear functions given by equations (2.6c) and (2.6d).

Following the analysis presented in Section 2.3, a general stochastic model for the earthquake ground motion acceleration, $\ddot{a}(t)$, obtained by filtering a modulated zero mean Gaussian white noise signal through a second order linear filter, is defined as

$$-\ddot{a}(t) = 2\zeta_g\omega_g\dot{x}_g(t)b_1 + \omega_g^2 x_g(t)b_2, \qquad (3.1d)$$

where $x_g(t)$ is the solution of the following equation

$$\ddot{x}_g + 2\zeta_g\omega_g\dot{x}_g + \omega_g^2 x_g = e(t)\xi(t), \qquad (3.1e)$$

with

$$x_g(0) = \dot{x}_g(0) = 0, \tag{3.1f}$$

and $e(t)$, $\xi(t)$ are defined in Section 2.3 by equations (2.27d)- (2.27f).

By setting $b_1 = b_2 = 1$, the Kanai-Tajimi model is recovered, while $b_1 = 1$, $b_2 = 0$ corresponds to the model defined by the equations (2.27a)-(2.27c). The equation of motion, (3.1), can be put into the following m-dimensional stochastic differential equation form

$$\frac{d\mathbf{u}}{dt} = \mathbf{a}(\mathbf{u}) + e(t)\mathbf{w}(t), \tag{3.2}$$

with $m = n + 4$ and $\mathbf{u}$, $\mathbf{w}(t)$, $\mathbf{a}(\mathbf{u})$ defined as

$$\mathbf{u}^{\mathbf{T}} = \{x, \dot{x}, \phi_1, ..., \phi_n, x_g, \dot{x}_g\} \tag{3.3a}$$

$$w_m(t) = \xi(t);\ w_i(t) = 0 \quad for\ i = 1, ..., m-1 \tag{3.3b}$$

$$\begin{aligned}
&a_1(\mathbf{u}) = u_2 \\
&a_2(\mathbf{u}) = -2\varsigma\omega_0 u_2 - \alpha_0\omega_0^2 u_1 + 2\varsigma_g\omega_g b_1 u_m + \omega_g^2 b_2 u_{m-1} - \omega_0^2 \sum_{i=1}^{n} \alpha_i g_1(u_{i+2}, u_2, x_{y_i}) \\
&a_j(\mathbf{u}) = g_2(u_j, u_2, x_{y_{j-2}}) \quad j = 3, ..., m-2 \\
&a_{m-1}(\mathbf{u}) = u_m \\
&a_m(\mathbf{u}) = -2\varsigma_g\omega_g u_m - \omega_g^2 u_{m-1}
\end{aligned} \tag{3.3c}$$

The system governed by equations (3.2) and (3.3) is a nonlinear dynamic system subjected to nonparametric stochastic excitation. For the case of filtered white noise excitation, the problem can be rigorously formulated in terms of the diffussion equation for the probability density of the response process. In this chapter, the method of generalized equivalent linearization is used for the

calculation of approximate velocity and displacement response statistics. For a rigorous examination of the theory of stochastic processes and nonlinear random vibration, see Ito (2), Stratonovich (3), (4), Caughey (6), Lin (7) or Crandall and Mark (8).

3.3 Equivalent linear system.

The equivalent linearization technique is a method applied directly to the equation of motion of the system. It was introduced independently by Booton (15) and Caughey (14). Later the method was generalized by Iwan and Yang (16), Spanos and Iwan (19), Atalik and Utku (17) and for general nonstationary response, by Iwan and Mason (18). The idea of the method is to approximate the nonlinear stochastic equation

$$\frac{d\mathbf{u}}{dt} = \mathbf{a}(\mathbf{u}) + e(t)\mathbf{w}(t) \tag{3.2}$$

by a linear equation,

$$\frac{d\mathbf{y}}{dt} = \mathbf{A}\mathbf{y} + e(t)\mathbf{w}(t). \tag{3.4}$$

The parameters of the equivalent linear system are calculated such that the norm of the difference between the two sets of equations is minimized by $\mathbf{y}(t)$, the solution of equation (3.4). The minimization is performed in the mean value sense. That is, one looks for the set of parameters A_{ij}, components of the matrix $\mathbf{A}$, which will minimize the expected value of the norm of the error ϵ^*, defined as

$$\epsilon^* = \epsilon^{\mathrm{T}}(\mathbf{y})\epsilon(\mathbf{y}), \tag{3.5a}$$

where

$$\epsilon(\mathbf{y}) = \mathbf{a}(\mathbf{y}) - \mathbf{A}\mathbf{y}. \tag{3.5b}$$

The case most examined and for which the following analysis is valid, is the case of zero mean response of a nonlinear system subjected to zero mean Gaussian white noise excitation.

From the minimization of the mean of ϵ^*, an expression for the parameters of the linear system is obtained in the form

$$E[\mathbf{y}\mathbf{y}^{\mathbf{T}}]\mathbf{A} = E[\mathbf{y}\mathbf{a}^{\mathbf{T}}(\mathbf{y})]. \tag{3.6}$$

Atalik and Utku(17), by considering a Gaussian distributed process $\mathbf{y}$, and assuming continuity of the partial derivatives in equation (3.7), obtained the following expression for $\mathbf{A}$

$$A_{ij} = E[\frac{\partial a_i}{\partial u_j}|_{\mathbf{u}=\mathbf{y}}]. \tag{3.7}$$

For Gaussian white noise excitation, $\mathbf{y}$, the solution of equation (3.4) is a multidimensional Gaussian distributed process, and the covariance matrix satisfies the following covariance equation:

$$\frac{d}{dt}\mathbf{Q} = \mathbf{A}\mathbf{Q} + \mathbf{Q}\mathbf{A}^{\mathbf{T}} + \mathbf{B}\mathbf{D}\mathbf{B}^{\mathbf{T}}, \tag{3.8a}$$

where

$$\mathbf{Q}(t_0) = \mathbf{Q_0} \tag{3.8b}$$

and

$$Q_{ij} = E[y_i y_j]. \tag{3.8c}$$

For $\mathbf{w}(t)$ given by (3.3b) and (2.27d)-(2.27f), it is implied that

$$(BDB^T)_{ij} = \delta_{im}\delta_{jm}e^2(t)S_0. \tag{3.9}$$

By applying equation (3.7), and for $\mathbf{a}(\mathbf{u})$ given by (3.3c), the following expression for the matrix $\mathbf{A}$ is obtained:

$$\mathbf{A} = \left(\begin{array}{cc|ccc|cc} 0 & 1 & 0 & \dots & 0 & 0 & 0 \\ -\alpha_0\omega_0^2 & -B_0 & -\alpha_1\omega_0^2 C_{21} & \dots & -\alpha_n\omega_0^2 C_{2n} & \omega_g^2 b_2 & 2\zeta_g\omega_g b_1 \\ \hline 0 & C_{41} & C_{31} & \mathbf{0} & 0 & 0 & 0 \\ \vdots & \vdots & \mathbf{0} & \ddots & \mathbf{0} & \vdots & \vdots \\ 0 & C_{4n} & 0 & \mathbf{0} & C_{3n} & 0 & 0 \\ \hline 0 & 0 & 0 & \dots & 0 & 0 & 1 \\ 0 & 0 & 0 & \dots & 0 & -\omega_g^2 & -2\zeta_g\omega_g \end{array}\right), \tag{3.10}$$

where

$$B_0 = 2\zeta\omega_0 + \omega_0^2 \sum_{i=1}^{n} \alpha_i C_{1i}, \tag{3.11}$$

and for $i = 1, ..., n$

$$C_{1i} = E\left[\left.\frac{\partial g_1(x_1, x_2, x_3)}{\partial x_2}\right|_{x_1=u_{i+2}, x_2=u_2, x_3=x_{y_i}}\right] \tag{3.12a}$$

$$C_{2i} = E\left[\left.\frac{\partial g_1(x_1, x_2, x_3)}{\partial x_1}\right|_{x_1=u_{i+2}, x_2=u_2, x_3=x_{y_i}}\right] \tag{3.12b}$$

$$C_{3i} = E\left[\left.\frac{\partial g_2(x_1, x_2, x_3)}{\partial x_1}\right|_{x_1=u_{i+2}, x_2=u_2, x_3=x_{y_i}}\right] \tag{3.12c}$$

$$C_{4i} = E\left[\left.\frac{\partial g_2(x_1, x_2, x_3)}{\partial x_2}\right|_{x_1=u_{i+2}, x_2=u_2, x_3=x_{y_i}}\right]. \tag{3.12d}$$

It should be pointed out that the functions $g_1(x_1, x_2, x_3)$, $g_2(x_1, x_2, x_3)$ are not continously differentiable in a rigorous sense. Nevertheless, it can be considered that the derivative of the unit step function $h(x)$, defined as

$$h(x) = \begin{cases} 1, & \text{if } x \geq 0; \\ 0, & \text{otherwise} \end{cases} \tag{3.13a}$$

exists in a weak sense, and is equal to

$$\frac{\partial h}{\partial x} = \delta(x). \tag{3.13b}$$

In the previous equation $\delta(x)$ is the Dirichlet delta function.

By substituting equations (2.6c) and (2.6d) into (3.12), an expression for the coefficients $(C_{ji}, j = 1, ..., 4; i = 1, ..., n)$ is obtained. This expression is a generalization of the results obtained by Asano and Iwan (48), and is given by

$$C_{1i} = \frac{x_{y_i}}{\sqrt{2\pi}\sigma_{\dot{x}}} \operatorname{erfc}\left(\frac{x_{y_i}}{\sqrt{2\sigma_{\phi i}(1-\rho_i^2)}}\right) \tag{3.14}$$

$$C_{2i} = \text{erf}\left(\frac{x_{y_i}}{\sqrt{2\sigma_{\phi i}}}\right) - \frac{x_{y_i} e^{-\frac{x_{y_i}^2}{2\sigma_{\phi i}}}}{\sqrt{2\pi\sigma_{\phi i}}} \text{erfc}\left(\frac{x_{y_i}\rho_i}{\sqrt{2\sigma_{\phi i}(1-\rho_i^2)}}\right) \tag{3.15}$$

$$C_{3i} = -\frac{1}{\pi}\sqrt{\frac{\sigma_{\dot{x}}(1-\rho_i^2)}{\sigma_{\phi i}}}\, e^{-\frac{x_{y_i}^2}{2\sigma_{\phi i}(1-\rho_i^2)}} - \frac{\rho_i x_{y_i}}{\sigma_{\phi i}}\sqrt{\frac{\sigma_{\dot{x}}}{2\pi}}\, e^{-\frac{x_{y_i}^2}{2\sigma_{\phi i}}}\left[1+\text{erfc}\left(\frac{x_{y_i}\rho_i}{\sqrt{2\sigma_{\phi i}(1-\rho_i^2)}}\right)\right] \tag{3.16}$$

$$C_{4i} = \frac{1}{2}\left(1+\text{erf}\left(\frac{x_{y_i}}{\sqrt{2\sigma_{\phi i}}}\right)\right) - \frac{1}{\sqrt{\pi}}\int_{\frac{x_{y_i}}{\sqrt{2\sigma_{\phi i}}}}^{\infty} e^{-t^2}\text{erf}\left(\frac{\rho_i}{\sqrt{1-\rho_i^2}}t\right)dt, \tag{3.17}$$

where $\sigma_{\phi i}$, $\sigma_{\dot{x}}$, $\sigma_{\dot{x}\phi i}$, ρ_i are defined by the following relations

$$\sigma_{\dot{x}} = Q_{22} = E[\dot{x}^2] \tag{3.18a}$$

$$\sigma_{\phi i} = Q_{i+2,i+2} = E[\phi_i^2] \tag{3.18b}$$

$$\sigma_{\dot{x}\phi i} = Q_{2,i+2} = E[\dot{x}\phi_i] \tag{3.18c}$$

$$\rho_i = \frac{\sigma_{\dot{x}\phi i}}{\sqrt{\sigma_{\dot{x}}\sigma_{\phi i}}}. \tag{3.18d}$$

In equation (3.18), erf(x) and erfc(x) are the error function and the complementary error function respectively, defined as

$$\text{erf(x)} = \frac{1}{\sqrt{\pi}}\int_{-x}^{x} e^{-t^2}dt \tag{3.19a}$$

and

$$\text{erfc(x)} = 1 - \text{erf(x)}. \tag{3.19b}$$

An approximate solution for the transient response covariance matrix, Q, can be obtained by solving the set of simultaneous equations (3.7) and (3.8) for the particular values of the parameters of the equivalent linear system given by the relations (3.10)-(3.12) and (3.14-3.19). The integration of equations (3.7),

(3.8a) is in general done numerically. It should be pointed out that the expression (3.17) for $(C_{4i};\ i=1,...,n)$ contains an infinite integral, which cannot be expressed in terms of elementary functions and a numerical integration will require a high computational effort. Asano and Iwan (48) have shown that for small values of $(\rho_i;$ i=1,...,n), equation (3.17) can be replaced by

$$C_{4i} = \frac{1}{2}\left(1+\mathrm{erf}\left(\frac{x_{y_i}}{\sqrt{2\sigma_{\phi i}}}\right)\right) - \frac{1}{\pi}e^{-\frac{x_{y_i}^2}{2\sigma_{\phi i}}}\frac{\rho_i}{\sqrt{1-\rho_i^2}}, \qquad (3.17')$$

which corresponds to the first term in the series expression of the infinite integral in the equation (3.17). For cases of practical interest, the error introduced by using equation (3.17') instead of (3.17) is negligible while the computational effort is reduced by about 25 times.

Because the probability density function of the response of a linear system subjected to zero mean Gaussian excitation is a zero mean Gaussian distribution, the covariance matrix, $\mathbf{Q(t)}$, gives a full probabilistic description for the response statistics.

As shown in Appendix A, in the case of a stationary excitation and if a stationary solution of the covariance equation exists, the spectral density function, Φ_{xx}, and the transfer function, $H_x(i\omega)$, of the displacement response are given by

$$\Phi_{xx}(\omega) = \frac{S_0}{(2\pi)}\frac{4\varsigma_g^2\omega_g^2 b_1^2\omega^2+\omega_g^4 b_2^2}{(\omega_g^2-\omega^2)^2+4\varsigma_g^2\omega_g^2\omega^2}\frac{1}{(R_x^2+I_x^2)} \qquad (3.20)$$

and

$$\frac{1}{H_x(i\omega)} = R_x + iI_x, \qquad (3.21)$$

where

$$R_x = (\alpha_0\omega_0^2-\omega^2)+\omega^2\omega_0^2\sum_{i=1}^{n}\frac{\alpha_i C_{2i}C_{4i}}{\omega^2+C_{3i}^2} \qquad (3.22a)$$

$$I_x = \omega\left[B_0-\omega_0^2\sum_{i=1}^{n}\frac{\alpha_i C_{2i}C_{3i}C_{4i}}{\omega^2+C_{3i}^2}\right]. \qquad (3.22b)$$

3.4 Numerical results of equivalent linearization.

Consider the bilinear hysteretic system illustrated in Figure 3.1. The equation of motion is given by

$$\ddot{x} + 2\zeta\omega_0\dot{x} + \alpha_0\omega_0^2 x + (1-\alpha_0)\omega_0^2 g_1(\phi, \dot{x}, Y) = -\ddot{a}(t) \tag{3.23a}$$

and

$$\dot{\phi} = g_2(\phi, \dot{x}, Y), \tag{3.23b}$$

with g_1 and g_2 given by equation (2.6). By introducing the state variable, ϕ, a third-order equation of motion for the drift response variables is obtained, while the equation of motion given by equation (3.23) becomes independent of the time history of the response. For the analysis presented in this section, the excitation model given by equation (2.27), is considered, i.e. $b_1 = 1$ and $b_2 = 0$ in equation (3.1d).

For the case of a bilinear hysteretic system, the normalized excitation peak frequency, ω_g', normalized time, τ, ductility ratio, μ_x, and normalized excitation RMS value, σ_a' can be defined as follows (Appendix B):

$$\omega_g' = \frac{\omega_g}{\omega_0} \tag{3.24a}$$

$$\tau = \omega_0 t \tag{3.24b}$$

$$\mu_x = \frac{x}{Y} \tag{3.24c}$$

and

$$\sigma_a' = \frac{\sigma_a}{\omega_0^2 Y} = \frac{\sqrt{S_0\omega_g\zeta_g}}{\omega_0^2 Y}. \tag{3.24d}$$

Without loss of generality, the analysis for the elastic, perfectly plastic system governed by equation (3.23), is done for the normalized system corresponding to parameters values

$$Y = 1 \qquad \text{and} \qquad \omega_0 = 1, \tag{3.25}$$

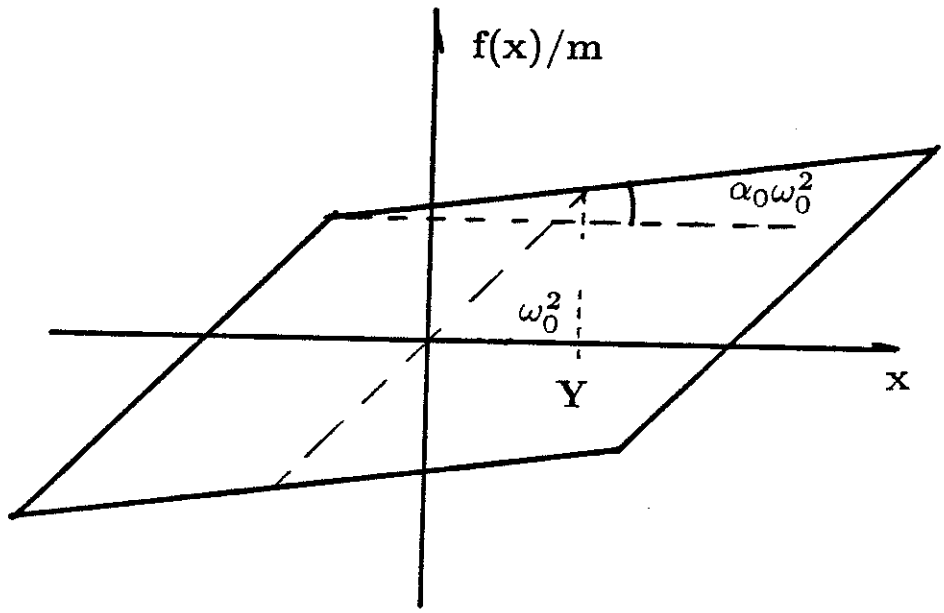

Figure 3.1
The bilinear hysteretic model.

while the results obtained are given in terms of the dimensionless groups defined by (3.24).

By applying the equivalent linearization described in Section 3.3, the transient mean square value for the displacement and velocity response are obtained. In Figures (3.2) and (3.3), the results predicted by this approximate solution scheme are compared to numerical simulation results for cases corresponding to $\alpha_0 = 0.1$, and for $\omega_g/\omega_0 = 0.50$ and 1.0, respectively. The very good agreement between the two sets of results suggests that equivalent linearization can be succesfully used for the prediction of transient response statistics. It can be also noticed that for stationary excitation, the solution for displacement and velocity response becomes stationary in mean square value. In order to illustrate the accuracy of equivalent linearization, a parametric investigation for the stationary response statistics is presented in this section. The seismic excitation model, described by equation (2.27), is used in the analysis that follows.

In Figure 3.4, the variation of the RMS value of the response with the normalized RMS value of the excitation and with α_0 is examined for bandwidth of excitation $\zeta_g = 0.50$. From the results presented in Figure 3.4, it can be noticed that for $\omega_g/\omega_0 \approx 1$, the displacement response of the bilinear hysteretic system is smaller than the response of the corresponding linear system ($\alpha_0 = 1$). A similar conclusion can be drawn from the results illustrated in Figure 3.5, for bandwidth of excitation $\zeta_g = 0.10$.

In Figure 3.6, the dependence of the response statistics on the characteristic frequency of the excitation is examined for $\alpha_0 = 0.1$, and for bandwidth of excitation, $\zeta_g = 0.50$. It can be concluded that a very strong dependence on the strength of the excitation is observed for $\omega_g/\omega_0 < 1$, while for ω_g/ω_0, a weaker dependence is noted.

The results presented in Figures 3.4, 3.5 and 3.6 suggest that the RMS value

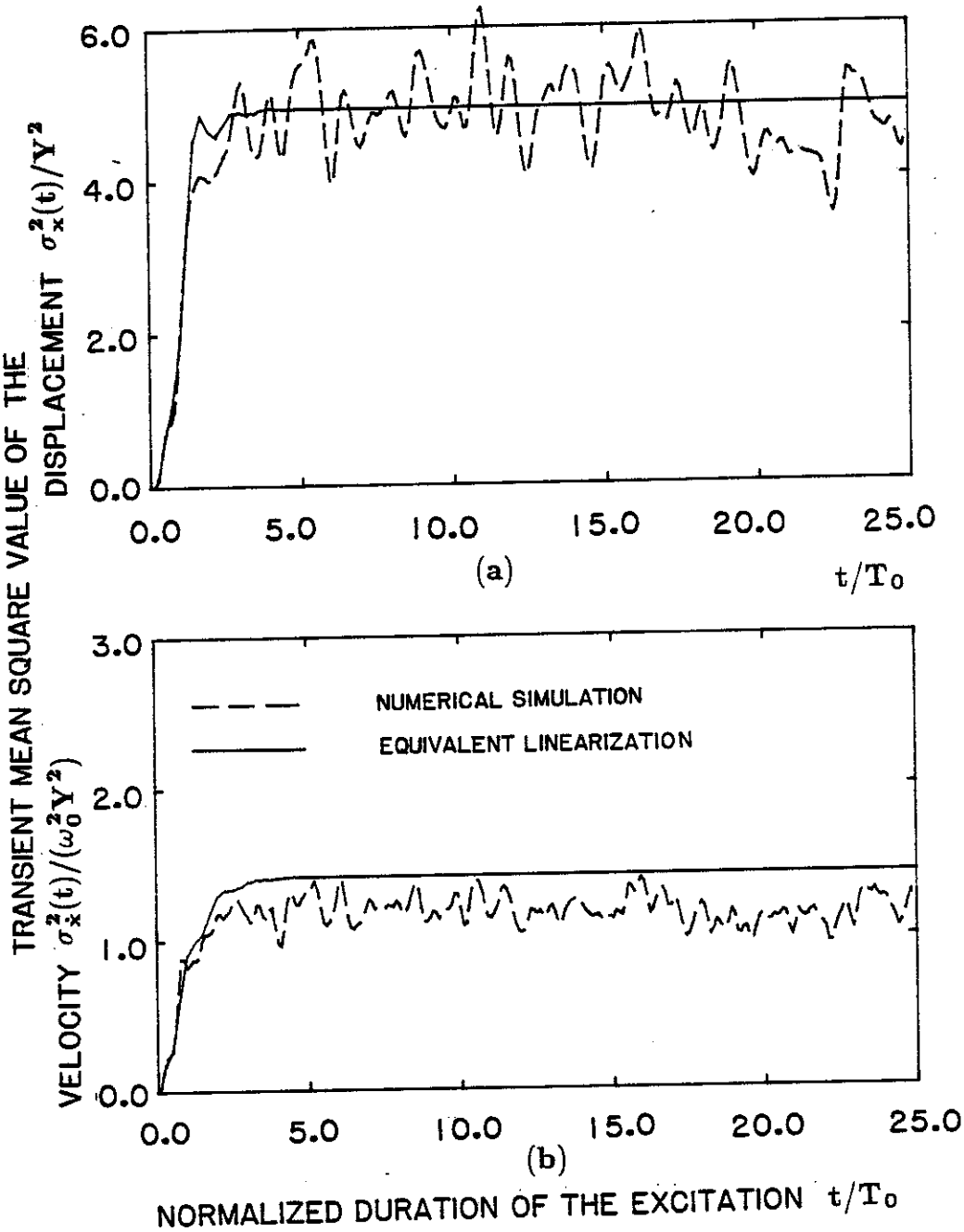

Figure 3.2
Covariance of Nonstationary Response. Bilinear hysteretic system subjected to filtered white noise excitation (eqn. 2.27), S_0=2.0, ς_g=0.50, ω_g/ω_0=0.50, α_0=0.10 and ς=0.05. (a) Displacement response. (b) Velocity response.

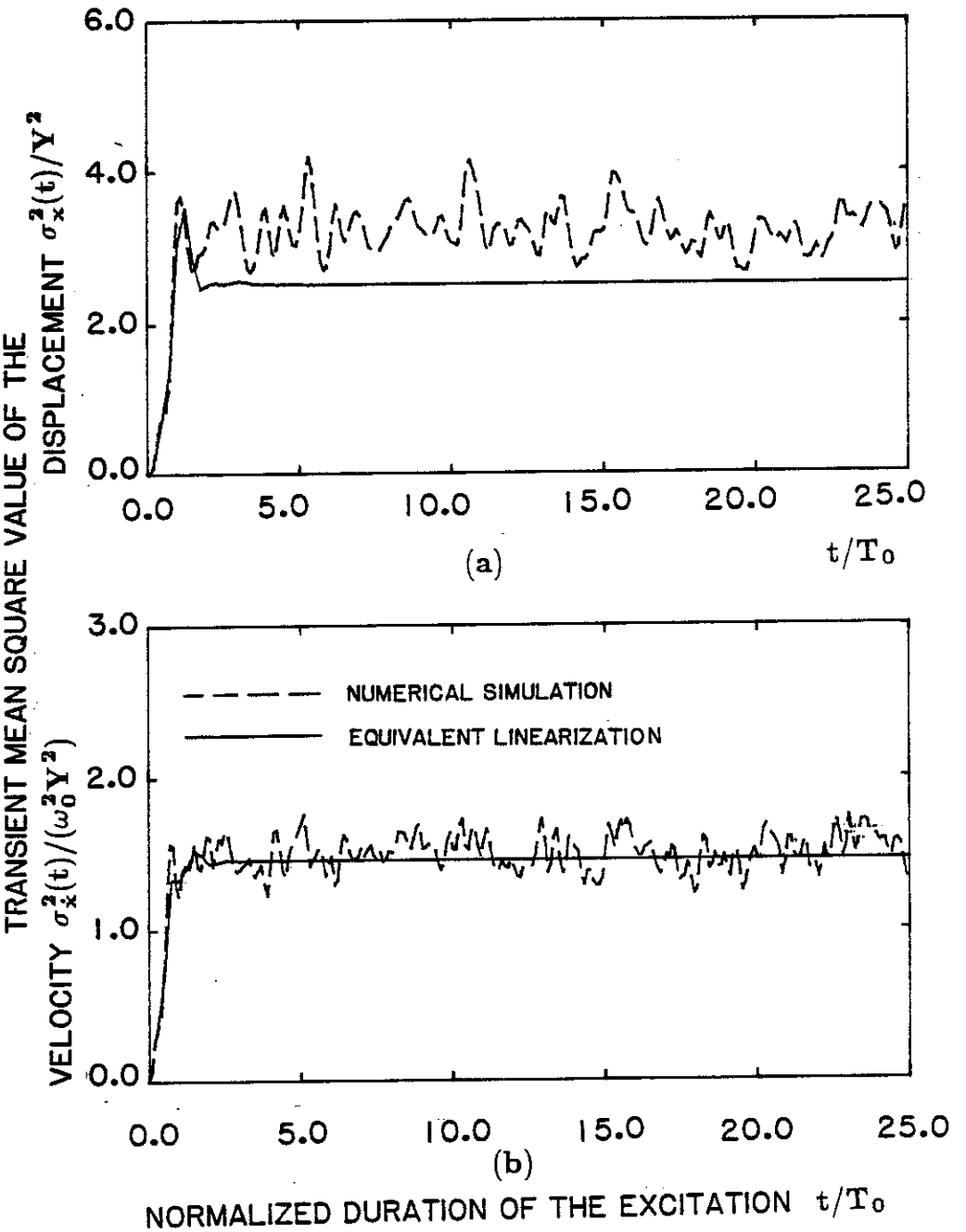

Figure 3.3
Covariance of Nonstationary Response. Bilinear hysteretic system subjected to filtered white noise excitation (eqno 2.27), S_0=2.0, ς_g=0.50, ω_g/ω_0=1.0, α_0=0.10 and ς=0.05. (a) Displacement response. (b) Velocity response.

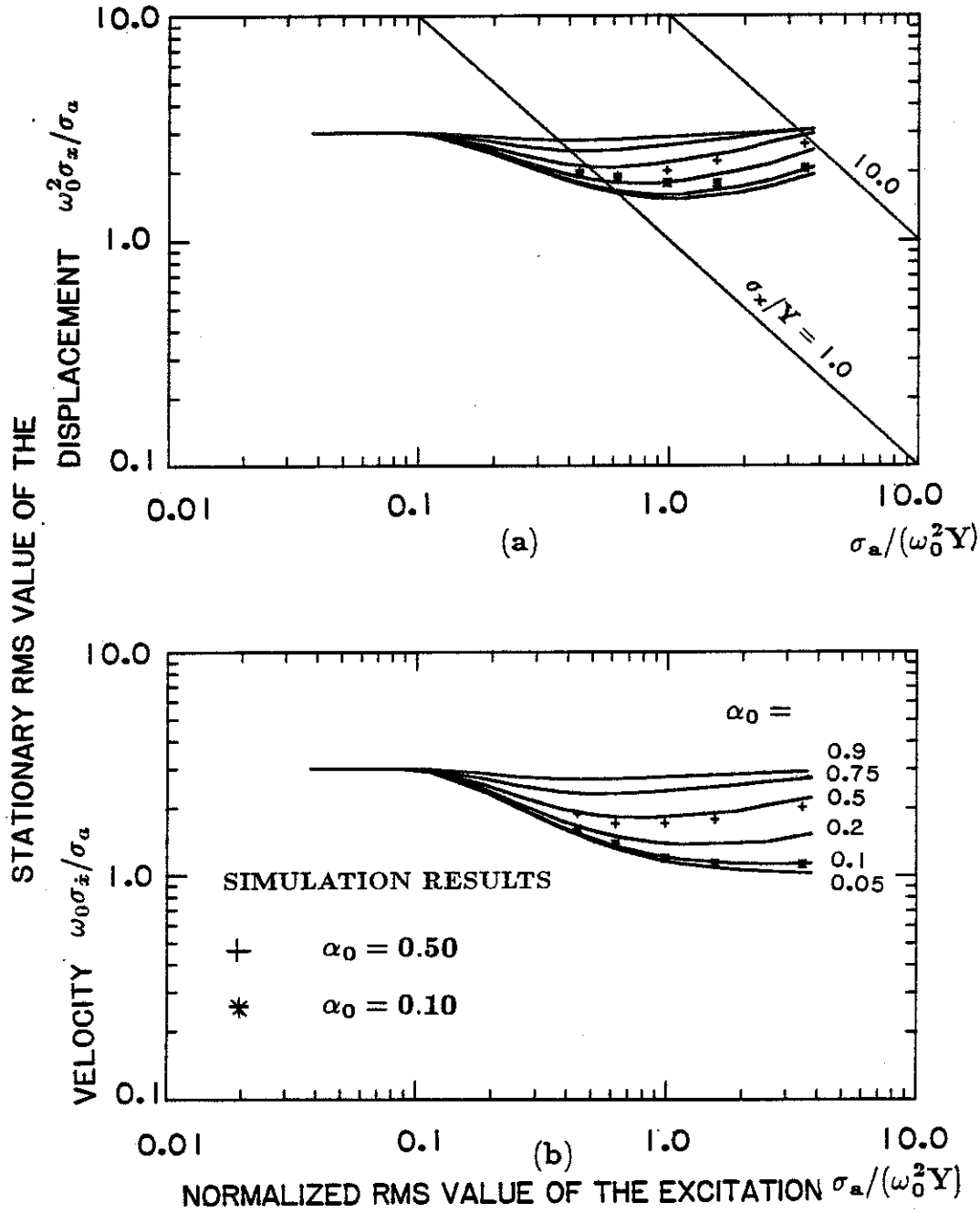

Figure 3.4
Dependence of the Stationary RMS response levels on the strength of the excitation and α_0, for bandwidth of the excitation, ζ_g=0.50, and ω_g/ω_0=1.0 and ζ=0.05. (a) Displacement response. (b) Velocity response.

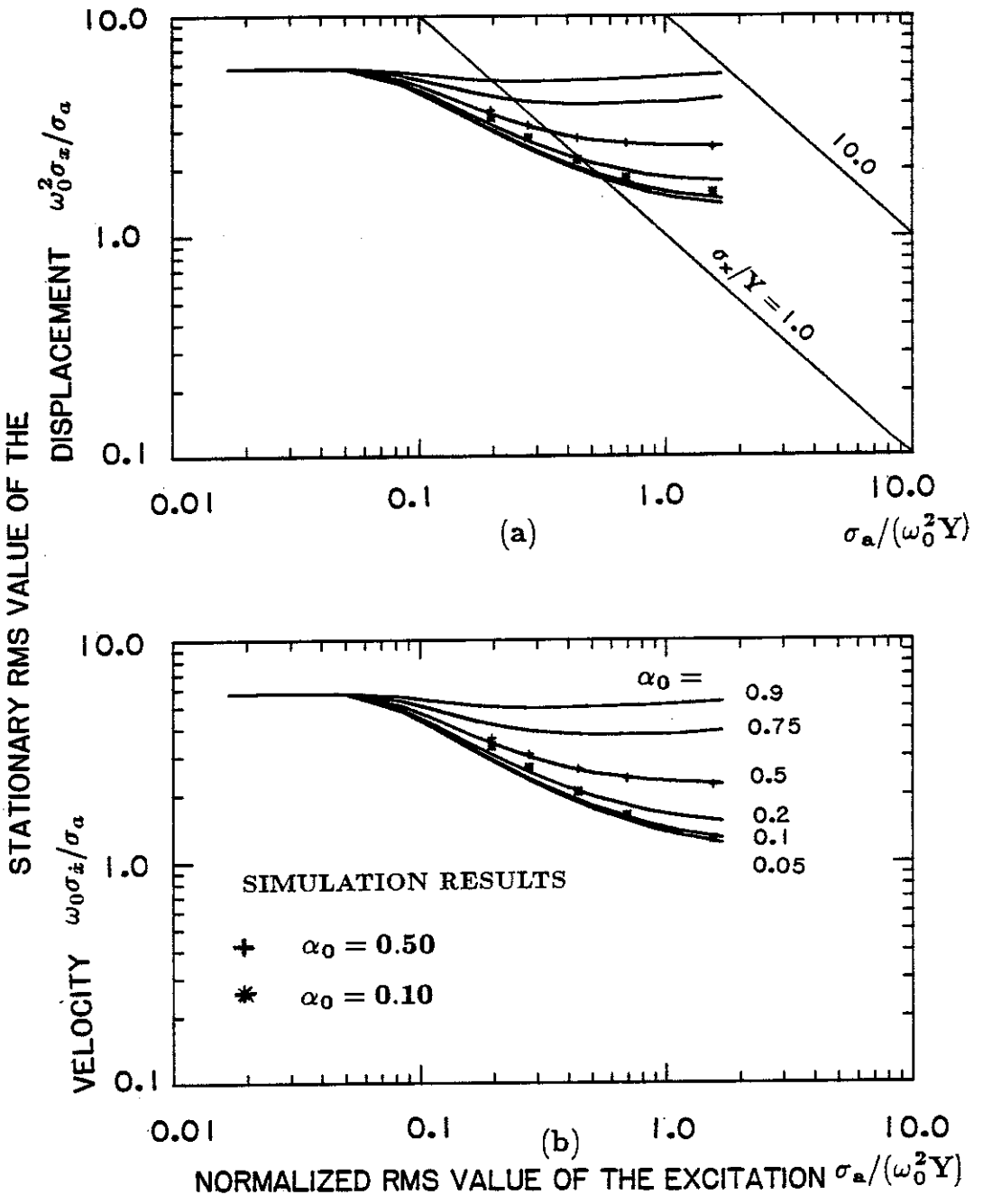

Figure 3.5
Dependence of the Stationary RMS response levels on the strength of the excitation and α_0, for bandwidth of the excitation, ζ_g=0.10, and for ω_g/ω_0=1.0 and ζ=0.05. (a) Displacement response. (b) Velocity response.

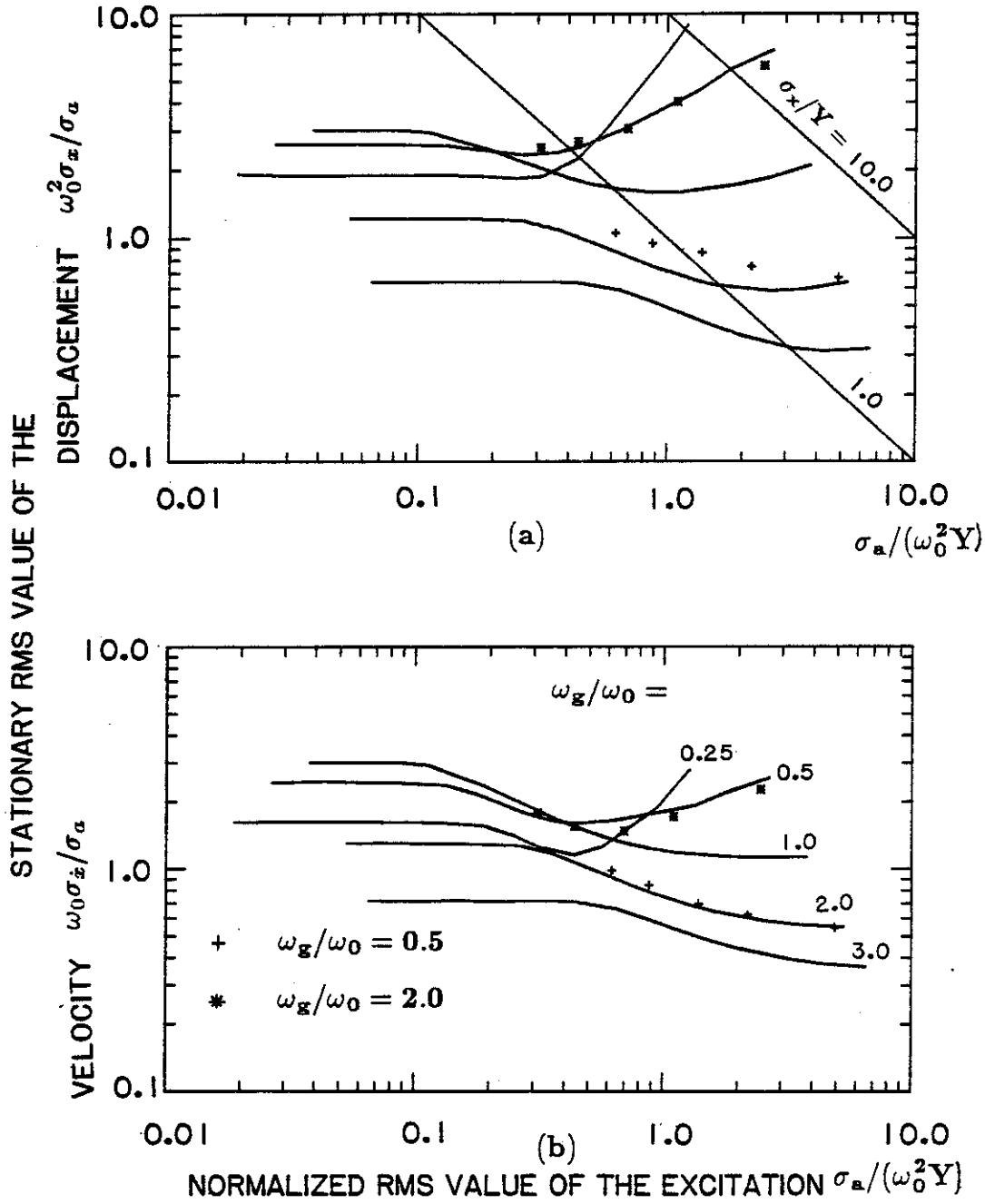

Figure 3.6
Dependence of the Stationary RMS response levels on the strength and characteristic frequency of the excitation. $\alpha_0 = 0.10$, ζ_g=0.50 and ζ=0.05. (a) Displacement response. (b) Velocity response.

for the displacement and velocity response predicted by the approximate solution are in very good agreement with the simulation data, even for small values of α_0, and for the whole range of inelastic response. Less accurate estimates are obtained for the displacement statistics and for cases corresponding to $\omega_g/\omega_0 > 1$. But even in these cases the maximum error is 25 percent, which implies that equivalent linearization, presented in Section 3.3, can be succesfully used in the prediction of second-order response statistics for the bilinear hysteretic system.

In Figure 3.7b, a comparison between the RMS value of the displacement response of a bilinear hysteretic system and a smooth multilinear hysteretic system, is presented. The restoring force of the related hysteretic systems are illustrated in Figure 3.7a. It can be noticed that equivalent linearization gives even better results for the case of a multilinear hysteretic system. As expected, the bilinear hysteretic systems gives the asymptotic behaviour of the multilinear hysteretic system for cases corresponding to elastic and strong inelastic response.

3.5 Comparison between second- and third-order equivalent linear systems.

Consider the bilinear hysteretic system illustrated in Figure 3.1, for which the equation of motion is given by

$$\ddot{x} + 2\zeta\omega_0\dot{x} + f(x,\dot{x},t) = \eta(t), \tag{3.26a}$$

where $\eta(t)$ is a white noise excitation, with autocorrelation function given by

$$E[\eta(t)\eta(t+\tau)] = S_0\delta(\tau), \tag{3.26b}$$

and $f(x,\dot{x},t)$ is the normalized hysteretic restoring force. By applying the Krylov-Bogoliubov method of equivalent linearization, Caughey (43), derived an analytical expression for the parameters ω_{eq} and ζ_{eq}, of a second-order equivalent linear system.

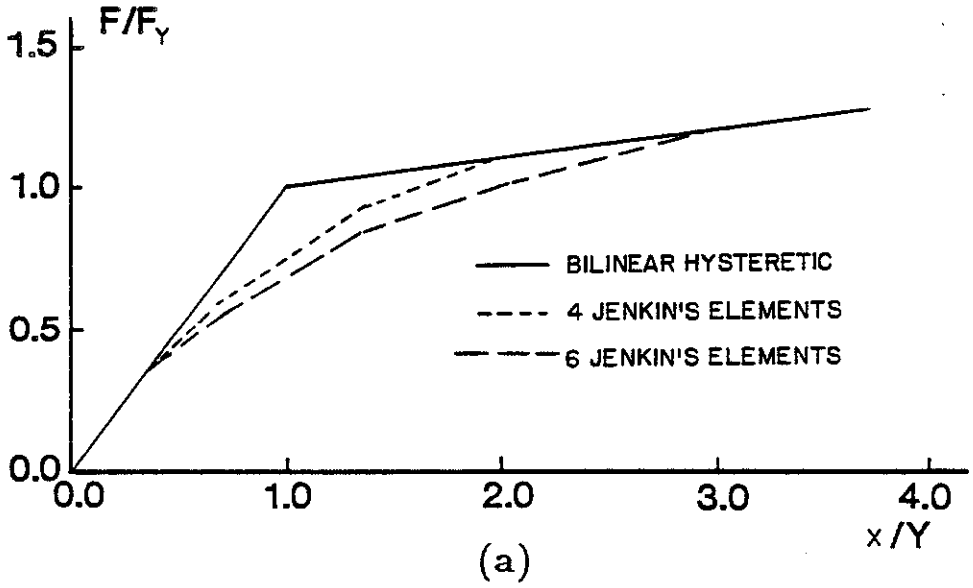

(a)

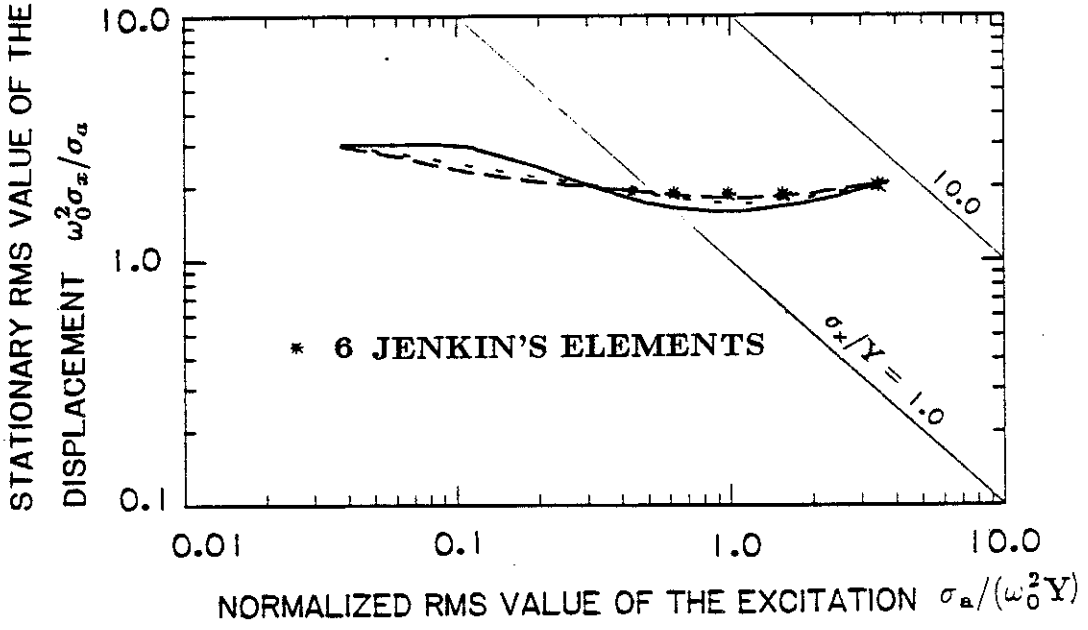

(b)

Figure 3.7
Comparison of the Stationary RMS response levels of a bilinear and multilinear hysteretic system. (a) Force-deflection diagram of the examined models. (b) Displacement response.

The equation of motion of the second-order equivalent linear system is given by

$$\ddot{x} + 2\zeta_{eq}\omega_{eq}\dot{x} + \omega_{eq}^2 x = \eta(t), \tag{3.27a}$$

with

$$\left(\frac{\omega_{eq}}{\omega_0}\right)^2 = 1 - \left[\frac{8(1-\alpha_0)}{\pi}\right]\int_1^\infty (z^{-3} + (\lambda z)^{-1})(z-1)^{1/2} e^{-z^2/\lambda} dz \tag{3.27b}$$

and

$$\zeta_{eq} = \zeta(\omega_0/\omega_{eq}) + (\omega_0/\omega_{eq})^2(1-\alpha_0)(\pi\lambda)^{-1/2}\mathrm{erfc}(\lambda^{-1/2}). \tag{3.27c}$$

The parameter λ is expressed in terms of the stationary RMS value of the displacement response, σ_x^2, or

$$\lambda = 2\sigma_x^2/Y^2. \tag{3.27d}$$

Iwan and Lutes (44) showed that in the case of a nearly elasto-plastic system, or $\alpha_0 = 1/21$, the second-order equivalent linear system is not able to accurately predict the displacement statistics. It was suggested that for an elasto-plastic system, the drift component of the response can not be modeled by a second-order linear system. In Figure 3.8, the stationary RMS values of the displacement response, obtained by the equivalent linearization described in Section 3.3, are compared with numerical simulation results, and with the correponding approximate solution of equation (3.27). It can be noted that for values of σ_x/Y between $(0.0, 0.4)$, the third order equivalent linear system gives similar results to the second order system. For higher values of σ_x/Y, though, the results of the third order system are more accurate.

In Figure 3.9, the power spectral density of the response predicted by the second- and third-order equivalent linear systems is compared with the corresponding numerical simulation results. Recall that for a second-order equivalent

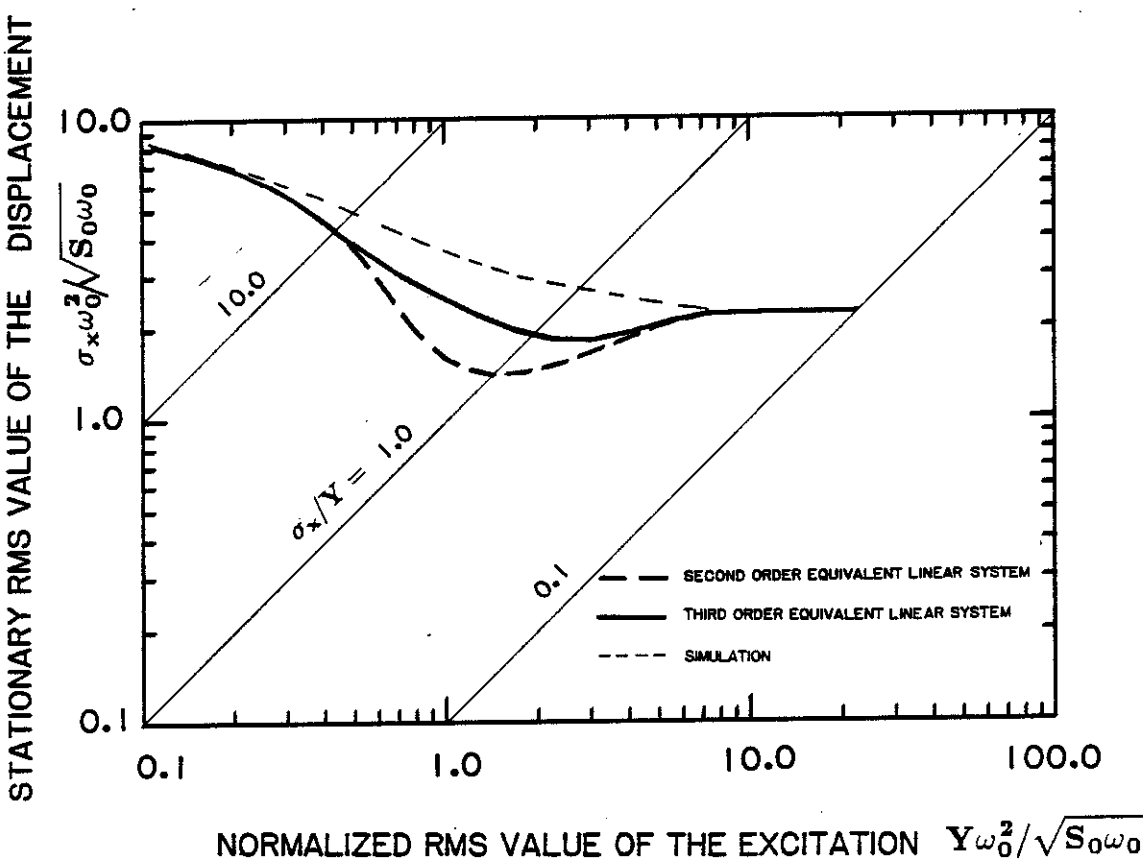

Figure 3.8
Comparison of the RMS value of the displacement response obtained by the second- and third-order equivalent linearization. Bilinear hysteretic model subjected to white noise excitation, α_0=1/21 and ς=0.05.

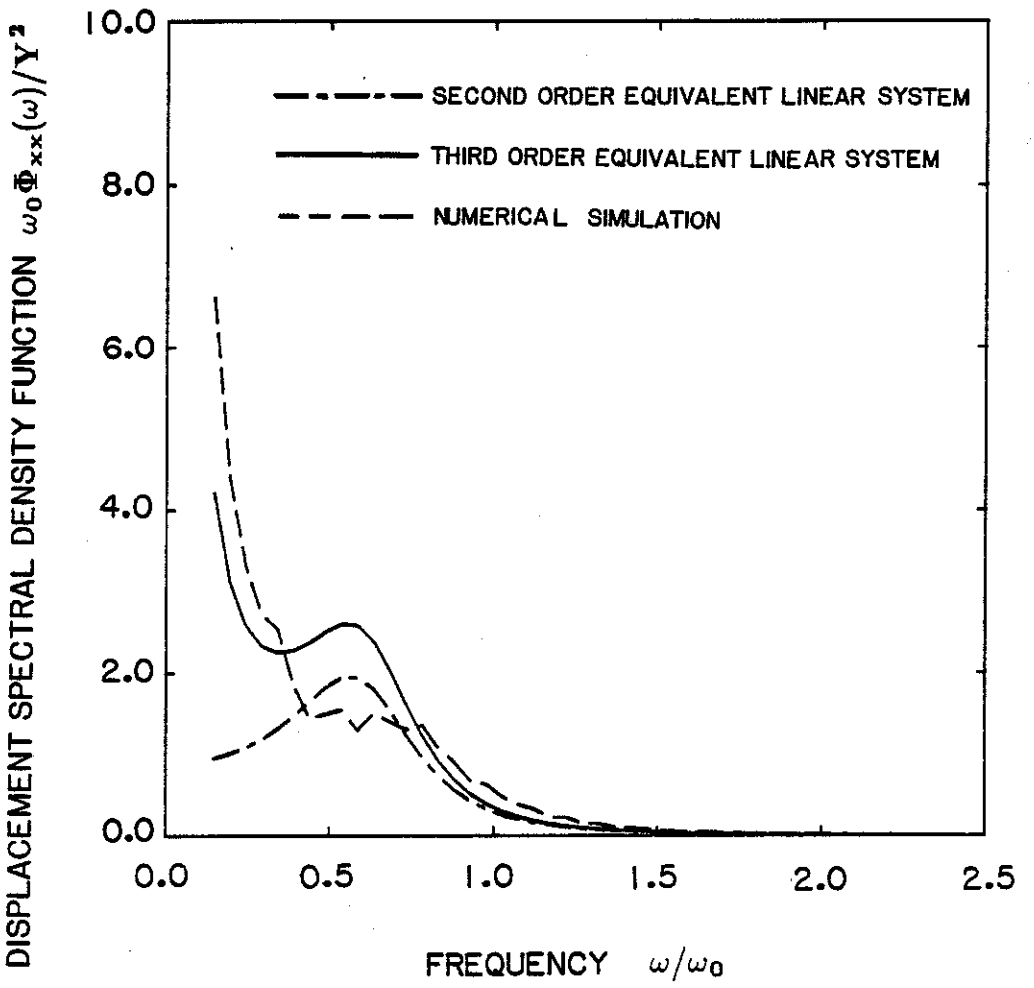

Figure 3.9
Spectral density function of the displacement response. Bilinear hysteretic system subjected to white noise excitation, S_0=1.0, ζ=0.05 and α_0=0.10. Comparison of the approximate results obtained by second- and third-order equivalent linearization with numerical simulation results.

linear system, subjected to white noise excitation, the power spectral density function of the displacement response is given by

$$\Phi_{xx}(\omega) = \frac{S_0}{(2\pi)} \frac{1}{(\omega_{eq}^2 - \omega^2)^2 + 4\zeta_{eq}^2 \omega_{eq}^2 \omega^2}. \tag{3.28}$$

By applying the results derived in Appendix B, an expression for $\Phi_{xx}(\omega)$ for the case of the third-order linear system is obtained as

$$\Phi_{xx}(\omega) = \frac{S_0}{2\pi(R_x^2 + I_x^2)}, \tag{3.29a}$$

with

$$R_x = (\alpha_0 \omega_0^2 - \omega^2) + \omega^2 \omega_0^2 \frac{(1-\alpha_0) C_2 C_4}{\omega^2 + C_3^2} \tag{3.29b}$$

$$I_x = \omega \left[2\zeta + (1-\alpha_0)\omega_0^2 C_1 - \omega_0^2 \frac{(1-\alpha_0) C_2 C_3 C_4}{\omega^2 + C_3^2} \right]. \tag{3.29c}$$

From the results presented in Figure 3.9, it can be concluded that the third-order linear system gives a much better approximation for the frequency content of the displacement response. The two peaks structure of the power spectral density, $\Phi_{xx}(\omega)$, should be attributed to the elastic component of the displacement and to the drift of the hysteretic system.

The analysis presented in this section indicates that the second moments of response are not sufficient for the description of hysteretic behaviour. In particular, is suggested that for large inelastic response, the drift of hysteretic systems becomes the most significant response variable. This implies that for a better understanding of hysteretic behaviour, the dependence of the drift on system and excitation parameters should be examined. In Section 3.6, the drift is defined for the case of a bilinear hysteretic system, while in Section 3.7 a detailed examination of the frequency content of the hysteretic response is presented. Finally, in Chapters 4 and 5, the random response of an elasto-plastic system is examined by formulating the problem in terms of the drift process.

3.6 Drift of a bilinear hysteretic system.

For the bilinear hysteretic system illustrated in Figure 3.1, the drift, $z(t)$, is defined as

$$z(t) = x(t) - y(t). \tag{3.30}$$

Because equivalent linearization described in Section 3.3 is formulated in terms of the elastic component of the displacement, $y(t)$, second-order statistics for the drift, $z(t)$, can be obtained from the response statistics of the variable x and y. Recall that $y(t)$ is given by

$$y(t) = g_1(\phi(t), \dot{x}(t), Y) \tag{3.31}$$

with g_1 defined by equation (2.6c). By substituting equation (3.31) into (3.30), the following expressions for the mean and the mean square value of the drift are obtained:

$$E[z(t)] = 0 \tag{3.32a}$$

and

$$\sigma_z^2 = E[z^2] = E[x^2] - 2E[xg_1(\phi, \dot{x}, Y)] + E[g_1^2(\phi, \dot{x}, Y)]. \tag{3.32b}$$

Numerical results for the transient RMS value of the drift obtained from equation (3.32b), are illustrated in Figure 3.10. A very good agreement between the approximate results and the simulation data is noticed. From the results presented in Section 3.5, it can also be concluded that in the case of white noise excitation, the low frequency content of the displacement response is predicted by equivalent linearization. This implies that for white noise excitation, the second moments and the frequency content of the drift response are accurately predicted by the third-order equivalent linear system. A more detailed discussion on this issue is presented in Section 3.7.

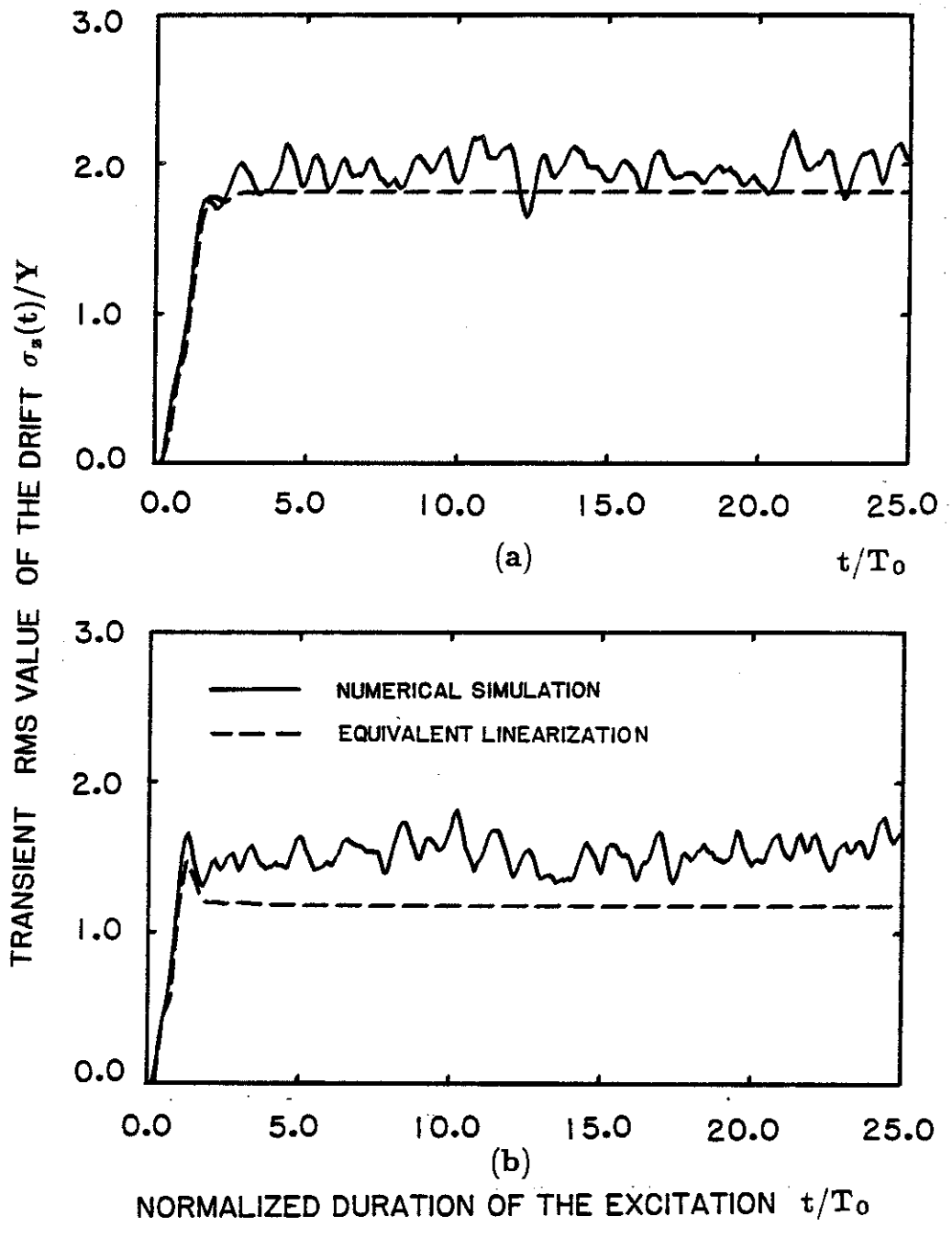

Figure 3.10
Transient RMS value of the drift response. Bilinear hysteretic system, S_0=2.0, ς_g=0.50, α_0=0.10 and ς=0.05. (a) ω_g/ω_0=0.50 (b) ω_g/ω_0=1.0.

3.7 On the frequency content of the displacement response.

In Section 3.3, an expression for the spectral density function of the displacement response of a multilinear hysteretic system, was obtained for the excitation model described by equation (2.27). In the particular case of a bilinear hysteretic system, equation (3.20), becomes

$$\Phi_{xx}(\omega) = \frac{S_0}{(2\pi)} \frac{4\zeta_g^2\omega_g^2\omega^2}{(\omega_g^2-\omega^2)^2+4\zeta_g^2\omega_g^2\omega^2} \frac{1}{(R_x^2+I_x^2)}, \tag{3.33}$$

with R_x and I_x, given by equation (3.29b) and (3.29c). A comparison with simulation data for Φ_{xx} is illustrated in Figure 3.11 for the case $\omega_g/\omega_0 = 0.50$, $S_0 = 2.0$ and bandwidth of excitation $\zeta_g = 0.50$. In contrast with the case of white noise excitation, it can be noticed that the third-order equivalent linear system is not able to predict the low frequency content of the displacement response, corresponding to the drift of the system.

This observation can be generalized for excitation models satisfying

$$\Phi_{aa}(0) = 0. \tag{3.34a}$$

From equation (3.29), it is implied that the zero frequency content of the displacement response of the equivalent linear system is given by

$$\Phi_{xx}(0) = \frac{\Phi_{aa}(0)}{\alpha_0^2}. \tag{3.34b}$$

Hence, for $\Phi_{aa}(0) = 0$ and from equation (3.34b), it is implied that $\Phi_{xx}(0) = 0$. From the simulation results presented in Figures 3.9 and 3.11, it can be concluded that the low frequency content of the displacement response is nonzero, regardless of the seismic excitation model. Because the ground motion acceleration spectrum satisfies equation (3.34a), it is also implied that equivalent linearization cannot be used for the prediction of the low frequency content of the displacement response of hysteretic structural systems.

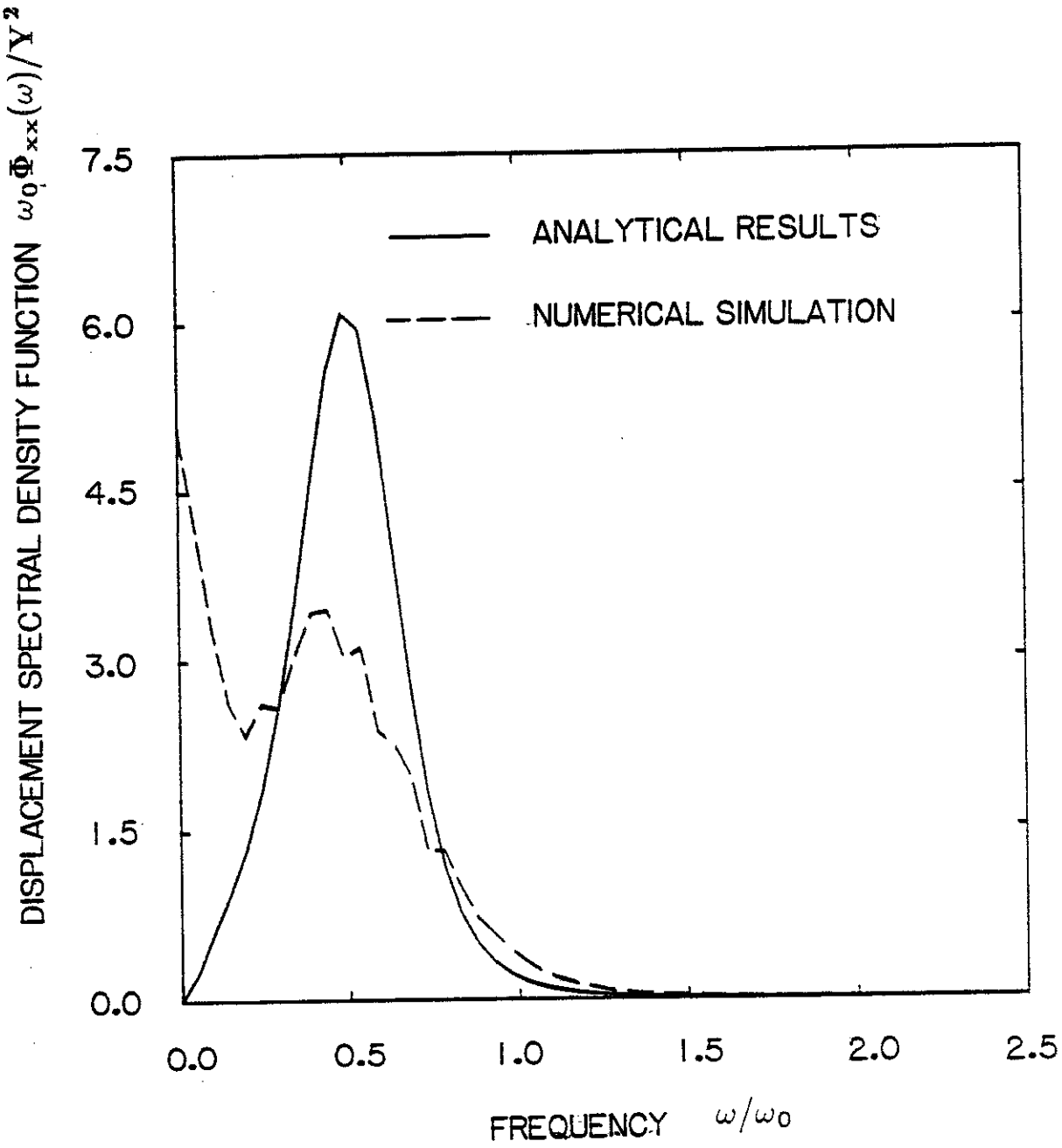

Figure 3.11
Spectral density function of the displacement response, for an excitation with no zero frequency content. S_0=2.0, ς=0.05, α_0=0.10 and ω_g/ω_0=0.50.

Finally, in Figure 3.12, a numerical simulation study of the influence of the excitation frequency content on the displacement response of a bilinear hysteretic system is presented. The two excitation models used in this study are described by the same RMS value and characteristic frequency at $\omega_g/\omega_0 = 1.0$. It can be noted that the low frequency content of the excitation has a significant influence on the drift response. The model A is the Kanai-Tajimi filter, often used in the modeling of the seismic excitation. As mentioned in Section 2.3, the Kanai-Tajimi filter does not accurately represent the low frequency content of the ground motion acceleration spectrum. In contrast, the excitation model B, is also obtained by filtering a white noise signal through a second order linear filter (equation 2.27), but satisfies the condition $\Phi_{aa}(0) = 0$. Based on this observation, it is suggested that the excitation model B should be used in the analysis of hysteretic structural response to earthquake excitation.

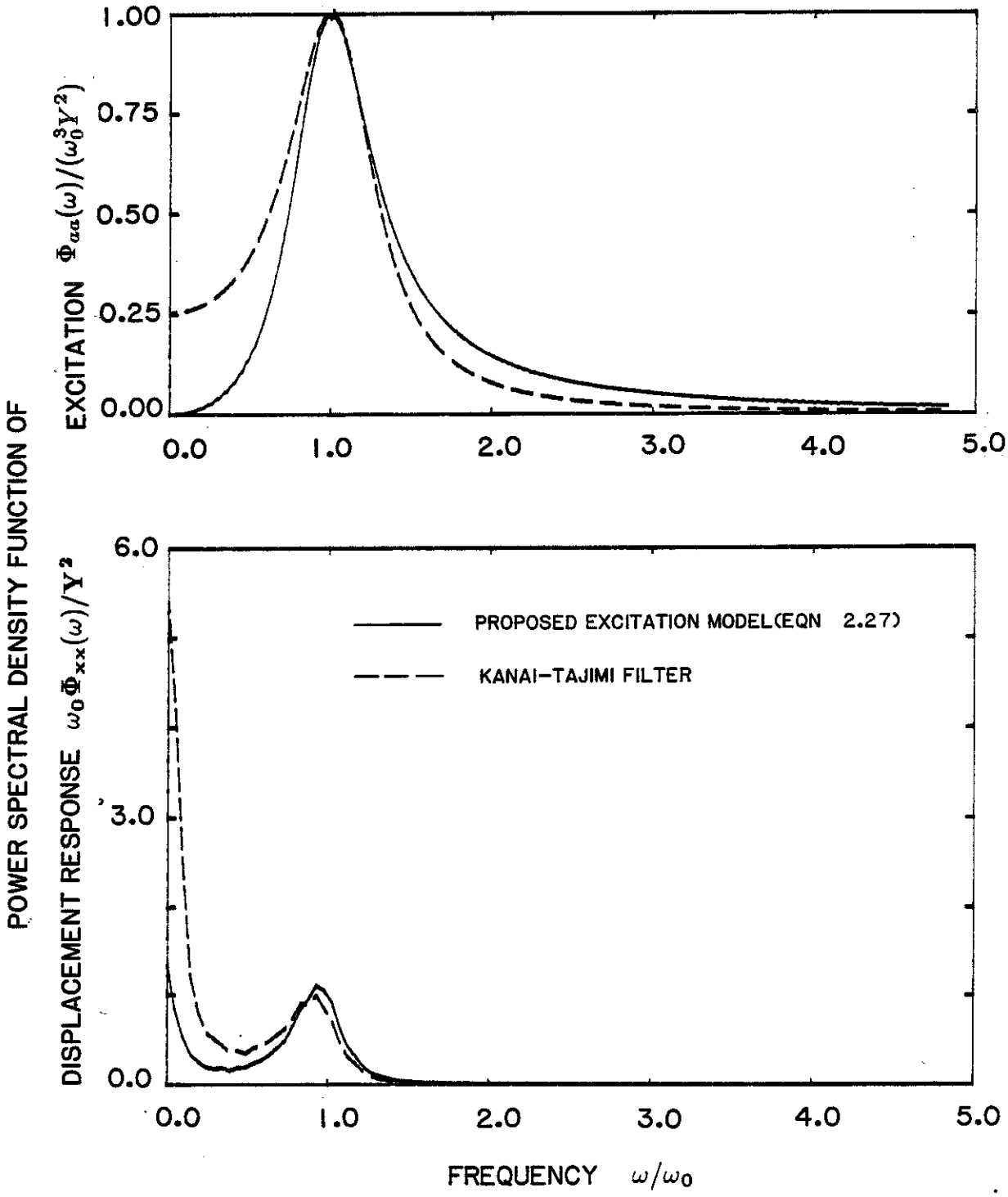

Figure 3.12
The influence of excitation low frequency content on the drift response of a bilinear hysteretic system. α_0=0.10 and ς=0.05. Comparison between Kanai-Tajimi filter and the proposed excitation model (numerical simulation).

3.8 Concluding remarks.

In this chapter, the response of a multilinear hysteretic system to stochastic seismic excitation was examined. It was concluded that the second-order displacement and velocity response statistics can be accurately predicted by equivalent linearization, for the case of strictly positive parameters α_0, $(\alpha_i \; i = 1, ..., n)$. The good agreement between the approximate results and the numerical simulation results was noticed for a broad range of excitation and system parameters.

The equivalent linearization used in this chapter was also compared to the second order equivalent linearization, introduced by Caughey. It was shown that the transfer function of the higher order linear system is able to represent the peak frequencies associated with the elastic component and the drift of the displacement response. Nevertheless, for excitation models characterized by no zero frequency content, it was shown that the response frequency content cannot be modeled by any equivalent linear system with a bounded transfer function. This suggests that the drift represents a characteristic feature of the hysteretic response behaviour, and that for a better understanding of the process, further investigation is required. To this end, the analysis presented in Chapters 4 and 5 is related to the formulation of the hysteretic response in terms of the drift process.

Chapter 4. THE ELASTIC, PERFECTLY PLASTIC SYSTEM.

4.1 Introduction.

In Chapter 3 a general class of hysteretic systems was examined. It was shown that for a multilinear hysteretic system and for strictly positive model parameters α_0, $(\alpha_i,\ i = 1, ..., n)$ in the constitutive equation (2.10), the second moments of the displacement and velocity response can be accurately predicted with the use of the equivalent linearization technique. The drift component of the displacement was defined for the case of a bilinear hysteretic system and it was concluded that the equivalent linear system cannot predict the frequency content of the drift response for the case of a stationary excitation with no zero frequency content. The analysis presented in Section 4.3 will show that for the same class of excitation models, and in the limiting case corresponding to $\alpha_0 = 0$, equivalent linearization fails to predict the nonstationarity of the displacement response. This suggests that the nature of the drift can not be explained in terms of an equivalent linear system and that for a better understanding of the process further investigation is required.

In this chapter, the random response of the elastic, perfectly plastic system is examined. By considering the drift as the sum of yield increments associated with the inelastic response, the problem can be formulated in terms of the yield increment process, as will be shown in Section 4.4. It will be concluded that an exact diffusion equation for the process cannot be obtained. For this reason, discrete Markov process models for the drift of an elasto-plastic system are introduced in Section 4.5. These models give a physical interpretation for the process, while providing information regarding the response statistics and a measure of structural safety in terms of survival probabilities for type-D barrier crossings. Although defined for the random response of the elasto-plastic system,

they also offer the basis for the understanding of hysteretic response behaviour in general.

In Section 4.6, the analytical results predicted by the discrete Markov process models are compared with Monte Carlo simulation results. It will be concluded that even if the probabilistic structure of the yield increment process is extremely complex, for long duration of the stationary excitation the drift statistics can be obtained using the properties of the simplified discrete Markov processes. A discussion of this issue is presented in Section 4.7.

4.2 Equation of motion.

For the case of an elastic, perfectly plastic system, illustrated in Figure 4.1, subjected to the stochastic seismic excitation model defined by equation (2.27), the equations of motion (2.6) and (2.27) are reduced to the form

$$\ddot{x} + 2\zeta\omega_0\dot{x} + \omega_0^2 g_1(\phi, \dot{x}, Y) = 2\zeta_g\omega_g\dot{x}_g \tag{4.1a}$$

$$\dot{\phi} = g_2(\phi, \dot{x}, Y) \tag{4.1b}$$

$$\ddot{x}_g + 2\zeta_g\omega_g\dot{x}_g + \omega_g^2 x_g = e(t)\xi(t), \tag{4.1c}$$

with initial conditions

$$x(0) = \dot{x}(0) = \phi(0) = x_g(0) = \dot{x}_g(0) = 0. \tag{4.1d}$$

In Appendix B it is shown that by an appropriate change of variables, a normalized excitation peak frequency, ω_g', normalized time, τ, ductility ratio, μ_x, and normalized RMS value of the excitation, σ_a', can be defined as follows

$$\omega_g' = \frac{\omega_g}{\omega_0} \tag{4.2a}$$

$$\tau = \omega_0 t \tag{4.2b}$$

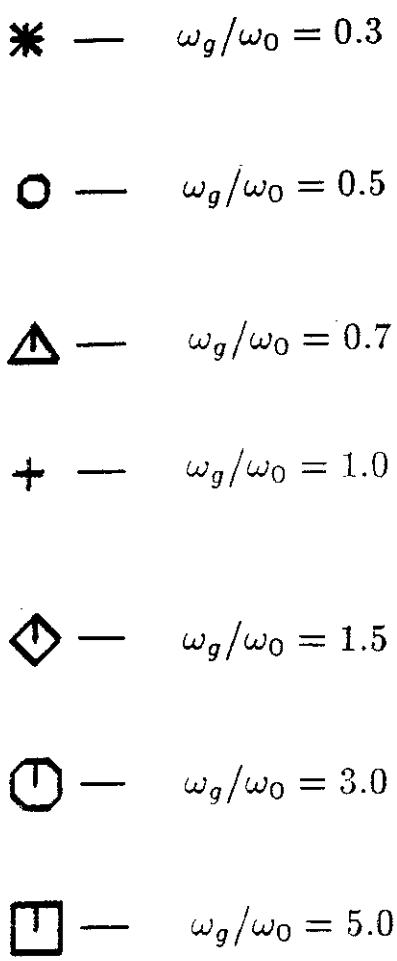

Figure 4.0
Legend of the numerical simulation data for the response statistics of an elasto-plastic system.

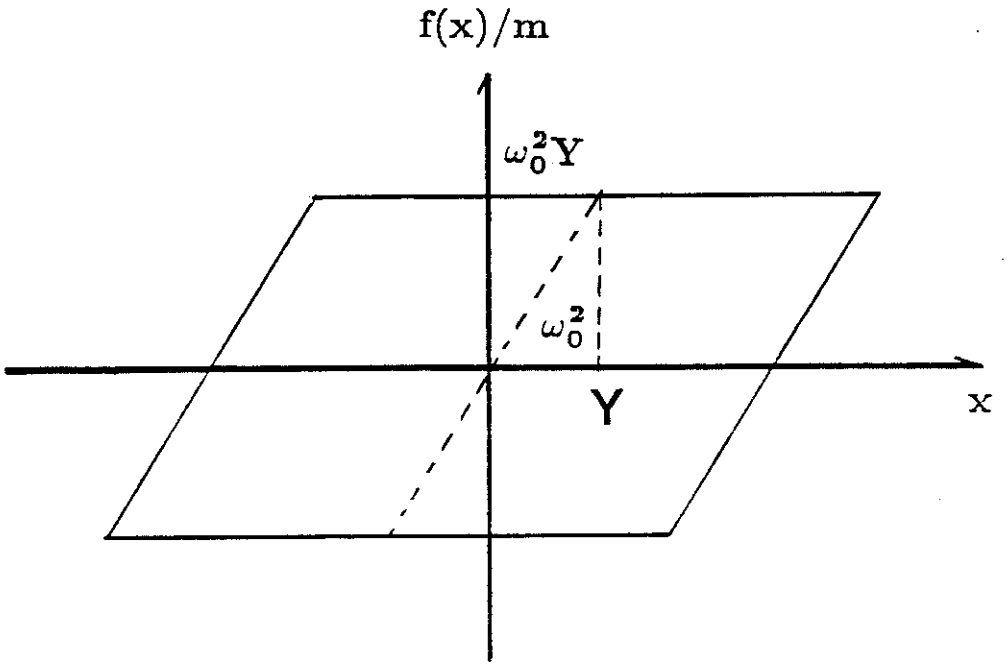

Figure 4.1
The elasto-plastic system.

$$\mu_x = \frac{x}{Y} \tag{4.2c}$$

and

$$\sigma'_a = \frac{\sigma_a}{\omega_0^2 Y} = \frac{\sqrt{S_0 \omega_g \zeta_g}}{\omega_0^2 Y}. \tag{4.2d}$$

Without loss of generality, the analysis for the elastic, perfectly plastic system governed by equation (4.1) is based on the normalized system corresponding to parameters values

$$Y = 1 \qquad \text{and} \qquad \omega_0 = 1, \tag{4.3}$$

while the results obtained are given in terms of the dimensionless groups defined by (4.2).

4.3 Equivalent linear system.

4.3.1 Formulation.

Following the procedure developed in Chapter 3, an equivalent linear system associated to the elasto-plastic system governed by equation (4.1), can be defined. It should be pointed out that the normalized restoring force in (4.1a) does not depend on the displacement x. This implies that the stochastic differential equation (3.2) for the response vector $\mathbf{u}$ represents a set of uncoupled equations, corresponding to the linear equation

$$\dot{u}_1 = a_1(\mathbf{u}) = u_2 \tag{4.4a},$$

and the nonlinear stochastic differential equation

$$\dot{u}_i = a_i(u_2, u_3, u_4, u_5) + e(t) w_i(t) \quad \text{for } i = 2, ..., 5, \tag{4.4b}$$

with

$$\begin{aligned} a_2(\mathbf{u}) &= -2\zeta u_2 + 2\zeta_g \omega_g u_5 - g_1(u_3, u_2, 1) \\ a_3(\mathbf{u}) &= g_2(u_3, u_2, 1) \\ a_4(\mathbf{u}) &= u_5 \\ a_5(\mathbf{u}) &= -2\zeta_g \omega_g u_5 - \omega_g^2 u_4 \end{aligned} \tag{4.5}$$

and g_1, g_2 defined by (2.6). Because equation (4.4b) does not depend on u_1, the parameters of the equivalent linear system C_{11}, C_{21}, C_{31}, C_{41}, are determined only by the response statistics of the variables (u_2, u_3, u_4, u_5) and are given by equations (3.14)-(3.17). This suggests that for an elasto-plastic system, the covariance matrix for the response variables $(\dot{x}, \phi, x_g, \dot{x}_g)$ can be obtained independently of the response statistics related to the displacement x.

4.3.2 Comparison of the approximate results to numerical simulation results.

In Figure 4.2, the results for the mean square value displacement and velocity response obtained by the equivalent linearization technique are compared with the corresponding simulation results obtained from a set of 250 samples, for the case $\omega_g = 1$, $\zeta_g = .50$, $\zeta = 0.01$ and S_0=0.40. The two sets of results seem to agree with respect to the velocity response statistics, while for the case of the mean square value displacement, equivalent linearization is not able to predict the divergent response behaviour. Instead, the solution for the equivalent linear system exhibits stationary behaviour. This kind of result is typical for the case of the excitation model defined by (2.27), corresponding to an excitation with zero low frequency content, as will be shown in Section 4.3.3.

In Figures 4.3a, 4.3b, a parametric investigation for the stationary RMS value of the velocity response is shown. The results obtained by equivalent linearization are compared with numerical simulations for the case $\zeta = 0.01$, and for $\zeta_g = 0.50$ and 0.25 respectively. From this analysis, it appears that the equivalent linearization technique can be used only for the calculation of the velocity response statistics.

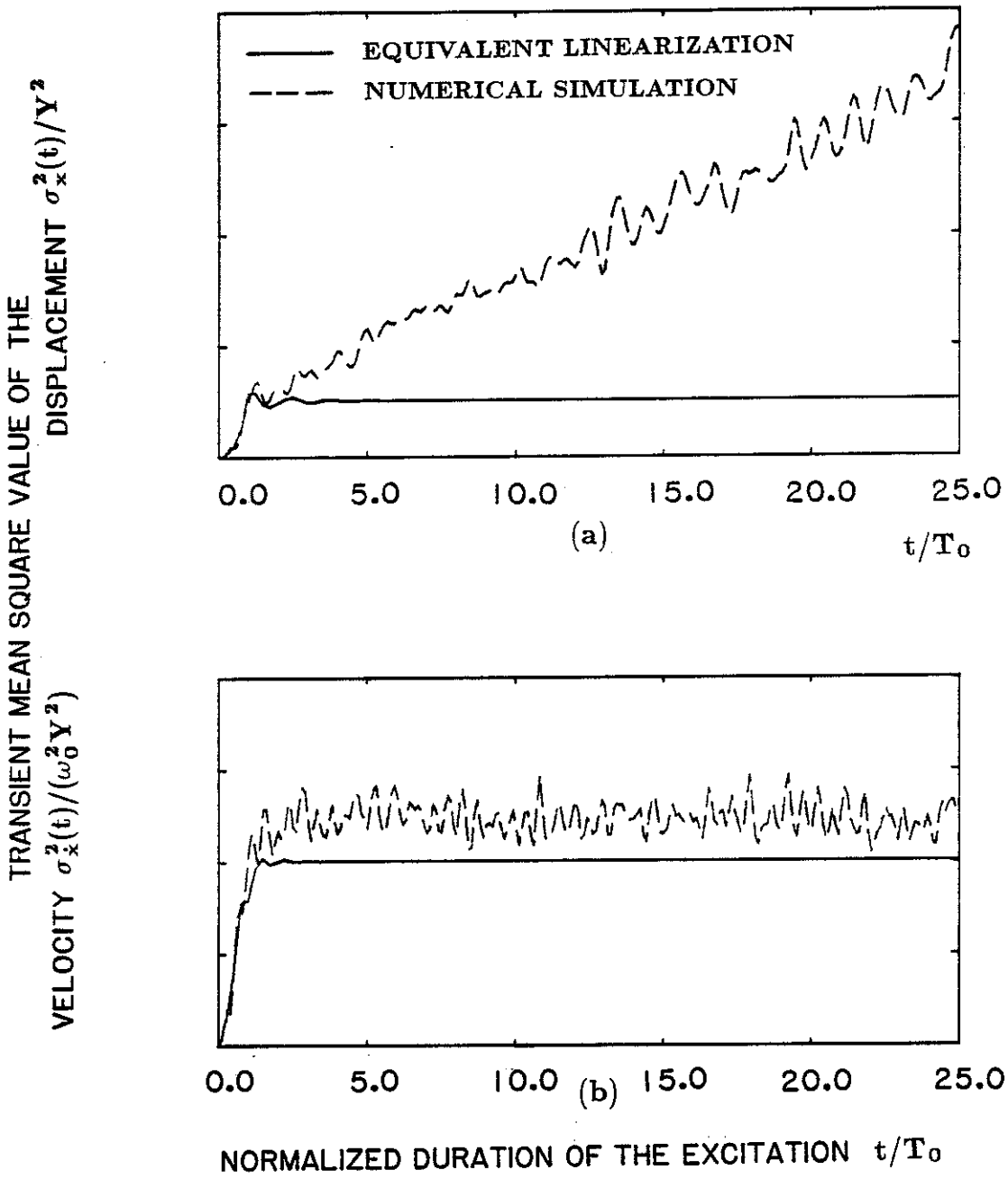

Figure 4.2
Nonstationary Covariance of the response of an elasto-plastic system. Equivalent linearization cannot predict the linearly divergent covariance of the displacement response, if the acceleration spectrum satisfies the condition $\Phi_{aa}(0)=0$. $S_0=0.40$, $\varsigma_g=0.50$, $\omega_g/\omega_0=1.0$ and $\varsigma=0.01$. (a) Displacement response. (b) Velocity response.

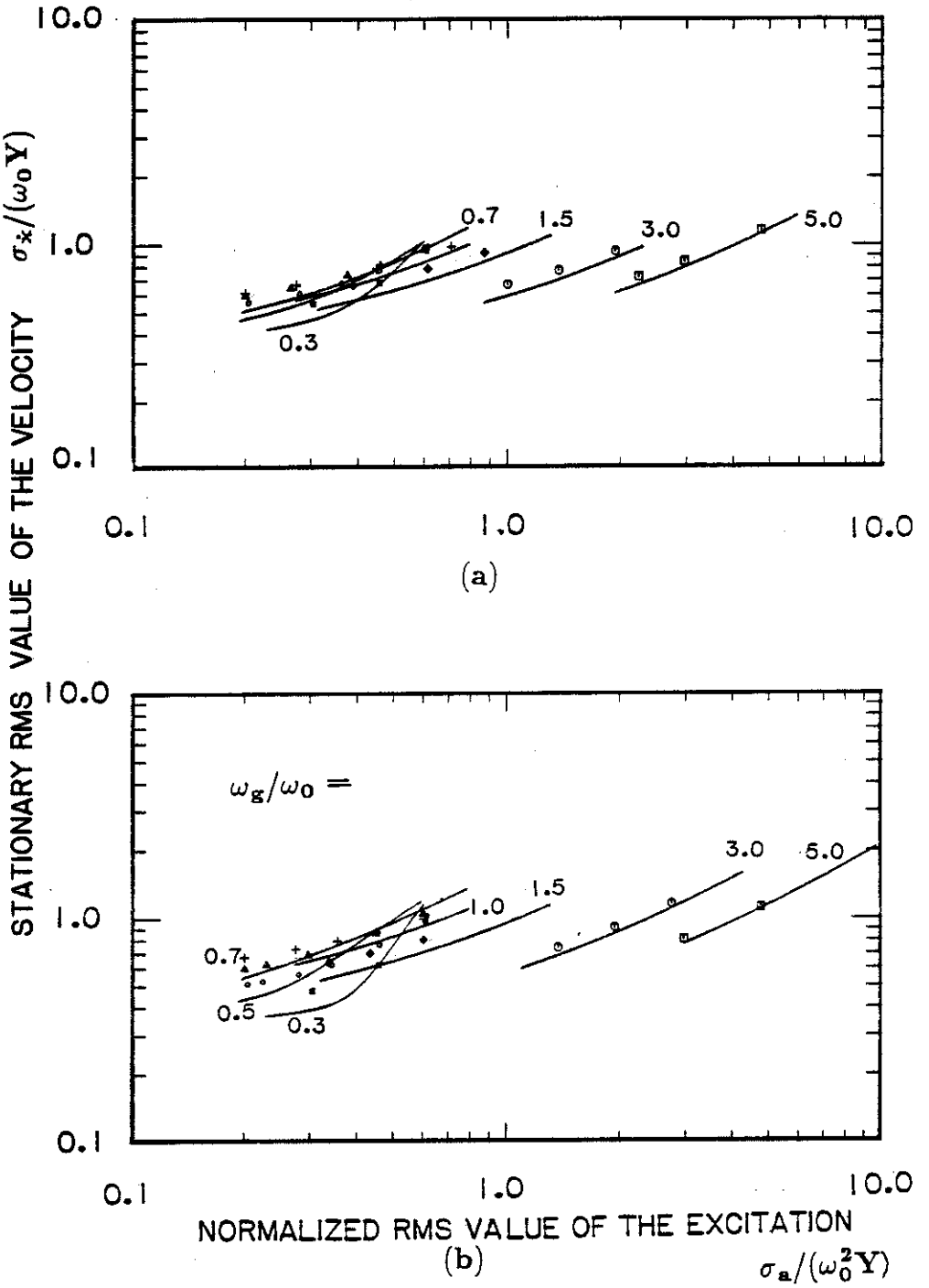

Figure 4.3
Parametric investigation for the stationary RMS value of the velocity response. Bandwidth of the excitation (a) ζ_g=0.50 (b) ζ_g=0.25. Legend of the simulation data given in Figure 4.0.

4.3.3 Interpretation of results.

Consider a two-dimensional stochastic process $(x, \dot{x})$, for which $\dot{x}$, the time derivative of the process x, is a stationary stochastic process with spectral density function $\Phi_{\dot{x}\dot{x}}(\omega)$. Then for $t \to \infty$ the following asymptotic expression for the mean square value of the process x is obtained (Crandall, Lee, Williams (45)):

$$\sigma_x^2(t) \asymp 2\pi\Phi_{\dot{x}\dot{x}}(0)t \qquad \text{as } t \to \infty. \tag{4.6}$$

Following the calculations performed in Appendix A, an expression for the spectral density function of the velocity response, $\dot{x}$, of the equivalent linear system can be derived. In the case of an elasto-plastic system with $\alpha_0 = 0$ and $n = 1$, this expression is

$$\Phi_{\dot{x}\dot{x}}(\omega) = \Phi_{aa}(\omega)\frac{1}{R_{\dot{x}}^2 + I_{\dot{x}}^2}, \tag{4.7a}$$

where $\Phi_{aa}(\omega)$ is the spectral density function for the stationary excitation process $\tilde{a}(t)$. $R_{\dot{x}}$ and $I_{\dot{x}}$ are given by

$$R_{\dot{x}} = \omega\left[\frac{C_{21}C_{41}}{\omega^2 + C_{31}^2} - 1\right] \tag{4.7b}$$

$$I_{\dot{x}} = 2\zeta + C_{11} - \frac{C_{21}C_{31}C_{41}}{\omega^2 + C_{31}^2}. \tag{4.7c}$$

For $\omega = 0$, substituting (4.7) into (4.6) yields

$$\sigma_x^2(t) \asymp 2\pi\frac{\Phi_{aa}(0)}{(2\zeta + C_{11} - C_{21}C_{41}/C_{31})^2}t \qquad \text{as } t \to \infty. \tag{4.8}$$

This implies that equivalent linearization predicts a linear divergent behaviour for the mean square value of the displacement only in the case of an excitation with $\Phi_{aa}(0) \neq 0$. Monte Carlo simulation results and the analysis presented in the following sections suggest that the linear divergent behaviour for the mean square value of the drift is a property of the elasto-plastic system subjected to

stationary stochastic excitation, and is not dependent upon the frequency content of the excitation. This implies that for long duration seismic excitation, in which the acceleration spectrum satisfies the condition $\Phi_{aa}(0) = 0$, the equivalent linearization results cannot be used for the calculation of the mean square value displacement and drift response. It is also implied that the drift of a hysteretic system can not be explained in terms of an associated linear system and further investigation is required for understanding the drift process.

Finally, as suggested in Section 4.3.2, the response statistics for the variables $(\dot{x}, \phi)$ are accurately predicted by equivalent linearization. This can be viewed as a consequence of the fact that the equation of motion represents a set of uncoupled equations for which the response statistics of the variables $(\dot{x}, \phi)$ possess a stationary solution and are independent of the response statistics associated with the displacement response x.

4.4 Formulation in terms of the drift process.

4.4.1 On the relationship between drift and yield increment process.

In section 4.3 it was shown that the statistics for the drift component of the response of an elasto-plastic system subjected to stochastic excitation cannot be predicted by an associated linear system and that for a better understanding of the hysteretic response behaviour, the nature of the drift of hysteretic systems should be examined. The objective of this section is to formulate the problem in terms of the drift component of the displacement response and to discuss the related diffusion equation.

Consider an elasto-plastic system subjected to a zero mean stationary Gaussian stochastic excitation, $\tilde{a}(t)$. Such a system and the corresponding normalized restoring force are illustrated in Figure 4.1. Without loss of generality, consider the simplified case corresponding to $\omega_0 = 1$ and $Y = 1$, for which case the

equation of motion is given by

$$\ddot{x} + 2\zeta\dot{x} + y = -\ddot{a}(t) \tag{4.9a}$$

and

$$\dot{y} = \dot{x}g(y), \tag{4.9b}$$

where y is the elastic component of the response, ζ accounts for the additional viscous damping, while $g(y)$ is given by

$$g(y) = \begin{cases} 0 & \text{if } |y| = 1 \text{ and } y\dot{x} > 0; \\ 1 & \text{otherwise.} \end{cases} \tag{4.9c}$$

For such a system, the drift, z, is defined as the inelastic component of the response, or

$$z = x - y. \tag{4.10}$$

A time history sample of $z(t)$ is illustrated in Figure 4.4 for the model parameter values $S_0 = 0.40$, $\omega_g = 1.0$, $\zeta_g = 0.50$ and $\zeta = 0.01$. It can be noticed that the drift response exhibits three distinct types of behaviour, associated with elastic response and yielding in the positive and negative direction, respectively. The three states S_1, S_2, S_3 so defined are illustrated in Figure 4.5 and correspond to the elastic state S_3, or

$$S_3 = \{(x, \dot{x}, y) |\ \ni\ |y| < 1\ \}, \tag{4.11a}$$

the plastic state S_1, associated with yielding in the positive direction, or

$$S_1 = \{(x, \dot{x}, y) |\ \ni\ y = 1\ \}, \tag{4.11b}$$

and S_2 corresponding to yielding in the negative direction, or

$$S_2 = \{(x, \dot{x}, y) |\ \ni\ y = -1\ \}. \tag{4.11c}$$

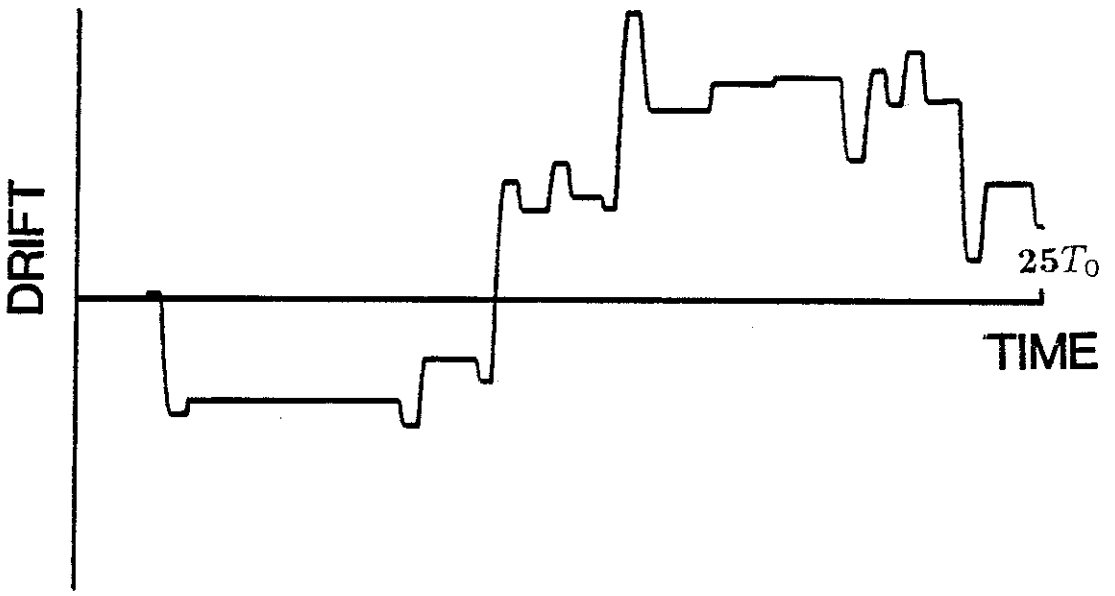

Figure 4.4
Time history of the drift response.

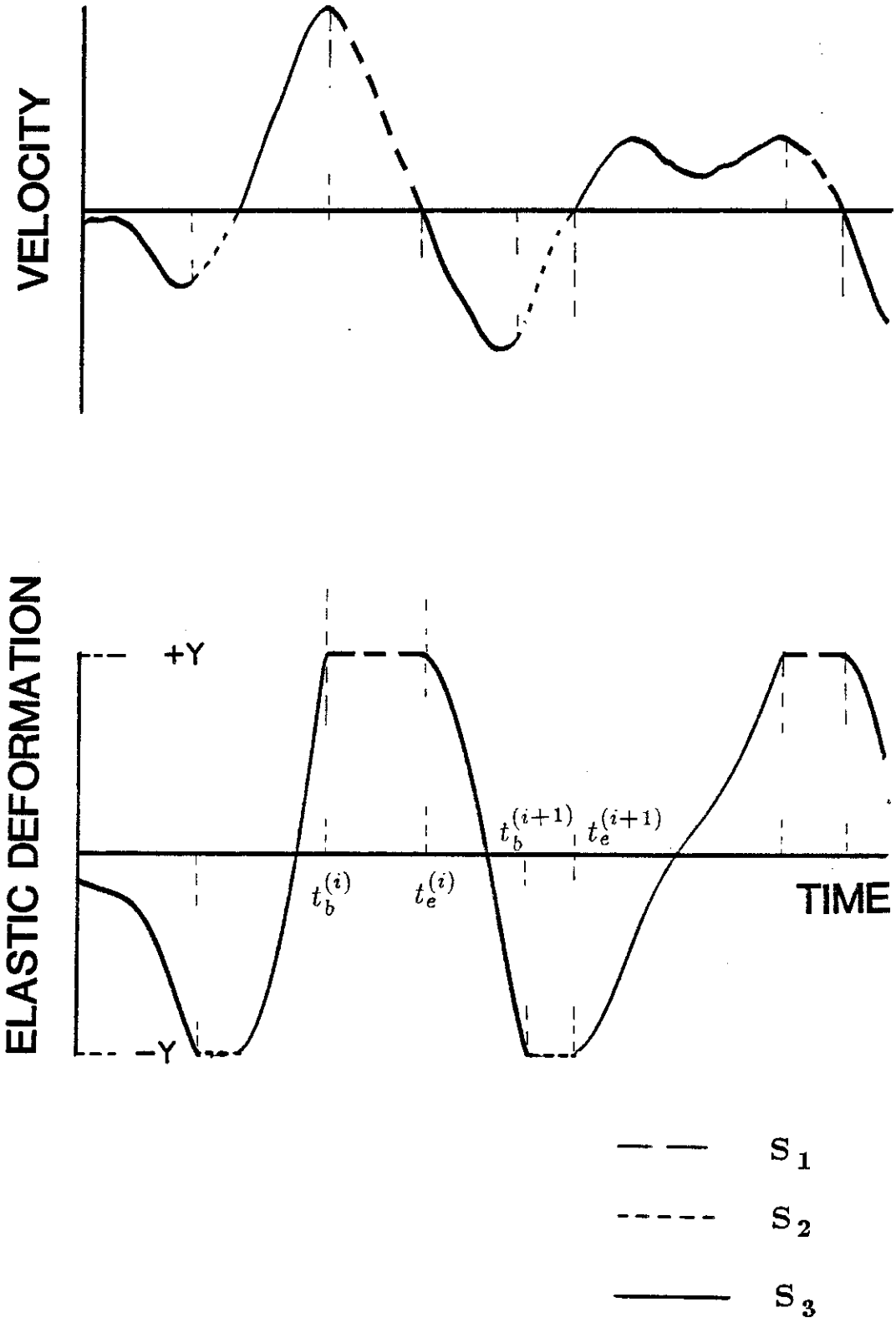

Figure 4.5
The response states S_3, corresponding to elastic behaviour, and S_1 and S_2, corresponding to yielding in positive and negative direction, respectively.

Define d_i as the yield increment associated with the i^{th} yield occurance, or

$$d_i = z(t_e^{(i)}) - z(t_b^{(i)}), \tag{4.12}$$

where $t_b^{(i)}$ and $t_e^{(i)}$ represent the beginning and the ending time of the i^{th} yield increment, respectively. In equation (4.12), $t_b^{(i)}$ and $t_e^{(i)}$ are also random variables with $t_b^{(i)} < t_e^{(i)}$ and $\dot{z}(t_e^{(i)}) = 0$. For the response belonging to the plastic state S_1, or for

$$(x(t), \dot{x}(t), y(t)) \in S_1, \tag{4.13a}$$

the equation of motion is given by

$$y(t) = 1 \tag{4.13b}$$

and

$$\ddot{z}(t) + 2\zeta\dot{z}(t) + 1 = -\ddot{a}(t). \tag{4.13c}$$

For the response belonging to the plastic state S_2, or for

$$(x(t), \dot{x}(t), y(t)) \in S_2, \tag{4.14a}$$

the equation of motion is

$$y(t) = -1 \tag{4.14b}$$

and

$$\ddot{z}(t) + 2\zeta\dot{z}(t) - 1 = -\ddot{a}(t). \tag{4.14c}$$

Finally, for the case of elastic response, or for

$$(x(t), \dot{x}(t), y(t)) \in S_3, \tag{4.15a}$$

the equation of motion is

$$\dot{z}(t) = 0 \tag{4.15b}$$

and

$$\ddot{y}(t) + 2\zeta\dot{y}(t) + y(t) = -\tilde{a}(t). \tag{4.15c}$$

The analysis in this chapter is carried out using the excitation model defined by (2.27), or

$$-\tilde{a}(t) = 2\zeta_g\omega_g\dot{x}_g(t) \tag{4.16a}$$

$$\ddot{x}_g(t) + 2\zeta_g\omega_g\dot{x}_g(t) + \omega_g^2 x_g(t) = \xi(t), \tag{4.16b}$$

corresponding to the case $T_s \rightarrow \infty$ and for $\xi(t)$, a zero mean Gaussian white noise process with spectral density function $S_0/2\pi$. As discussed in Section 2.3.4., for the stochastic seismic excitation model governed by equation (4.16), the model parameters ω_g, ζ_g and S_0 represent the peak frequency, spectral bandwidth and strength of the excitation, respectively.

The four-dimensional random process, $\mathbf{u}^{(\mathbf{i})\,\mathbf{T}}$, is defined as

$$\mathbf{u}^{(\mathbf{i})\,\mathbf{T}} = \{\dot{z}(t_b^{(i)}), y(t_b^{(i)}), x_g(t_b^{(i)}), \dot{x}_g(t_b^{(i)})\}. \tag{4.17}$$

Now, $(z(t), y(t), x_g(t), \dot{x}_g(t))$ is the solution of the stochastic differential equations (4.13)-(4.16) with continuity conditions

$$\dot{z}(t_{b_+}^{(i)}) = \dot{y}(t_{b_-}^{(i)}) \tag{4.18a}$$

$$\dot{z}(t_{e_-}^{(i)}) = \dot{y}(t_{e_+}^{(i)}) = 0 \tag{4.18b}$$

and

$$y(t_{b_-}^{(i)}) = y(t_{e_+}^{(i)}) = \pm 1 \tag{4.18c}$$

By definition, $t_b^{(i)}$ is the first passage time associated with the first passage of the barrier level $y(t_b^{(i)}) = \pm\ 1$ for initial conditions $y(t_e^{(i-1)}) = 1$ or $y(t_e^{(i-1)}) = -1$. Similarly, $y(t_e^{(i)})$ is the first passage time associated with the first passage of the barrier $\dot{z}(t_e^{(i)}) = 0$, and for initial conditions $\dot{z}(t_b^{(i)})$. From equations (4.13)-(4.18) and from the definitions of $t_b^{(i)}$ and $t_e^{(i)}$, it is implied that $\mathbf{u}^{(\mathbf{i})}$ is a discrete

Markov process. But from the results presented in Section 4.3, it can be assumed that $(z(t), y(t), x_g(t), \dot{x}_g(t))$ is a stationary stochastic process, which implies that the diffusion equation for the process $\mathbf{u^{(i)}}$ can be assumed independent of i.

Consider a time T, for which $n(T)$ yield increments have occured between $t = 0$ and $t = T$, such that

$$t_e^{(n(T))} < T < t_e^{(n(T)+1)}. \tag{4.19}$$

Then for large T

$$z(T) \approx \sum_{i=1}^{n(T)} d_i \tag{4.20}$$

The relation (4.20) holds in an approximate sense, in order to account for the possibility of an yield occurence at the time T.

The yield increment d_i is defined by (4.12) as

$$d_i = z(t_e^{(i)}) - z(t_b^{(i)}). \tag{4.12}$$

For $\mathbf{u^{(i)}}$ stationary in i, the yield increment process d_i can be considered as a zero mean stationary process described by the probability density functions

$$\begin{aligned} &p_{d_1}(d_i) = p_{d_1}(d_{i+i_0}) \\ &p_{d_1,d_2}(d_i, d_j) = p_{d_1,d_2}(d_{i+i_0}, d_{j+i_0}) \\ &\vdots \\ &p_{d_1,\ldots,d_k}(d_{i_1}, \ldots, d_{i_k}) = p_{d_1,\ldots,d_k}(d_{i_1+i_0}, \ldots, d_{i_k+i_0}). \end{aligned} \tag{4.21}$$

The second moments Q_j, of the yield increment process d_i are defined as

$$Q_j = E[d_i d_{i+j}]. \tag{4.22}$$

By applying equation (4.20), the mean and the mean square value of the drift are given by

$$E[z(T)] \approx 0, \tag{4.23a}$$

$$E[z^2(T)] \approx E[(\sum_{i=1}^{n(T} d_i)^2]. \qquad (4.23b)$$

For large T, the random process $n(T)$ can be considered independent on $(d_i, i = 1, ..., n(T))$, which implies that

$$E[z^2(T)] \approx E[n(T)Q_0+2(n(T)-1)Q_1+2(n(T)-2)Q_2+...+2Q_{(n(T)-1)}]. \quad (4.24)$$

In equation (4.24), the expectation is taken with respect to the random variable $n(T)$. From equation (4.24), it can be seen that the second moment of the drift response can be calculated if the probabilistic structure of the yield increment process and of the random process, $n(T)$, are known.

The probabilistic structure of the process d_i, defined by equation (4.19) can be derived from the diffusion equation of the process $\mathbf{u}^{(i)}$. But the calculation of the diffusion equation for the process $\mathbf{u}^{(i)}$ involves two first passage problems, associated with the first passage times $t_b^{(i)}$ and $t_e^{(i)}$, and no exact solutions for these problems are available at this time. However, based on the linear divergence of the mean square value drift, it can be assumed that for large $n(T)$, the following approximate expression can be derived for the autocorrelation functions of the yield increment process

$$n(T)Q_0 + 2(n(T) - 1)Q_1 + 2(n(T) - 2)Q_2 + ... + 2Q_{(n(T)-1)} \approx An(T)Q_0 + E_0. \qquad (4.25)$$

A justification for equation (4.25) will be given in Section 4.5, when analysing the discrete Markov process models for the drift. For the case of mutually independent yield increments, the coefficient A is equal to one. For this reason A is defined as correlation factor, and will give a measure of the yield increments correlation.

Substituting (4.25) into (4.24) yields

$$E[z^2(T)] \approx E_0 + AQ_0E[n(T)] = E_0 + \nu_Y TAQ_0, \qquad (4.26)$$

where ν_Y is the expected value for the rate of yield occurences. In the case of a stationary excitation, the stationarity of the yield increment process is approximately achieved after the first yield occurence. Define

$$T_{ex} = E[t_b^{(1)}] \tag{4.27a}$$

as the expected time of the first yield occurance. It can be assumed that for $t > T_{ex}$, the mean square value drift exhibits a linear divergent behaviour. Then for $t > T_{ex}$, equation (4.26) may be written in the following equivalent form:

$$\sigma_z^2(t) = E[z^2(t)] \approx \epsilon_0' Q_0 + \nu_Y A Q_0 (t - T_{ex}). \tag{4.27b}$$

From equation (4.27) it can be noticed that the mean square value drift is determined from the response statistics Q_0, ν_Y, ϵ_0' and A. In Sections 4.4.2 and 4.4.3 it will be shown that the first order probability density of the yield increment process can be derived from the stationary probability density of the velocity response. Due to the complexity of the problem, an analytical expression for the correlation factor A can not be determined. For this reason, discrete Markov process models for the drift are introduced in Section 4.5. Based on these models and on the Monte Carlo simulation results presented in Section 4.6, an approximate expression for A is obtained.

4.4.2 Response statistics for the upcrossing velocity process

Because of the symmetry involved in the problem, consideration need only to be given to the case corresponding to yielding in positive direction, or for $y = 1$. As shown in Figure 4.5, at time $t_b^{(i)}$ the response leaves the elastic state S_3 with an upcrossing velocity $\dot{z}(t_b^{(i)})$ and yielding will occur until the velocity $\dot{z}(t)$ becomes equal to zero. But, as discussed in Section 4.4.1, the Markov process $\mathbf{u}^{(i)}$ possesses a stationary solution, which implies that a stationary solution for the yield increment, yield duration and upcrossing velocity processes will exist. To account for both plastic states S_1 and S_2, the absolute value of the upcrossing velocity $v_y^{(i)}$ is defined as follows:

$$v_y^{(i)} = |\dot{z}(t_b^{(i)})|. \tag{4.28}$$

From the continuity equation (4.18a), it is implied that the stationary probability density function of the process v_y, $p_{v_y}(v_y)$, is related to the the stationary probability density $p^s_{\dot{x}y}(\dot{x}, y)$ of the response variables $(\dot{x}, y)$ corresponding to the elastic state S_3. Based on the definition of the conditional probability for a discrete process, Karnopp and Scharton (39) showed that this relationship is given by

$$p_{v_y}(v_y) = \lim_{\epsilon \longrightarrow 0} \frac{p^s_{\dot{x}y}(v_y, 1-\epsilon)}{\int_0^\infty p^s_{\dot{x}y}(\dot{x}, 1-\epsilon)d\dot{x}} \quad for\ v_y \geq 0. \tag{4.29}$$

Equation (4.29) was also used by Vanmarcke and Veneziano (40) and Grossmayer (41), for the calculation of drift increment statistics. A more careful look at the relationship between $p_{v_y}(v_y)$ and $p^s_{\dot{x}y}(\dot{x}, y)$ will prove that equation (4.29) is actually in error.

Consider $\{x, \dot{x}\}$, a two-dimensional stochastic process, for which it is desired to calculate the conditional probability density $p_{\dot{x}}(\dot{x}, t_0 | x = x_0)$, conditional upon the upcrossing of the barrier level $x = x_0$ for $t \in (t_0, t_0 + dt)$. Then, $p_{\dot{x}}$

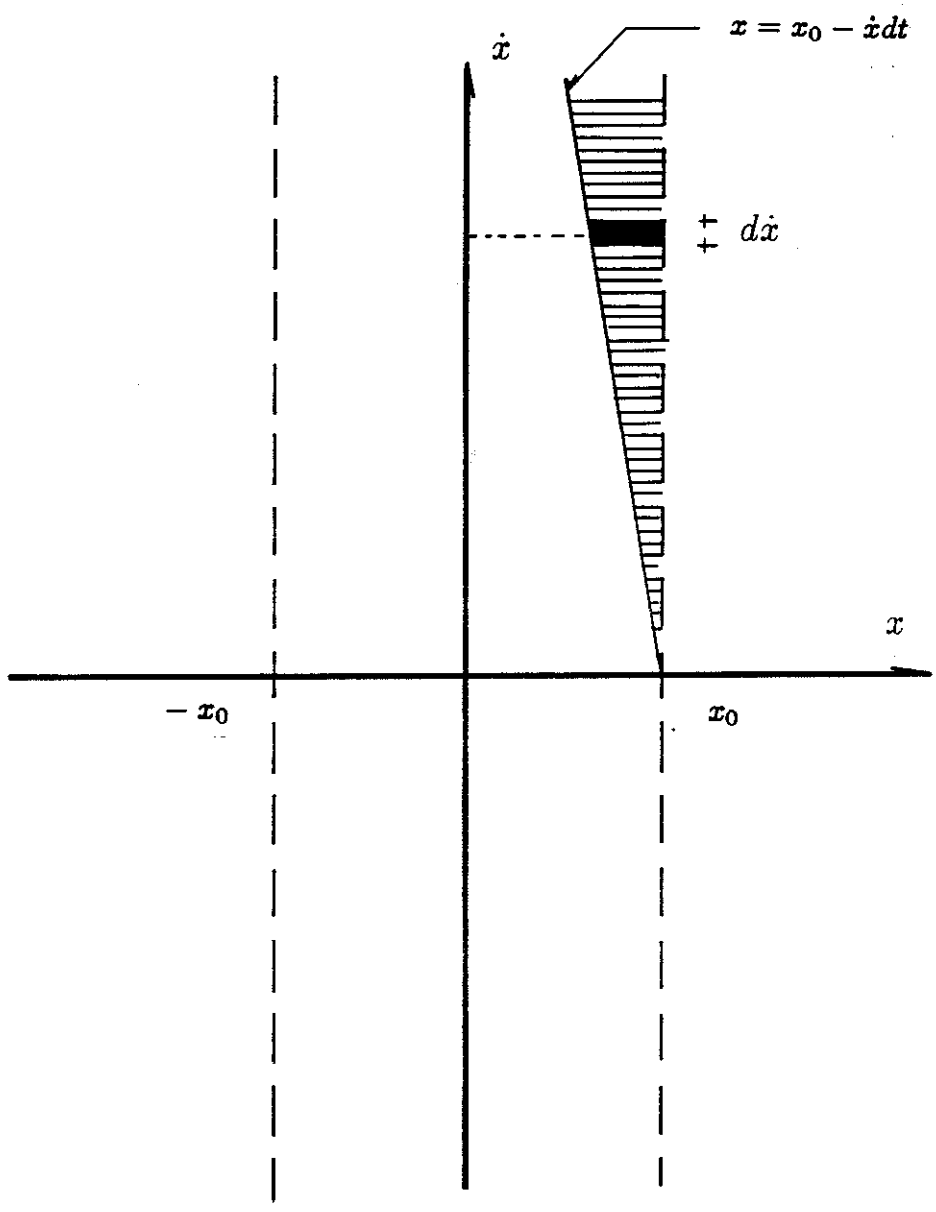

Figure 4.6
Phase plane of the stochastic process $(x, \dot{x})$. The marked domain corresponds to trajectories for which upcrossing of the threshold $x = x_0$ occurs at times $\tau \in (t, t + dt)$.

should satisfy the condition

$$\int_{-\infty}^{\infty} p_{\dot{x}}(\dot{x}, t_0|x = x_0)d\dot{x} = 1. \tag{4.30}$$

But from Figure 4.6, it can be seen that

$$p_{\dot{x}}(\dot{x}, t_0|x = x_0)d\dot{x} = A^* \int_{x_0 - \dot{x}dt}^{x_0} p_{x\dot{x}}(x, \dot{x}, t_0)dxd\dot{x}, \tag{4.31a}$$

or

$$p_{\dot{x}}(\dot{x}, t_0|x = x_0)d\dot{x} = A^* \dot{x} p_{x\dot{x}}(x = x_0, \dot{x}, t_0)d\dot{x}dt, \tag{4.31b}$$

where A^* is a constant that is determined from equation (4.30). Hence, the following expression for $p_{\dot{x}}$ is derived

$$p_{\dot{x}}(\dot{x}, t_0|x = x_0) = \frac{\dot{x} p_{x\dot{x}}(x = x_0, \dot{x}, t_0)}{\int_0^{\infty} \dot{x} p_{x\dot{x}}(x = x_0, \dot{x}, t_0)d\dot{x}}. \tag{4.32}$$

Using equation (4.32), and for stationary probability density function, the correction for equation (4.29) is given by

$$p_{v_y}(v_y) = \lim_{\epsilon \to 0} \frac{v_y p^s_{\dot{x}y}(v_y, 1 - \epsilon)}{\int_0^{\infty} \dot{x} p^s_{\dot{x}y}(\dot{x}, 1 - \epsilon)d\dot{x}} \quad for\ v_y \geq 0. \tag{4.33}$$

Of special interest is the case corresponding to Gaussian distributed probability density $p^s_{\dot{x}y}(v_y, 1)$, or

$$p^s_{\dot{x}y}(v_y, 1) = B^* e^{-\frac{v_y^2}{2b^2}}. \tag{4.34}$$

From (4.33) and (4.34)

$$p_{v_y}(v_y) = \frac{v_y}{2b^2} e^{-\frac{v_y^2}{2b^2}}. \tag{4.35}$$

The mean and mean square values for the upcrossing velocity v_y are then calculated as

$$E[v_y] = \sqrt{\frac{\pi}{2}} b, \tag{4.36a}$$

$$E[v_y^2] = 2b^2. \tag{4.36b}$$

4.4.3 First-order probability density for the yield increment process.

To account for both plastic states S_1 and S_2, the absolute value of the drift increment $d_y^{(i)}$ and yield duration $t_y^{(i)}$ are defined as follows:

$$d_y^{(i)} = |d_i| \tag{4.37a}$$

$$t_y^{(i)} = t_e^{(i)} - t_b^{(i)}; \tag{4.37b}$$

$d_y^{(i)}$ and $t_y^{(i)}$ are stationary random processes and $d_y^{(i)}$ given by

$$d_y^{(i)} = \int_{t_b^{(i)}}^{t_b^{(i)}+t_y^{(i)}} |\dot{z}(t)|dt. \tag{4.38}$$

Without loss of generality, consider that the time $t = 0$ represents the beginning of a yield increment in the positive direction. In this case, the equation of motion for the velocity $v(t) = \dot{z}(t)$ is given by

$$\dot{v} + 2\zeta v + 1 = -\tilde{a}(t) \quad \text{for } t \in (0, t_y), \tag{4.39a}$$

where t_y is the first passage time of the barrier level $v = 0$, or

$$v(t_y) = 0, \tag{4.39b}$$

given that at time $t = 0$

$$v(0) = v_y, \tag{4.39c}$$

v_y is a random variable with probability density function given by (4.33). The drift increment d_y, defined by (4.38) can be expressed in terms of $v(t)$ as

$$d_y = \int_0^{t_y} v(t)dt. \tag{4.40}$$

From the formulation of the problem, it is implied that t_y represents the stopping time of a first passage problem and as a consequence, exact solutions

for the probability distributions of t_y and d_y are very difficult to obtain. Instead, the following approximate solution is defined.

Consider the excitation $-\ddot{a}(t)$ to be composed of a deterministic mean value $m_0(t)$ and the random process $\epsilon(t)$, or

$$-\ddot{a}(t) = m_0(t) + \epsilon(t), \tag{4.41}$$

and assume that for small yield durations $|\frac{\epsilon(t)}{m_0(t)}| \ll 1$, and that $m_0(t)$ remains constant during the yield occurance. Then, for $\varsigma \ll 1$, the stochastic differential equation (4.39a) reduces to the deterministic equation

$$\dot{v} + 1 \approx m_0, \tag{4.42}$$

with $v(0) = v_y$. The assumption regarding the constant value of the mean value for the excitation is justified in the case of small duration yield occurences and for the excitation model described by a single peak spectral density function and zero low frequency content. Indeed, in this case the excitation exhibits oscillations at the characteristic frequency ω_g and strong autocorrelation for small time differences.

From equation (4.42) it is implied that

$$v(t) \approx v_y - (1 - m_0)t \quad \text{for } t \in (0, t_y) \tag{4.43}$$

and

$$t_y \approx \frac{v_y}{(1 - m_0)}. \tag{4.44}$$

From (4.40)

$$d_y \approx \frac{v_y^2}{2(1 - m_0)}. \tag{4.45}$$

The mean and mean square values for the drift increment and yield duration can be easily calculated as

$$E[t_y] = \frac{1}{(1 - m_0)} E[v_y], \tag{4.46}$$

$$E[d_y] = \frac{1}{2(1-m_0)} E[v_y^2]. \tag{4.47}$$

In the case corresponding to Gaussian distributed probability density, $p^s_{\dot{x}y}(v_y, 1)$, the following simplified expressions for the yield increment statistics are obtained:

$$E[t_y] = \frac{1}{(1-m_0)} \sqrt{\frac{\pi}{2}} b \tag{4.48}$$

$$E[d_y] = \frac{1}{(1-m_0)} b^2 \tag{4.49}$$

and

$$E[d_y] = \frac{2}{(1-m_0)^2} b^4. \tag{4.50}$$

4.5 Two-state Markov process model for the drift of an elasto-plastic system.

In Section 4.4 it was shown that by expressing the drift as the sum of yield increments associated with inelastic behaviour, the random response of an elasto-plastic system is determined from the yield increment statistics. Because of the complexity of the problem, an exact solution of the diffusion equation for the yield increment process can not be obtained. For this reason, the analysis presented in this section is based on a simplified Markov process model for the drift. For this model, the second order statistics and an asymptotic expression for the first passage probability of type-D barrier levels are derived in Sections 4.5.2 and 4.5.3, respectively. A discussion on the generalization of the results for the actual yield increment process is presented in Section 4.5.4.

4.5.1 Discrete Markov process models.

Consider the two-state process, $S^{(i)}$, defined as the inelastic state in which the i^{th} yielding occured. Then the yield increment, d_i, is described by the magnitude, $d_y^{(i)}$, and the direction of yield occurence determined by the process $S^{(i)}$. For the models introduced in this section, it is considered that $d_y^{(i)}$ and $S^{(i)}$ are independent processes, or

$$p_{Sd_y}(S^{(i)}, d_y^{(i)}) = p_S(S^{(i)}) p_{d_y}(d_y^{(i)}). \tag{4.51}$$

It is also considered that the magnitude of the yield increments are mutually independent processes, while $S^{(i)}$ is a two-state Markov process, with transition probabilities, p^+ and p^-, defined as

$$p^+ = P(S_1|S_1) = P(S_2|S_2) \tag{4.52a}$$

and

$$p^- = P(S_1|S_2) = P(S_2|S_1), \tag{4.52b}$$

and $P(...)$ is defined as the probability of the event in parenthesis. Based on their definitions, it is implied that

$$p^+ + p^- = 1. \tag{4.52c}$$

Equations (4.51) and (4.52), imply that the transition probability for the stationary process, $(d_y^{(i)}, S^{(i)})$, is given by

$$p_{Sd_y}(d_y^{(i+j)}; S^{(i+j)}|d_y^{(i)}; S^{(i)}) = p_{d_y}(d_y^{(i+j)}) P(S^{(i+j)}|S^{(i)}). \tag{4.53}$$

For the simplified yield increment model the mean square value of the yield increment, Q_0, and the transition probabilities, p^+ and p^-, are equal to the corresponding values of the actual yield increment process. In order to account

for the possible correlation between the magnitude of yield increments, two extreme cases are considered, as follows.

For the deterministic steady-state response of an elasto-plastic system, the magnitude of yield increments is constant. Based on this observation, the type-A model is defined as a process with constant magnitude yield increments. The other extreme case corresponds to uncorrelated $d_y^{(i)}$. As shown in Section 4.4, the first order probability density of d_y is approximately exponentially distributed. For this reason, the type-B model is defined as a process with mutually independent and exponentially distributed magnitude of the yield increments.

4.5.2 First order probability density of the drift response.

The drift, $z^{(n)}$, is defined as the sum of yield increments, or

$$z^{(n)} = \sum_{i=1}^{n} d_i. \tag{4.54a}$$

This implies that for zero mean yield increments, the drift is a zero mean process, with covariance, $\sigma_z^{(n)^2}$, given by

$$\sigma_z^{(n)^2} = E[z^{(n)^2}] = nQ_0 + 2(n-1)Q_1 + ... + 2Q_{n-1}, \tag{4.54b}$$

where Q_j are the autocorrelation functions of the yield increment process. But for the yield increment model, with transition probability given by equation (4.53), Q_j is given by

$$Q_j = E[d_{i+j}d_i] = E[d_y^{(i+j)}d_y^{(i)}]E[\text{sgn}(d_{i+j}d_i)]. \tag{4.55a}$$

Because the $d_y^{(i)}$ were assumed mutually independent, it follows that

$$Q_j = E[\text{sgn}(d_{i+j}d_i)] \begin{cases} E[d_y^2], & \text{if } j = 0; \\ E^2[d_y], & \text{if } j \geq 1. \end{cases} \tag{4.55b}$$

Now, $S^{(i)}$ is a two-state Markov chain and because the yield increment is a zero mean, stationary process

$$P(S^{(i)} = S_1) = P(S^{(i)} = S_2) = \frac{1}{2}. \tag{4.56}$$

Following standard procedure for the treatment of Markov chains, it can be shown that

$$P(S^{(i+j)} = S_1 | S^{(i)} = S_1) = P(S^{(i+j)} = S_2 | S^{(i)} = S_2) = \frac{1}{2}[1 + (1 - 2p^-)^j], \tag{4.57a}$$

and that

$$P(S^{(i+j)} = S_1 | S^{(i)} = S_2) = P(S^{(i+j)} = S_2 | S^{(i)} = S_1) = \frac{1}{2}[1 - (1 - 2p^-)^j]. \tag{4.57b}$$

From equations (4.52), (4.56) and (4.57)

$$E[\mathrm{sgn}(d_{i+j} d_i)] = (1 - 2p^-)^j, \tag{4.58a}$$

which implies that

$$Q_j = \begin{cases} E[d_y^2], & \text{if } j = 0; \\ E^2[d_y](1 - 2p^-)^j, & \text{if } j \geq 1. \end{cases} \tag{4.58b}$$

Define

$$\beta_0 = 1 - 2p^-. \tag{4.59}$$

Then, by substituting (4.58), (4.59) into (4.54b), the following expression for $E[z^{(n)^2}]$ is obtained:

$$E[z^{(n)^2}] = nE[d_y^2] + 2E^2[d_y]\left[\frac{n\beta_0(1-\beta_0^{n-1})}{1-\beta_0} - \frac{\beta_0(1-\beta_0^{n-2})}{(1-\beta_0)^2} + ((n-1)\beta_0 - 1)\frac{\beta_0^{n-1}}{1-\beta_0}\right]. \tag{4.60}$$

For $n \to \infty$ this becomes

$$E[z^{(n)^2}] = n\left[E[d_y^2] + \frac{2E^2[d_y]\beta_0}{1-\beta_0}\right] - \frac{2\beta_0 E^2[d_Y]}{(1-\beta_0)^2}. \tag{4.61}$$

Equation (5.65) suggests that for the conditional random walk process examined in this section, the mean square drift is linearly divergent as $n \rightarrow \infty$, or

$$E[z^{(n)^2}] = nAQ_0 + E_0, \tag{4.62a}$$

where A is the correlation factor defined in Section 4.4, and is equal to

$$A = 1 + \frac{2E^2[d_y]}{E[d_y^2]} \frac{\beta_0}{1-\beta_0}. \tag{4.62b}$$

The " offset", E_0, is given by

$$E_0 = \frac{2\beta_0 E^2[d_y]}{(1-\beta_0)^2} = \epsilon_0 Q_0 \tag{4.62c}$$

and

$$\epsilon_0 = -\frac{2\beta_0 E^2[d_y]}{E[d_y^2]}. \tag{4.62d}$$

For the type-A process,

$$E^2[d_y] = E[d_y^2], \tag{4.63}$$

and the correletation factor A is given by

$$A = \frac{p^+}{p^-}; \tag{4.64a}$$

while ϵ_0 is given by

$$\epsilon_0 = \frac{(2p^- - 1)}{2p^{-2}}. \tag{4.64b}$$

In the case of the type-B process, the mean and the mean square value of d_y are related through the relationship

$$2E^2[d_y] = E[d_y^2], \tag{4.65}$$

which implies that for the type-B process, the correlation factor and the offset coefficients are given by

$$A = \frac{1}{2p^-} \tag{4.66a}$$

and

$$\epsilon_0 = \frac{(2p^- - 1)}{4p^{-2}}. \tag{4.66b}$$

For both processes A and B, it can also be shown that as $n \to \infty$, the drift, $z^{(n)}$, defined by (4.54a), becomes a Gaussian distributed process.

Grossmayer (41) defined the increment d_g as the sum of all successive yield increments in the same direction. The change of drift during an open loop , $d\eta$, was defined as

$$d\eta^{(i)} = \frac{d_g^{(i+1)} + 2d_g^{(i)} + d_g^{(i-1)}}{4}. \tag{4.67a}$$

From the definitions of the related processes, the coefficient A, for Grossmayer's model can be derived as

$$A = \frac{3}{32}(1 + \frac{p^+}{p^-})^2. \tag{4.67b}$$

4.5.3 First passage probability for the conditional random walk.

In Appendix C it is shown that for the type-B process, as $n \to \infty$, the survival probability for the type-D barrier at $|z| = b$, defined as

$$W_b^{(n)} = \text{Prob}(|z^{(i)}| < b \quad \forall i = 1, ..., n), \tag{4.68}$$

is just a function of the ratio between b and $\sigma_z^{(n)}$, and does not dependent on n. Hence,

$$W_b^{(n)} \approx p_0(\frac{b}{\sigma_z^{(n)}}). \tag{4.69a}$$

In equation (4.69a), $p_0(\gamma)$ represents the survival probability of Brownian motion for a type-D barrier at $|z| = \gamma t$, and is given by

$$p_0(\gamma) = \frac{4}{\pi} \sum_{k=0}^{\infty} \frac{(-1)^k}{(2k+1)} e^{-\frac{(2k+1)^2 \pi^2}{8\gamma^2}}. \tag{4.69b}$$

Because the type-A process is a conditional random walk with constant increments, for large n it will converge to a Wiener process. This implies that

the first passage probability of a type-D barrier level at $|z| = \gamma\sigma_z^{(n)}$ will again be given by $p_0(\gamma)$.

The connection with Brownian motion can be better understood if the increment $\Delta^{(i)}$ is defined as an average of k succesive yield increments $d^{(i)}$. Then, for $n = n_1 k$,

$$z^{(n)} = \sum_{i=1}^{n_1 k} d^{(i)} = \sum_{j=1}^{n_1} \left(\sum_{i=1}^{k} d^{((k-1)j+i)} \right) = k \sum_{j=1}^{n_1} \Delta^{(j)}. \tag{4.70}$$

For large enough k, the $\Delta^{(j)}$ can be considered as mutually independent and Gaussian distributed increments. Define the type-C model as a process with mutually independent and Gaussian distributed increments. The mean square value drift for the type-C process is then given by

$$\sigma_z^{(n)^2} \approx n\sigma_\Delta^2. \tag{4.71}$$

But from (4.62a)

$$E[z^{(n)^2}] = nAQ_0 + E_0. \tag{4.62a}$$

Hence,

$$A = \frac{\sigma_\Delta^2}{E[d_Y^2]}, \tag{4.72}$$

which relates the correlation factor A to the second moments of the Δ and d_Y processes.

For large n, the type-C process will behave like a random walk converging towards Brownian motion. This can be illustrated by considering the first passage problem for the process C and for a type-D barrier at $|z| = \gamma\sigma_z^{(n)}$. The transition probability density is given by

$$p^{(i)}(z) = \frac{1}{(2\pi)^{\frac{1}{2}}\sigma_\Delta} \int_{-\infty}^{\infty} e^{-\frac{(x-z)^2}{2\sigma_\Delta^2}} p^{(i-1)}(x)dx. \tag{4.73}$$

The survival probability is given by

$$W_b^{(n)} = \frac{1}{(2\pi)^{\frac{n}{2}}\sigma_\Delta^n} \underbrace{\int_{-\gamma\sigma_\Delta\sqrt{n}}^{\gamma\sigma_\Delta\sqrt{n}} \cdots \int_{-\gamma\sigma_\Delta\sqrt{n}}^{\gamma\sigma_\Delta\sqrt{n}}}_{n \text{ times}} e^{-\frac{x_1^2}{2\sigma_\Delta^2}} e^{-\frac{(x_2-x_1)^2}{2\sigma_\Delta^2}} \ldots e^{-\frac{(x_n-x_{n-1})^2}{2\sigma_\Delta^2}} dx_1 \ldots dx_n, \tag{4.74}$$

or by an appropriate change of variables, $t_i = \frac{x_i}{\sigma_\Delta\sqrt{n}}$,

$$W_b^{(n)} = \frac{1}{(2\pi n)^{\frac{n}{2}}} \underbrace{\int_{-\gamma}^{\gamma} \cdots \int_{-\gamma}^{\gamma}}_{n \text{ times}} e^{-\frac{nt_1^2}{2}} e^{-\frac{n(t_2-t_1)^2}{2}} \ldots e^{-\frac{n(t_n-t_{n-1})^2}{2}} dt_1 \ldots dt_n. \tag{4.75}$$

Equation (4.75) represents an approximate solution for the survival probability at time $t = 1$ for a Brownian motion and for the type-D barrier at $|z| = \gamma$. An approximate solution may be obtained by discretizing the time interval $(0, 1)$ into n time intervals, and applying the transition probability of the process at times $(t_j = \frac{j}{n},\ j = 0, ..., n-1)$. As $n \to \infty$, $W_b^{(n)}$ converges to $p_0(\gamma)$ defined by equation (4.69b). Based on numerical diffusion of the probability density function, it can be concluded that good estimates for $p_0(\gamma)$ can be obtained for $n \geq 10$.

For computational purposes, the series expansion expression for $p_0(\gamma)$, given by (4.69b), can be efficiently applied for low barrier levels, or for small γ. For high barrier levels, a similar expression for $p_0(\gamma)$ can be obtained (see Simon (10)), as

$$p_0(\gamma) = \text{Prob}(u \in \Gamma) - \text{Prob}(u \in B), \tag{4.76a}$$

where u is a normal distributed variable and Γ, B are defined as

$$\Gamma = (-\gamma, \gamma) \cup (3\gamma, 5\gamma) \cup (-3\gamma, -5\gamma) \cup \ldots \tag{4.76b}$$

and

$$B = (\gamma, 3\gamma) \cup (-\gamma, -3\gamma) \cup (5\gamma, 7\gamma) \cup \ldots. \tag{4.76c}$$

For large values of γ, by applying an asymptotic expansion for the complementary error function, an approximate expression for $p_0(\gamma)$ can be obtained as

$$p_0(\gamma) \approx 1 - \frac{2}{\gamma} e^{-\frac{\gamma^2}{2}} [1 - \frac{1}{\gamma^2}]. \tag{4.77}$$

The generalization of the properties derived in Sections 4.5.2 and 4.5.3, to the continous-in-time drift of an elasto-plastic system is discussed in Section 4.5.4, while a comparison of the analytical results with Monte Carlo simulation results is examined in Section 4.6.

4.5.4 Interpretation of results.

In this section, discrete Markov process models for the drift of elasto-plastic systems subjected to stationary stochastic excitation are examined. As discussed in Section 4.4.1, the mean square value drift can be expressed as a function of the yield increment statistics through equation (4.24), or

$$E[z^2(T)] \approx E[n(T)Q_0 + 2(n(T)-1)Q_1 + 2(n(T)-2)Q_2 + ... + 2Q_{(n(T)-1)}], \tag{4.24}$$

where expectation is taken with respect to the number of yield occurences, the random process $n(T)$. But for the discrete conditional random walk model it was shown that for large $n(T)$, equation (4.54b) can be expressed in terms of the correlation factor A and autocorrelation functions Q_0, as following:

$$n(T)Q_0 + 2(n(T)-1)Q_1 + 2(n(T)-2)Q_2 + ... + 2Q_{(n(T)-1)} \approx An(T)Q_0 + E_0. \tag{4.78}$$

As also mentioned in Section 4.4.1, it is suggested that even in the general case of a drift increment process, such a relationship should be valid. For autocorrelation functions of the actual yield increment process satisfying equation (4.78), the mean square value of the drift is linearly divergent, and is given by equation (4.26)

$$E[z^2(T)] \approx E_0 + AQ_0E[n(T)] = E_0 + \nu_Y TAQ_0, \tag{4.26}$$

where ν_Y is the expected value for the rate of yield occurences. In the case of a stationary excitation, the stationarity of the yield increment process is approximately achieved after the first yield occurence. Because the behaviour of the elasto-plastic system is different before and after this first occurence, a time shift T_1 is introduced in equation (4.26) corresponding to the start of the equivalent discrete Markov process. Then, for the discrete process, T_1 should satisfy the equation

$$\nu_Y(T_{ex} - T_1) = 1. \tag{4.80}$$

The approximate expression for the mean square drift is given by

$$\sigma_z^2(t) \approx \epsilon_0' Q_0 + \nu_Y A Q_0 (T - T_{ex}) \tag{4.81a}$$

and

$$\epsilon_0' = \epsilon_0 + A. \tag{4.81b}$$

For process A, substituting equation (4.64) into (4.81b), yields

$$\epsilon_0' = \frac{(4p^- - 2p^{-2} - 1)}{2p^{-2}}. \tag{4.82a}$$

For process B, substituting (4.66) into (4.81b), yields

$$\epsilon_0' = \frac{4p^- - 1}{4p^{-2}}. \tag{4.82b}$$

Although the drift is a continuous process, equation (4.27b) suggests that for large $\nu_Y T$, the drift statistics can be predicted from the the properties of an associated discrete random process corresponding to $\nu_Y T$ yield increments.

Of the three random walk models for the drift (processes A, B and C) it appears that the most realistic approximation is given by the type-C process, which also offers an interpretation for the coefficient A. Recall that the process

C is defined as a random walk with Gaussian distributed increments $\Delta^{(i)}$ obtained by averaging k succesive yield increments $d_Y^{(i)}$. It is not clear, however, how large k should be in order to achieve the statistical independence of the increments $\Delta^{(i)}$. This implies that such a model cannot be used succesfully for the computation of the correlation factor A.

A more detailed examination of the applicability of the discrete Markov process models for the drift response of an elasto-plastic system is discussed in the next section.

4.6 Monte Carlo simulation study of the Brownian nature of the drift.

4.6.1 Introduction.

In Section 4.5, the properties of a conditional Markov process model for the drift of an elasto-plastic system were examined. The model was based on the assumption that the magnitude of the yield increments are mutually independent processes, while the direction of yield occurence is a two state Markov process corresponding to the plastic states S_1 and S_2. In order to account for the possible correlation between the magnitude of the yield increments, the processes A and B were defined for the modeling of strong and weak correlation, respectively. It was suggested that for large duration of the stationary stochastic excitation, the drift becomes a Brownian motion. No indication was given, however, on whether such large durations correspond to problems of practical significance. Because no analytical tools are available to examine this issue, a Monte Carlo simulation study of the elasto-plastic system subjected to stationary stochastic excitation is reported in this section.

The purpose of this numerical simulation study is to examine the applicability of the discrete Markov process models for drift of an elastoplastic system subjected to stochastic excitation. Based on the properties of the discrete model,

it is suggested that certain drift properties should be invariant with respect to system and excitation parameters. For this reason, the following properties are verified on the whole sample set of 54 simulation cases:

Property 1. -stationarity for the response variables $\dot{x}$, y, $d_y^{(i)}$, $t_y^{(i)}$, p^+, ν_Y, approximately for times $t > T_{ex}$.

Property 2. -Brownian motion nature of the drift for long duration of the stationary seismic excitation, which implies:

a. -linear divergent mean square value drift.

b. -zero mean Gaussian distribution of the drift response.

c. -distribution for the normalized peak drift response independent of t, and given by $p_0(\frac{z_{max}(t)}{\sigma_z(t)})$.

The system and excitation parameters used in this analysis are selected to represent cases of practical interest. In the 54 cases examined, the ratio between the characteristic frequency of the excitation and the natural frequency of the system is chosen as ω_g/ω_0 =0.3, 0.5, 0.7, 1.0, 1.5, 3.0 and 5.0, while the values ς_g= 0.25 and 0.50 are selected for the bandwidth of the excitation, to represent narrow and broad banded excitation, respectively. The results presented in this analysis mostly correspond to peak ductility ratios between one and ten, which is considered the domain of practical interest.

Because the objective of this study is to examine whether the Brownian motion model can be applied for excitation durations of practical interest, the duration of the simulated records is chosen as $25T_0$, were T_0 is the natural period of the system.

4.6.2 A Monte Carlo simulation program for the random response of an elasto-plastic system.

The simulation program used in this analysis is designed for the purpose of examining the properties of the yield increment and drift of an elasto-plastic system. Because the system responds linearly in each of the three states, S_1, S_2, S_3 defined by (4.11), the equation of motion is solved exactly for each case, or

$$\mathbf{x}^{(i+1)} = \mathbf{A_j}\mathbf{x}^{(i)} + \mathbf{B_j}\mathbf{a}^{(i+1)}, \tag{4.83a}$$

with

$$\mathbf{x}^{(i)^T} = \{x^{(i)}, \dot{x}^{(i)}\} \tag{4.83b}$$

$$\mathbf{a}^{(i+1)^T} = \{\ddot{a}^{(i+1)}, \ddot{a}^{(i)}\}, \tag{4.83c}$$

and $(\mathbf{A_j}, \mathbf{B_j};\ j = 1,2,3)$ correspond to the state S_j and for time steps dt=$T_0/100$, where T_0 is the natural period of the system. The transition times $t_b^{(k)}$, $t_e^{(k)}$, corresponding to the beginning and the ending time of the k^{th} yield occurence are numerically calculated as the solutions of the following equations

$$y(t_b^{(k)}) = \pm 1 \tag{4.84a}$$

and

$$\dot{x}(t_e^{(k)}) = 0. \tag{4.84b}$$

Because $t_b^{(i)}$ and $t_e^{(i)}$ are determined for each yield occurance, the duration of each yielding occurence

$$t_y^{(i)} = t_e^{(i)} - t_b^{(i)} \tag{4.84c}$$

and the corresponding yield increments

$$d^{(i)} = x(t_e^{(i)}) - x(t_b^{(i)}) \tag{4.84d}$$

are calculated.

From the 250 simulated records of the response variables $(x, \dot{x}, z, y)$, the corresponding transient mean square values are calculated, as well as the expected time of the first yield occurance T_{ex}^{sim}. It is observed that for times $t > T_{ex}^{sim}$, stationarity in mean square value for $(\dot{x}, y)$ is approximately achieved. Following the stationarity assumption it is also assumed that for $t > T_{ex}^{sim}$, the $(\dot{x}, y)$ process is ergodic, which enables the creation of large samples for the yield increment and velocity response. The sequence of yield increments is stored for each record, which allows the calculation of stationary transition probabilities p^+ and p^-.

As basic properties of a Wiener process, the Gaussian distribution and the survival probability of the drift response are also examined. The peak response distributions at times $t = 15T_0$ and $t = 25T_0$ and the drift probability distributions at times $t = 10T_0$ and $t = 20T_0$ are calculated for each simulation study. A discussion of the results is presented in Sections 4.6.3 and 4.6.4.

4.6.3 Correlation factor and first-order statistics.

For all 54 cases studied in this analysis, a linear divergence for the mean square value of the drift and stationarity in mean square value for the response variables $(\dot{x},y)$ is noticed. It is also verified that Property 1 is approximately valid for times $t > T_{ex}$. In order to illustrate the stationarity for the yield increment statistics, the simulated records are divided into ten equal time intervals of length $2.5T_0$, and the expected values $E^{(j)}[p^+]$, $\nu_Y^{(j)}$, $E^{(j)}[d_y]$ corresponding to the j^{th} time interval are calculated. It is noted that the specified statistics are independent of j, for $j \geq 3$, which implies that for future simulation studies, the ergodicity assumption can be applied for times $t \geq 5T_0$.

The linear divergence in mean square value of the drift implies that for $t > T_{ex}$, $\sigma_z^2(t)$ is approximately given by

$$\sigma_z^2(t) = \Delta(t - T_1), \tag{4.85a}$$

with

$$\Delta = A\nu_Y Q_0 \tag{4.85b}$$

$$T_1 = T_{ex} - \frac{\epsilon_0'}{A\nu_Y}, \tag{4.85c}$$

where A is the correlation factor defined as a function of the yield increment autocorrelation functions. Based on equation (4.85a), a numerical simulation estimate for the correlation factor, A, is obtained from a least square linear fit of the mean square value of the drift time history, and for $t > T_{ex}+T_0$. Following this approach, A is calculated as

$$A^{sim} = \frac{\Delta_{sim}}{\nu_Y^{sim} Q_0^{sim}}. \tag{4.86}$$

In Figure 4.7, a comparison is shown between the $(A_{sim}, \frac{p^+}{p^-})$ values obtained from Monte Carlo simulation and the analytical results predicted by the discrete

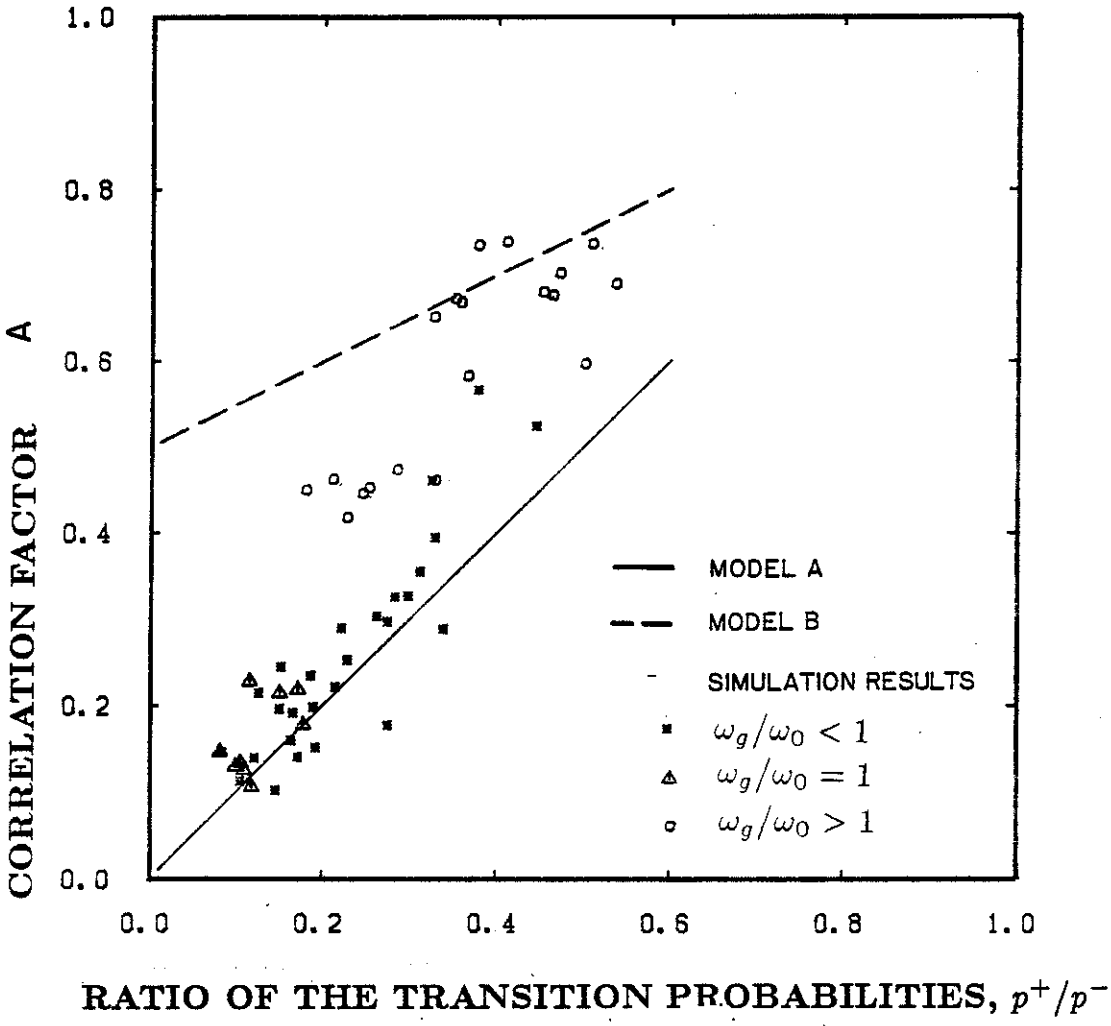

Figure 4.7
Correlation factor, A, versus the ratio of transition probabilities p^+/p^-. Comparison between analytical and numerical simulation results.

Markov process models. Recall that for type-A process, the correlation factor is given by

$$A = \frac{p^+}{p^-}, \tag{4.64a}$$

while for process B, by

$$A = \frac{1}{2p^-}. \tag{4.66a}$$

The correlation factor for Grossmayer's model is

$$A = \frac{3}{32}(1 + \frac{p^+}{p^-})^2. \tag{4.67b}$$

From the results presented in Figure 4.7, it can be seen that equation (4.64a), corresponding to the process A, is in better overall agreement with the simulation data. This suggests that for the actual process, the magnitude of the yield increments are not mutually independent. Nevertheless, for $\omega_g/\omega_0 > 1$ the simulated results show an increasing divergence from the process A model, while approaching the analytical results predicted by process B. It can be concluded that even if the dependence of the correlation factor, A, on system and excitation parameters is very complex, an approximate relation between A and $\frac{p^+}{p^-}$ can be derived. In the analysis presented in Chapter 5, it is assumed that A is given simply by

$$A = \frac{p^+}{p^-}. \tag{4.64a}$$

The transition probabilities p^+ and p^- also provide a measure of the narrowbandness of the response. For small values of p^+/p^-, the response is narrowbanded and a yield increment in one direction will be most probably followed by yielding in the opposite direction. In contrast, for larger values of p^+/p^-, the response becomes broadbanded and the sequence of yield increments approaches a random walk type of behaviour. It should be pointed out that this definition of narrowbandness of the response relates to the short duration behaviour of

the system. As it will be shown later in this section, the large time scale behaviour of the drift approaches a Brownian motion independent of the system and excitation parameters.

In Figure 4.8, the values for the offset coefficient, ϵ_0' obtained from numerical simulation studies are compared to the expression of ϵ_0' obtained from the discrete Markov process model (equation 4.82). It can be noticed that even if neither model is in very good agreement with simulation data, an approximate value $\epsilon_0' \approx 0.5$ gives good conservative estimates for the offset of the mean square value of the drift. For large durations of the excitation and for most problems of practical interest, the offset, E_0, becomes negligible. Nevertheless, for cases in which the offset is of practical significance, equation (4.27b), with $\epsilon_0' = 0.5$, can be used as a simple approximation for the transient mean square value drift response. An illustration of this simplified solution is shown in Figure 4.9.

Finally, in Figure 4.10, the probability distribution of the drift response at time $t = 20T_0$ is illustrated for the values of model parameters $S = 0.40$, $\omega_g = 1$, $\varsigma = 0.01$ and $\varsigma_g = 0.50$. The simulated data are obtained from a set of 2500 samples. It can be seen that the drift response indeed becomes Gaussian distributed. For actual structural systems, $20T_0$ corresponds to a duration of the excitation in the range (4-60) sec., and can be considered of practical interest.

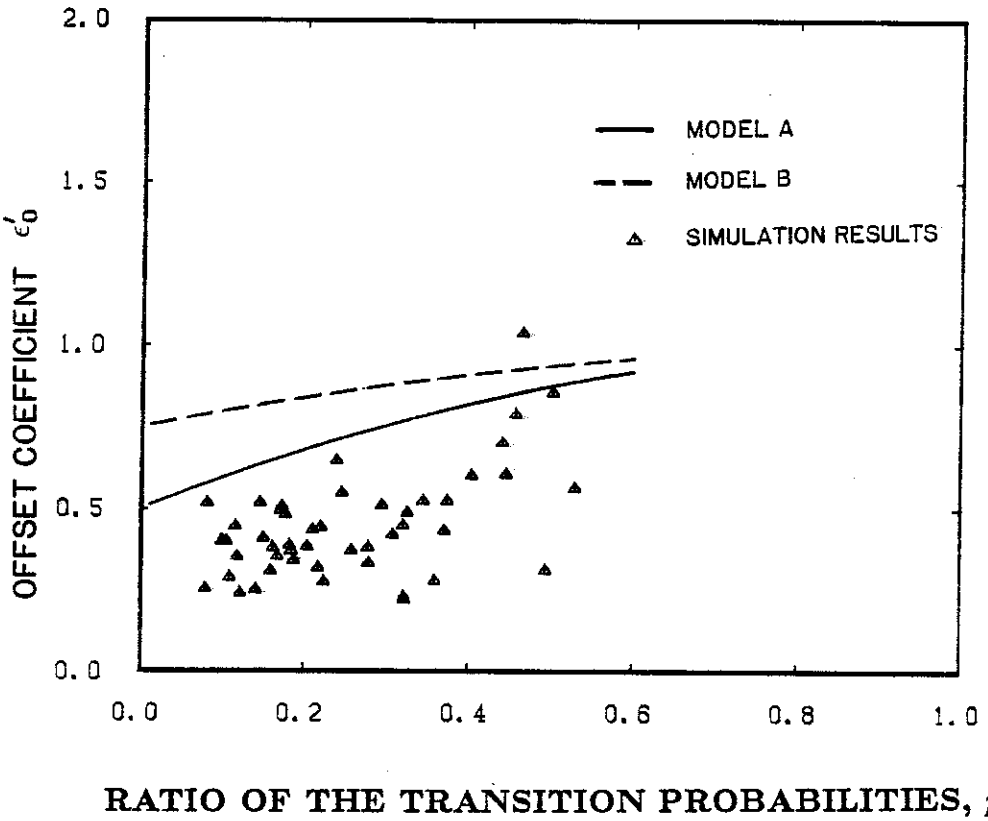

Figure 4.8
Offset coefficient, ϵ_0', versus the ratio of transition probabilities p^+/p^-. Comparison between analytical and numerical simulation results.

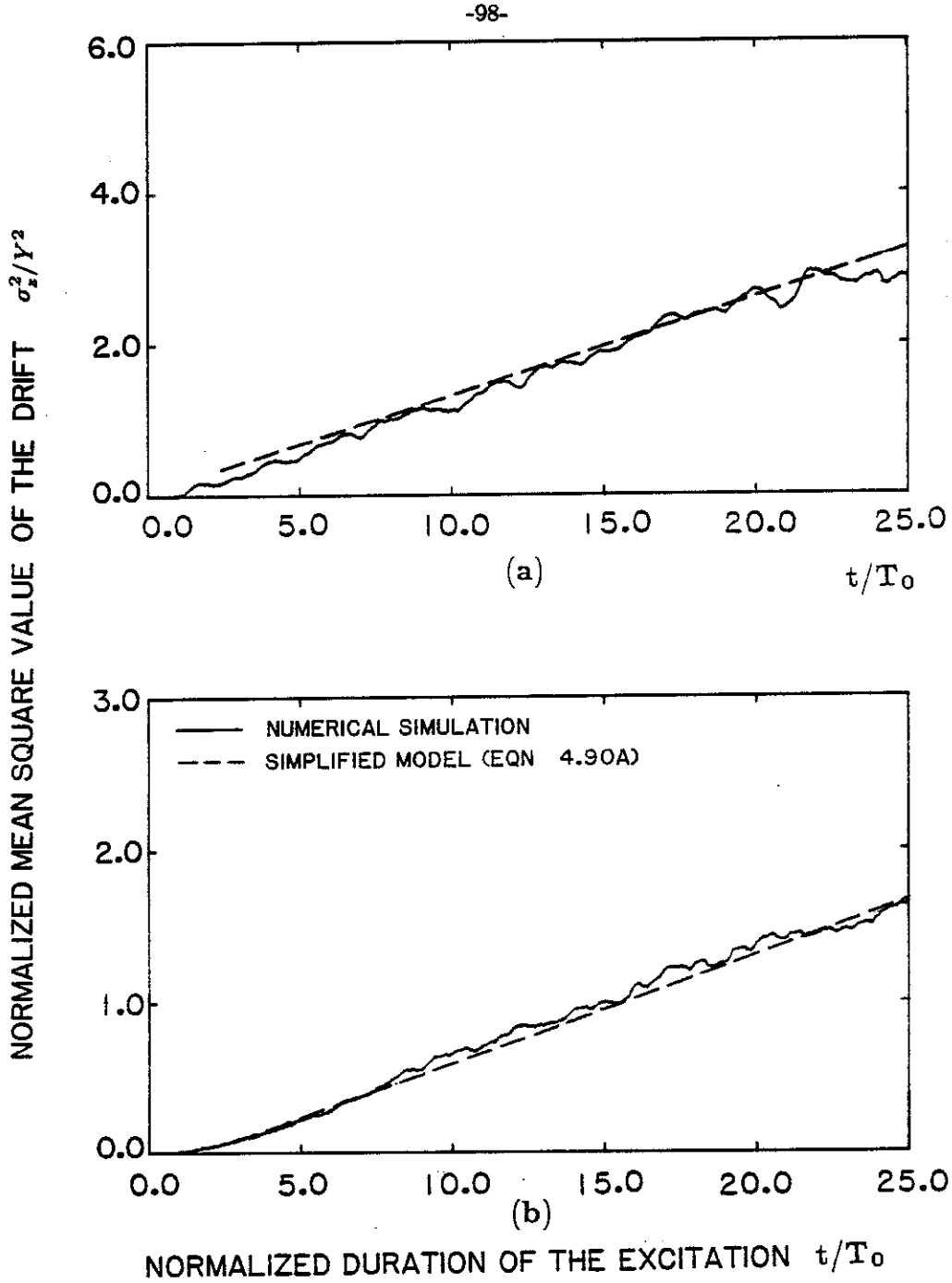

Figure 4.9
Transient mean square value of the drift obtained by the simplified equation (4.90a). (a) S_0=0.90, ω_g/ω_0=0.50, ζ_g=0.25. (b) S_0=2.5, ω_g/ω_0=3.0, ζ_g=0.25.

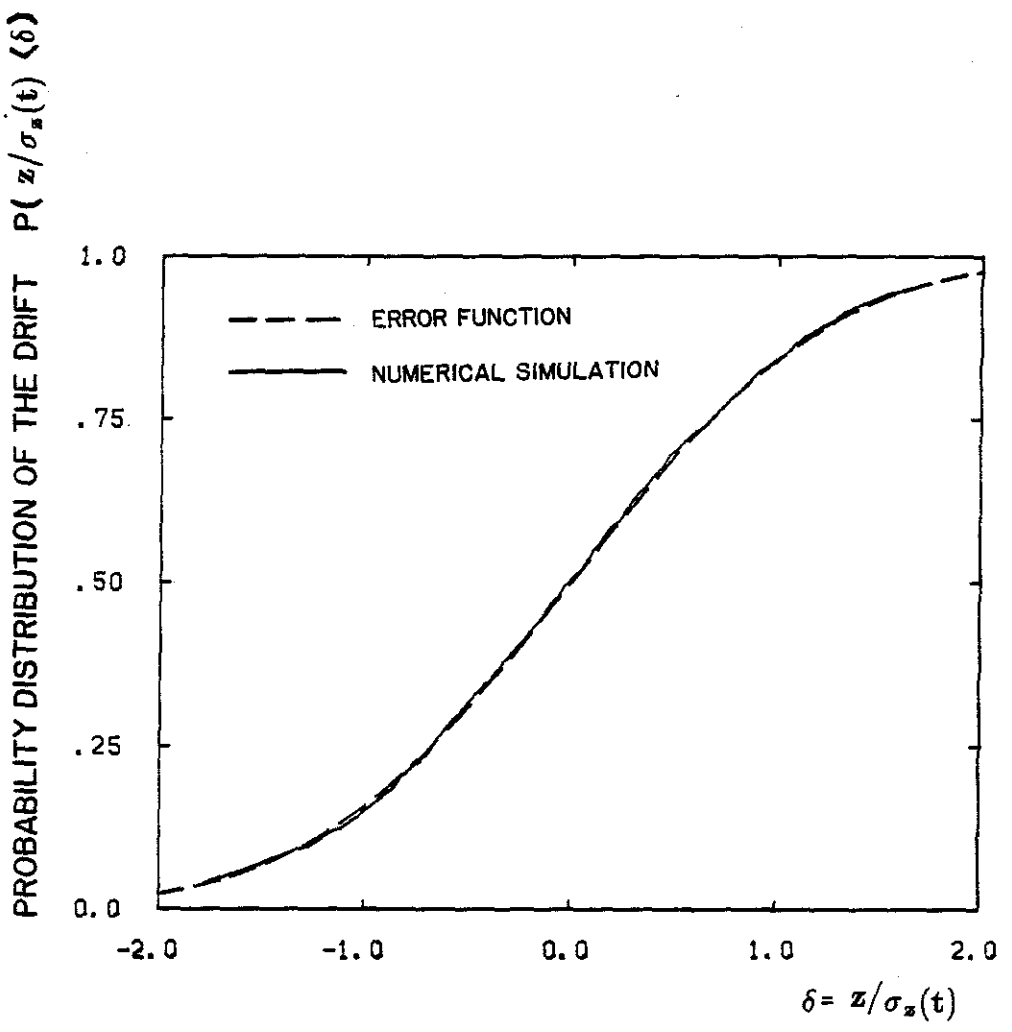

Figure 4.10
Probability distribution of the drift response at time $t = 20T_0$ and for S_0=0.40, ω_g/ω_0=1.0, ζ_g=0.50. Numerical simulation data obtained from 2500 samples of drift response.

4.6.4 The first passage problem.

For a Brownian motion, the first passage probability of a type-D barrier level at $|z| = \gamma\sigma_z(t)$ is equal to

$$\text{Prob}\left(\left|\frac{z(t)}{\sigma_z(t)}\right| < \gamma \quad \forall s \in (0,t)\right) = p_0(\gamma) \tag{4.87}$$

and is independent of t. Equation (4.87) also gives the probability distribution for the peak drift response

$$z_{max}(t) = \max_{s\in(0,t)} |z(s)|. \tag{4.88a}$$

From (4.87) and (4.88a) it is implied that

$$\text{Prob}\left(\left|\frac{z_{max}(t)}{\sigma_z(t)}\right| < \gamma\right) = p_0(\gamma). \tag{4.88b}$$

In Figure 4.11, the simulated probability distributions for the normalized peak drift response at $t = 15T_0$ and $25T_0$ are compared with the corresponding analytical curve $p_0(\gamma)$, for the parameters values $S_0 = 0.40$, $\varsigma_g = 0.50$, $\varsigma = 0.01$ and $\omega_g = 1.0$, and for 2500 simulated records. It can be seen that in this case, the analytical results are in excellent agreement with the simulation results. A statistical examination of the first passage probability is performed over the 54 cases considered in this analysis, as follows.

Define $\gamma_{j,i}(t)$, as the normalized peak drift response for the i^{th} studied case, corresponding to survival probability p_j. This implies that for the i^{th} set of excitation parameters, the survival probability for the drift response is given by

$$\text{Prob}\left(\frac{z_{max}(t)}{\sigma_z(t)} < \gamma_{j,i}(t)\right) = p_j. \tag{4.89a}$$

Consider the mean $m_\gamma^j(t)$ and the RMS value $\sigma_\gamma^j(t)$ of the variable $\gamma_{j,i}(t)$, defined as

$$m_\gamma^j(t) = \frac{1}{N}\sum_{i=1}^{N} \gamma_{j,i}(t) \tag{4.89b}$$

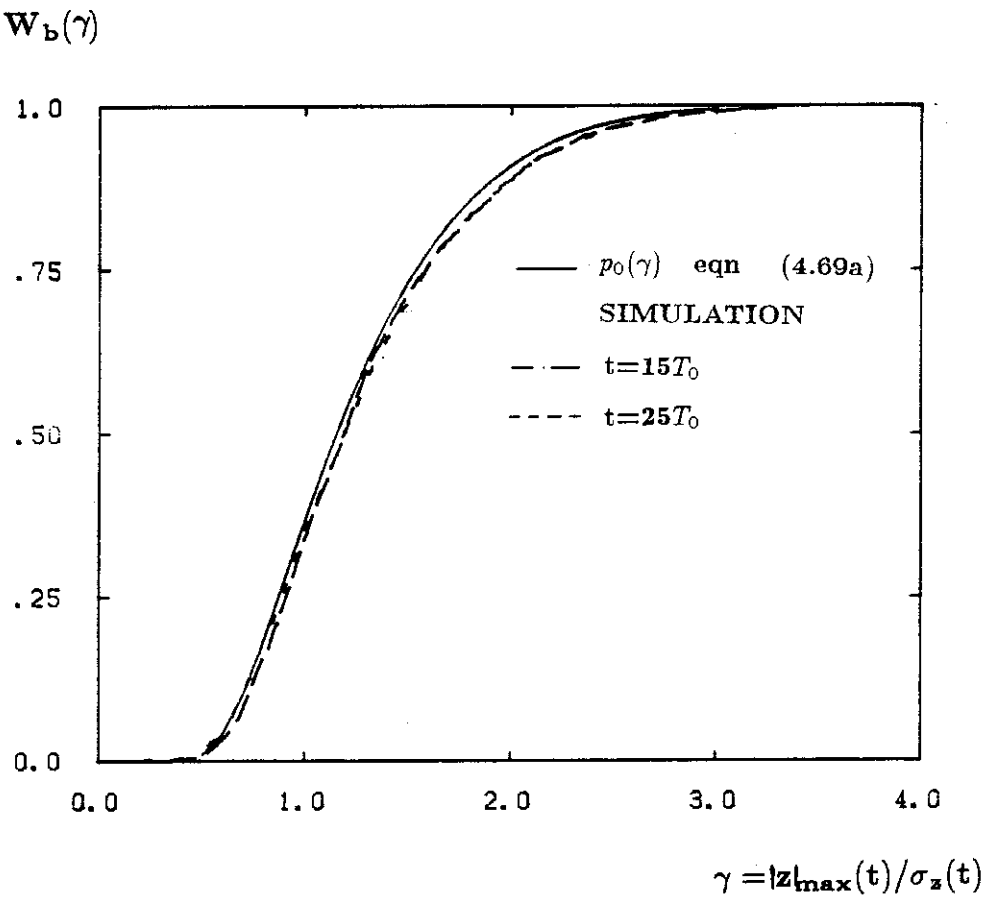

Figure 4.11
Probability distribution of the normalized peak drift response at time t=15T_0 and 25T_0, for S_0=0.40, ω_g/ω_0=1.0, ζ_g=0.50. Numerical simulation data obtained from 2500 samples of drift response. The results suggest the Brownian motion nature of the drift of an elasto-plastic system.

$$\sigma_\gamma^j(t)^2 = \frac{1}{N-1}\sum_{i=1}^{N}(\gamma_{j,i}(t) - m_j(t))^2. \qquad (4.89c)$$

where N is the number of simulation cases considered. In Figure 4.12a and 4.12b, the analytical prediction for the first passage probability distribution, $p_0(\gamma)$, is compared to the corresponding simulation results, $m_\gamma^j(t) \pm \sigma_\gamma^j(t)$, for cases corresponding to $\frac{\omega_a}{\omega_0} \leq 1$ and for durations $t = 25T_0$ and $t = 15T_0$, respectively. It can be noticed that the simulation results, calculated from a set of 36 samples, are in excellent agreement with the analytical prediction. Similar conclusions can be drawn for cases corresponding to $\frac{\omega_a}{\omega_0} \geq 1$, as illustrated in Figure 4.13. In this case the simulation results were calculated from a set of 27 samples. In Figures 4.12 and 4.13, the results are also compared to the approximate expression for $p_0(\gamma)$, given by equation (4.77). From this comparison, it can be concluded that the approximate expression (4.77), can be used for large values of the normalized peak response, or for $\gamma > 1.5$.

Finally, if one considers the small sample used for each simulation study (250 records), the results may be considered in excellent agreement with the analytical prediction.

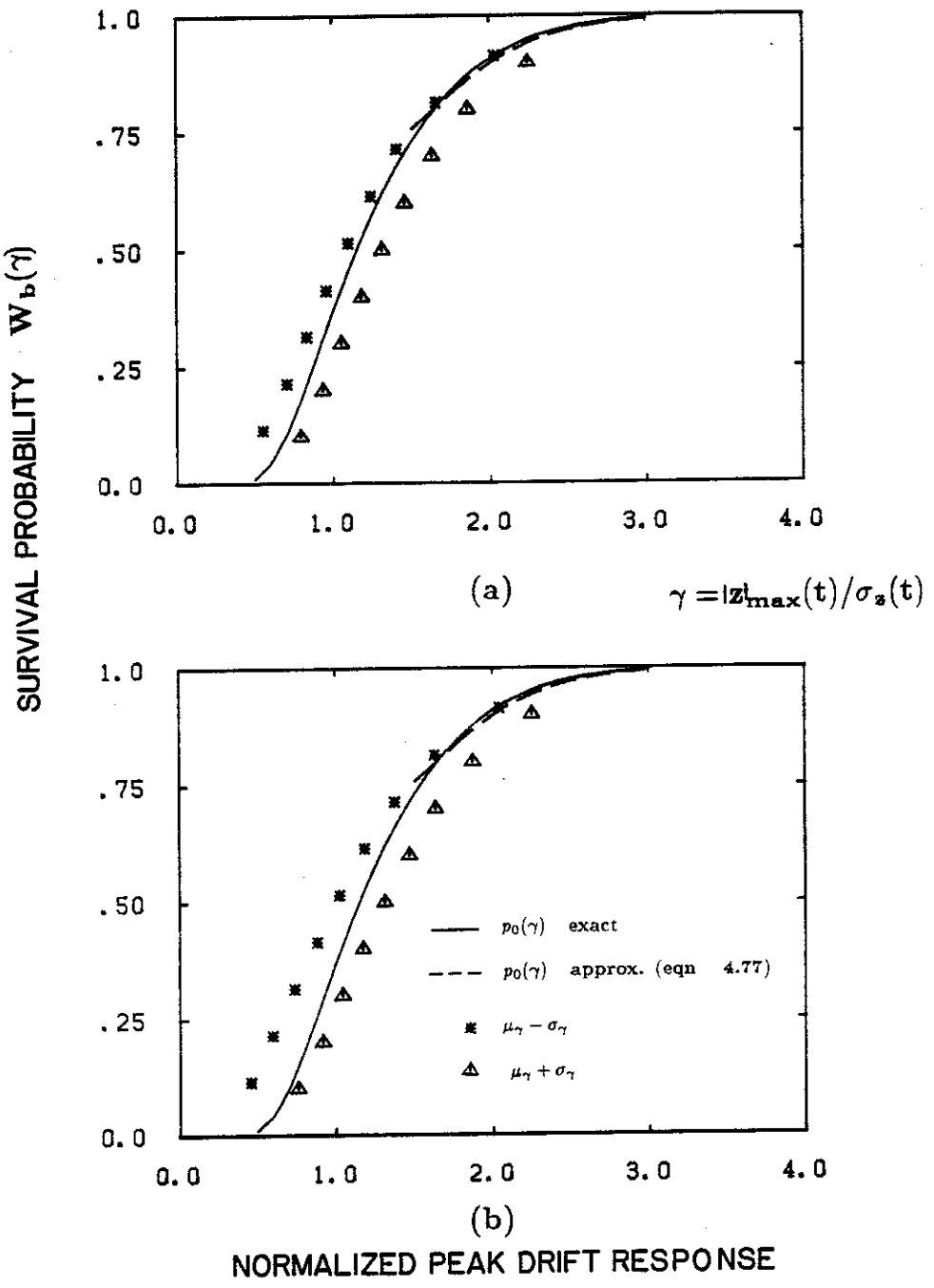

Figure 4.12
Statistical examination of the peak drift response probability distribution. Simulation data obtained for cases corresponding to $\omega_g/\omega_0 \leq 1$. The results are compared to the corresponding probability distribution of a Brownian motion. (a) $t = 25T_0$, (b) $t = 15T_0$.

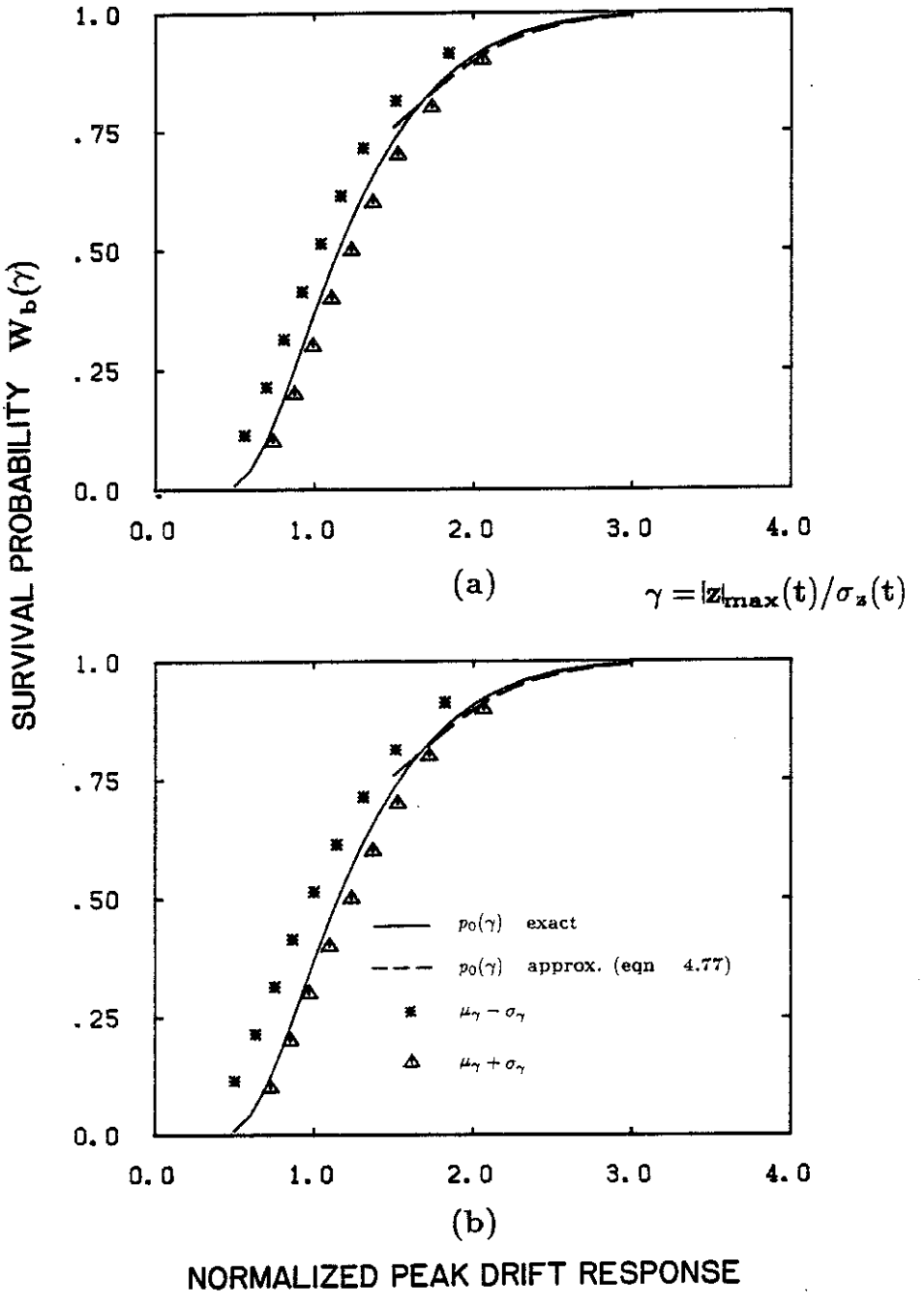

Figure 4.13
Statistical examination of the peak drift response probability distribution. Simulation data obtained for cases corresponding to $\omega_g/\omega_0 \geq 1$. The results are compared to the corresponding probability distribution of a Brownian motion. (a) $t = 25T_0$, (b) $t = 15T_0$.

4.7 Conclusion.

The analytical results and the simulation study presented in this Chapter suggest that for long duration strong motion excitation the elasto-plastic system exhibits a Brownian motion type of behaviour. Such behaviour is observed for durations of at least $15T_0$, which for an actual structural system corresponds to duration of approximately 3-45 sec. The implications of this observation are very significant for the analysis of the random response of elasto-plastic systems.

For the case of a stationary excitation, the drift response is a zero mean Gaussian distributed random process, with transient mean square value given approximately by

$$\sigma_z^2(t) \approx Q_0[0.5 + \nu_Y A(t - T_{ex})] \quad \text{for } t \geq T_{ex}. \tag{4.90a}$$

The peak drift probability distribution is approximately given by

$$\text{Prob}\left(\left|\frac{z_{max}(t)}{\sigma_z(t)}\right| < \gamma\right) = p_0(\gamma). \tag{4.90b}$$

It was shown that the dependence of the correlation factor, A, on system and excitation parameters is very complex. It also appears that an analytical expression for A is extremely difficult to obtain. From the results derived in Section 4.5 and their comparison with simulation results presented in Section 4.6, it can be concluded, however, that at least an approximate relation between A and the transition probabilities p^+ and p^- can be derived. The strong correlation between the two quantities also suggests the need of a solution scheme for the calculation of the transition probabilities p^+ and p^-. In the analysis presented in this thesis, it will be assumed that the correlation factor is simply given by

$$A = \frac{p^+}{p^-}. \tag{4.64a}$$

From these observations it is concluded that the random response of an elasto-plastic system subjected to stationary stochastic excitation is approximately determined by the conditional probabilities, p^+ and p^-, mean square value yield increment, Q_0, the mean rate of yield occurence, ν_Y, and the expected time of the first yield occurence, T_{ex}. Based on the analytical results obtained in this chapter, an approximate solution for the problem is introduced in Chapter 5.

The analysis presented in this chapter provides useful information regarding the nature of the displacement response behaviour. A measure of the narrow-bandness of the elastic component response is given by the transition probabilities p^+ and p^-. In contrast, the drift component of the response does not exhibit oscillatory behaviour and can be approximately considered as a Brownian motion.

Chapter 5. APPROXIMATE SOLUTION FOR THE RANDOM RESPONSE OF AN ELASTO-PLASTIC SYSTEM.

5.1 Introduction.

From the analysis presented in Chapter 4, it was concluded that the drift statistics can be approximately expressed in terms of the transition probabilities, p^+ and p^-, mean square value yield increment, Q_0, and the mean rate of yield occurance, ν_Y. Based on this observation, an approximate solution for the random reponse of an elasto-plastic system subjected to filtered white noise excitation is derived.

As will be shown later in this chapter, p^+, Q_0 and ν_Y can be calculated from the stationary probability density $p^s_{\dot{x}y}(\dot{x}, y)$, of the velocity, $\dot{x}$, and elastic component of the displacement response, y. Karnopp and Scharton (39), Vanmarcke and Veneziano (40) and Ditlevsen (42) calculated $p^s_{\dot{x}y}$ from the response of an associated linear system governed by equation (4.15c). It is understood that such an assumption is approximately valid only for the case of infrequent and small plastic deformations. To avoid this restriction, Grossmayer (41) calculated $p^s_{\dot{x}y}$ from the response statistics of an equivalent linear system, defined as the limit of a reccurent algorithm.

In the method presented in this chapter, there is no need for consideration of an associated linear system because, as shown in Section 4.3, the elasto-plastic system is formulated in terms of an additional response variable ϕ, correponding to the elastic component of the displacement response. In Section 4.3 it was also shown that the equivalent linear system defined by equations (3.7), (3.8) and (3.14)-(3.18) gives very good approximate results for the response statistics associated with the variables $(\dot{x}, \phi)$. But for $|\phi| < 1$, $y = \phi$ and $\dot{y} = \dot{x}$, which implies that $p^s_{\dot{x}y}$ can be calculated by the equivalent linearization technique and

is a zero mean two-dimensional Gaussian distribution. Based on $p^s_{\dot{x}y}$, the yield increment statistics are obtained in Section 5.2, while in Section 5.3, a new solution technique for the calculation of the mean rate of yield occurence, ν_Y is presented. Estimates for the transition probabilities, p^+ and p^-, are calculated in section 5.4, from an approximate solution of the first passage problem associated with the crossing of the yielding level by the y process. Finally, the results for the drift statistics obtained by this approximate solution scheme, are discussed in Section 5.4.5.

5.2 Yield increment statistics.

5.2.1 Response statistics for the upcrossing velocity process.

In Chapter 4 it was shown that the conditional probability density $p_{v_y}(v_y)$ can be expressed in terms of $p^s_{\dot{x}y}$ as

$$p_{v_y}(v_y) = \lim_{\epsilon \to 0} \frac{v_y p^s_{\dot{x}y}(v_y, 1-\epsilon)}{\int_0^\infty \dot{x} p^s_{\dot{x}y}(\dot{x}, 1-\epsilon) d\dot{x}} \quad \text{for } v_y \geq 0. \tag{4.33}$$

But, $p^s_{\dot{x}y}$ is a zero mean two dimensional Gaussian distribution with covariance matrix $\mathbf{Q}^s$ defined by (2.63c) and (3.3a). Thus

$$p^s_{\dot{x}y}(\dot{x}, 1) = \frac{1}{2\pi\sqrt{\det \mathbf{Q}^s}} \exp\left(-\frac{(\dot{x}-\mu_y)^2}{2s^2}\right), \tag{5.1a}$$

with

$$\mu_y = \frac{Q_{\dot{x}\phi}}{Q_{\phi\phi}} \tag{5.1b}$$

and

$$s^2 = \frac{Q_{\dot{x}\dot{x}} Q_{\phi\phi} - Q^2_{\dot{x}\phi}}{Q_{\phi\phi}}. \tag{5.1c}$$

From equations (4.33) and (5.1)

$$p_{v_y}(v_y) = \frac{1}{B^{(1)}} \exp\left(-\frac{(v_y-\mu_y)^2}{2s^2}\right), \tag{5.2a}$$

where $B^{(k)}$ is defined by

$$B^{(k)} = \int_0^\infty v_y^k \exp(-\frac{(v_y - \mu_y)^2}{2s^2}) dv_y \tag{5.2b}$$

A recurrent algorithm for the calculation of $B^{(k)}$'s is presented in Appendix D. From (5.2), the mean and mean square value for the upcrossing velocity v_y are then given by

$$E[v_y] = \frac{B^{(2)}}{B^{(1)}} \tag{5.3a}$$

$$E[v_y^2] = \frac{B^{(3)}}{B^{(1)}}. \tag{5.3b}$$

For most cases examined in this analysis

$$|Q_{\dot{x}\phi}| \ll \sqrt{Q_{\dot{x}\dot{x}} Q_{\phi\phi}}. \tag{5.4a}$$

Hence it can be assumed that $p_{\dot{x}y}^s$ is approximately a zero mean Gaussian distribution, which implies that the probability density $p_{v_y}(v_y)$ is approximately Rayleigh distributed, and given by

$$p_{v_y}(v_y) \approx \frac{v_y}{2b^2} exp(-\frac{v_y^2}{2b^2}). \tag{5.4b}$$

The RMS value b can be calculated from (4.36a) as

$$b = \sqrt{\frac{2}{\pi}} E[v_y]. \tag{5.4c}$$

This is used to define a simplified probability density function for the process v_y.

In Figure 5.1 and 5.2, the values for $E[v_y]$ and $E[v_y^2]$ obtained by equivalent linearization and equation (5.3), are compared with Monte Carlo simulation results for different values of S_0, ω_g/ω_0= 0.30, 0.50, 0.70, 1.0, 1.50, 3.0, 5.0 and for bandwidth of the excitation ζ_g= 0.25 and 0.50, respectively. The results are

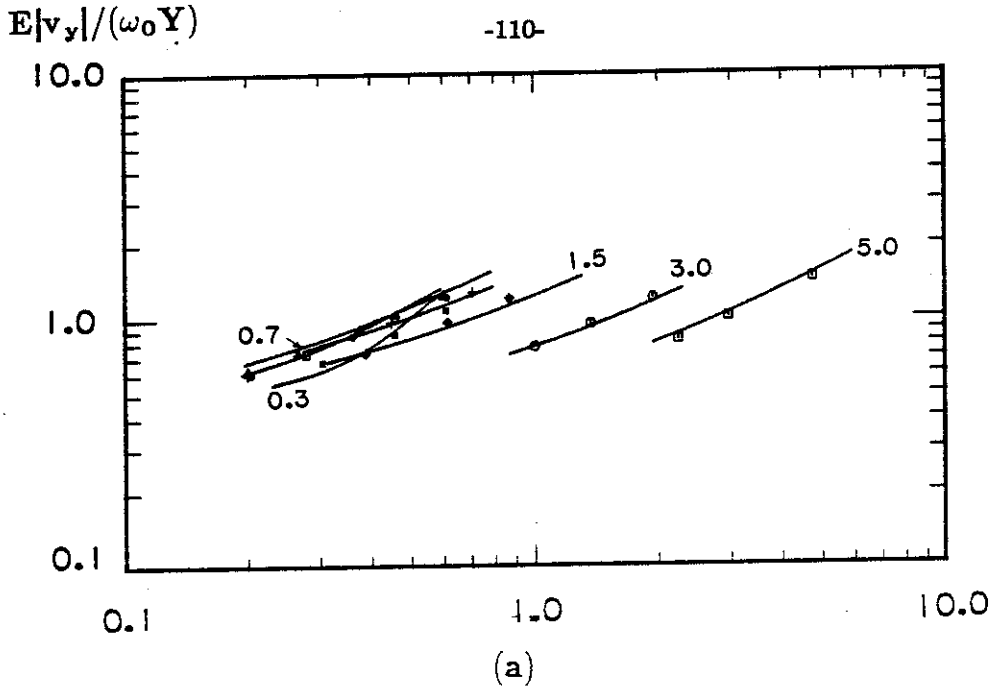

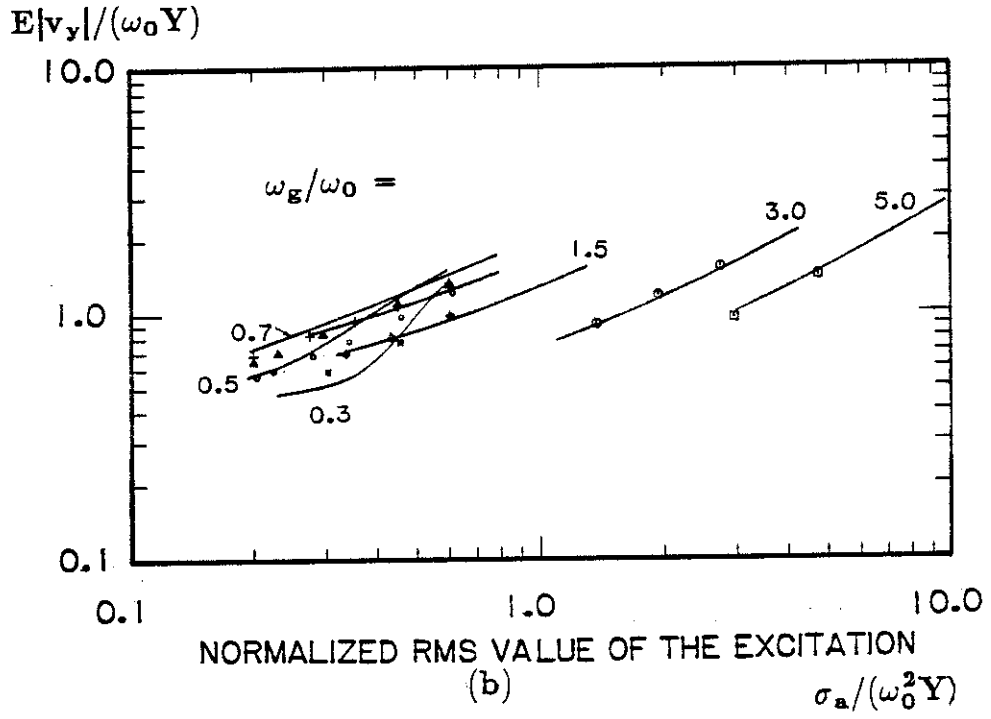

Figure 5.1
Parametric investigation for the stationary mean value of the upcrossing velocity, v_y, for the case of filtered modulated white noise excitation (eqno 2.27), ς=0.01. Bandwidth of the excitation (a) ς_g=0.50 (b) ς_g=0.25. Legend of simulation data given in Figure 4.0.

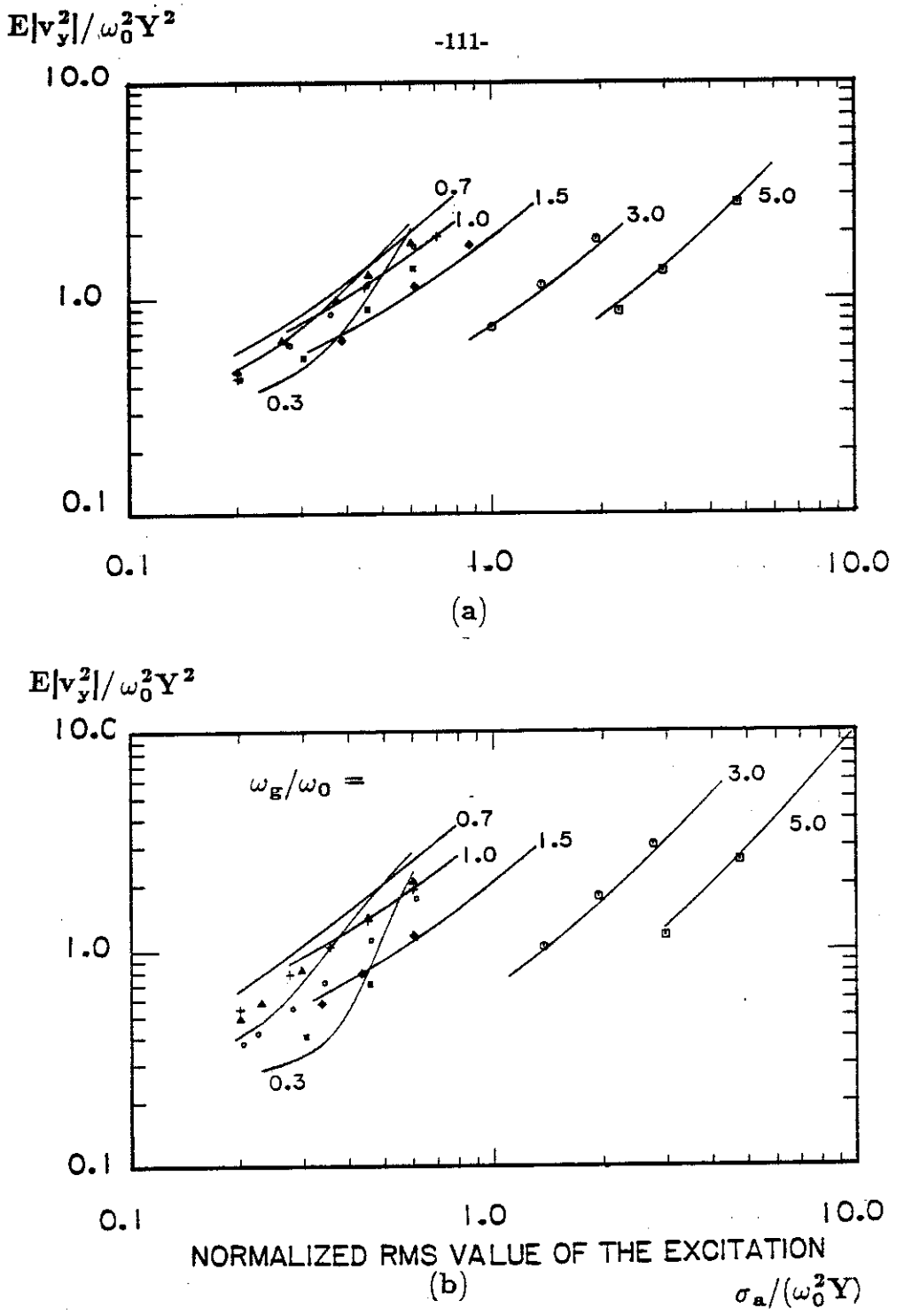

Figure 5.2
Parametric investigation for the stationary mean square value of the upcrossing velocity, v_y, for the case of filtered modulated white noise excitation (eqno 2.27), ς=0.01. Bandwidth of the excitation (a) ς_g=0.50 (b) ς_g=0.25. Legend of simulation data given in Figure 4.0.

presented in terms of the dimensionless groups defined by (4.2). It can be observed that the approximate solution gives very good overall results for a wide range of model parameters. Less accurate estimates are obtained for cases corresponding to $\omega_g/\omega_0 = 0.30,\ 0.50$ and weak excitation. The approximate Rayleigh distribution for the random varibale v_y is noticed for most cases examined.

5.2.2 Yield increment and yield duration statistics.

By substituting equation (5.2) in equations (4.46) and (4.47), the following expressions for the yield increment statistics are obtained:

$$E[t_y] = \frac{1}{(1-m_0)}\frac{B^{(2)}}{B^{(1)}} \tag{5.5}$$

$$E[d_y] = \frac{1}{2(1-m_0)}\frac{B^{(3)}}{B^{(1)}} \tag{5.6}$$

and

$$E[d_y^2] = \frac{1}{4(1-m_0)^2}\frac{B^{(5)}}{B^{(1)}}. \tag{5.7}$$

In equations (5.5)-(5.7), m_0 corresponds to the expected value of the excitation, conditional on yielding occurence in the positive direction. The equivalent linearization technique described in Section 4.3 was formulated in terms of the response variables $\{\dot{x}, \phi, x_g, \dot{x}_g\}$ and for an excitation model defined by equation (4.16a), as

$$-\ddot{a}(t) = 2\zeta_g\omega_g\dot{x}_g. \tag{4.16a}$$

By considering the transformation (4.16), an approximate zero mean three- dimensional Gaussian distribution for the response variables $(\dot{x}, \phi, -\ddot{a})$ can be derived. Call this solution $p_{\dot{x}\phi a}(\dot{x}, \phi, \ddot{a})$ and the related covariance matrix $\mathbf{Q}^s$.

Now,

$$y = g_1(\dot{x}, \phi, Y = 1), \tag{5.8}$$

and y=1 corresponds to the values $(\dot{x}, \phi) \in [0, \infty) \times [1, \infty)$. This implies that m_0 is given by

$$m_0 = \frac{\int_{-\infty}^{\infty} \int_0^{\infty} \int_1^{\infty} a p_{\dot{x}\phi a}(\dot{x}, \phi, a) d\phi d\dot{x} da}{\int_{-\infty}^{\infty} \int_0^{\infty} \int_1^{\infty} p_{\dot{x}\phi a}(\dot{x}, \phi, a) d\phi d\dot{x} da}. \tag{5.9}$$

By performing the integrations in equation (5.9), the following expression for m_0 is obtained:

$$m_0 = \frac{1}{\sqrt{2}} \frac{A_1 \frac{Q_{a\phi}}{Q_{\phi\phi}^{1/2}} \exp\left(-\frac{1}{2Q_{\phi\phi}}\right) + A_2 \frac{Q_{a\dot{x}}}{Q_{\dot{x}\dot{x}}^{1/2}}}{\int_{\frac{1}{\sqrt{2Q_{\phi\phi}}}}^{\infty} e^{-t^2} (1 + \mathrm{erf}(\frac{\rho}{\sqrt{1-\rho^2}} t)) dt}, \tag{5.10a}$$

where A_1, A_2 and ρ are given by

$$A_1 = 1 + \mathrm{erf}\left(\frac{Q_{\dot{x}\phi}}{\sqrt{2Q_{\phi\phi}(Q_{\dot{x}\dot{x}}Q_{\phi\phi} - Q_{\dot{x}\phi}^2)}}\right) \tag{5.10b}$$

$$A_2 = 1 - \mathrm{erf}\left(\sqrt{\frac{Q_{\dot{x}\dot{x}}}{2(Q_{\dot{x}\dot{x}}Q_{\phi\phi} - Q_{\dot{x}\phi}^2)}}\right) \tag{5.10c}$$

$$\rho = \frac{Q_{\dot{x}\phi}}{\sqrt{Q_{\dot{x}\dot{x}}Q_{\phi\phi}}}. \tag{5.10d}$$

In Figure 5.3, the approximate results for m_0 obtained from equivalent linearization and equation (5.9) are illustrated. It can be noticed that for $\omega_g/\omega_0 < 1$, m_0 is positive, while for $\omega_g/\omega_0 > 1$, m_0 is negative. For cases corresponding to $\omega_g/\omega_0 \approx 1$, m_0 is practically equal to zero.

By substituting equation (5.10) into equations (5.5)-(5.7), the expected values $E[t_y]$, $E[d_y]$, $E[d_y^2]$ are obtained. The approximate results are shown in Figures 5.4, 5.5 and 5.6 respectively. It can be noticed that the yield increment statistics are strongly dependent on the characteristic frequency and the RMS value of the excitation, while a weaker dependence on the bandwidth of the excitation is observed. For drift response of practical interest, and for $\omega_g/\omega_0 < 1$, large magnitude yield increments are observed. By comparison with Monte

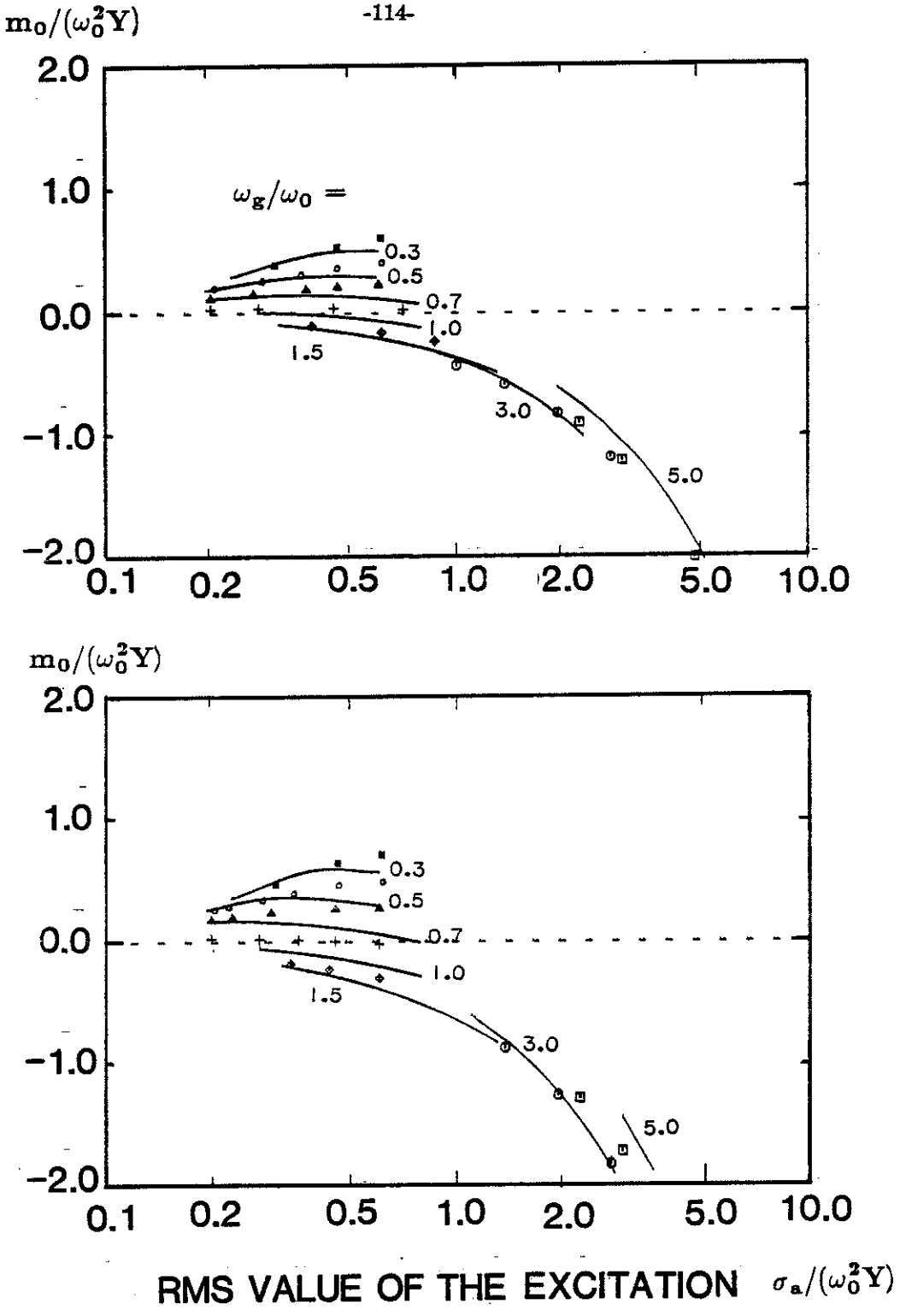

Figure 5.3
Variation of the conditional expected value, m_0, with the characteristic frequency and the strength of the excitation. (a) ζ_g=0.50 (b) ζ_g=0.25. Legend of the simulation data given in Figure 4.0.

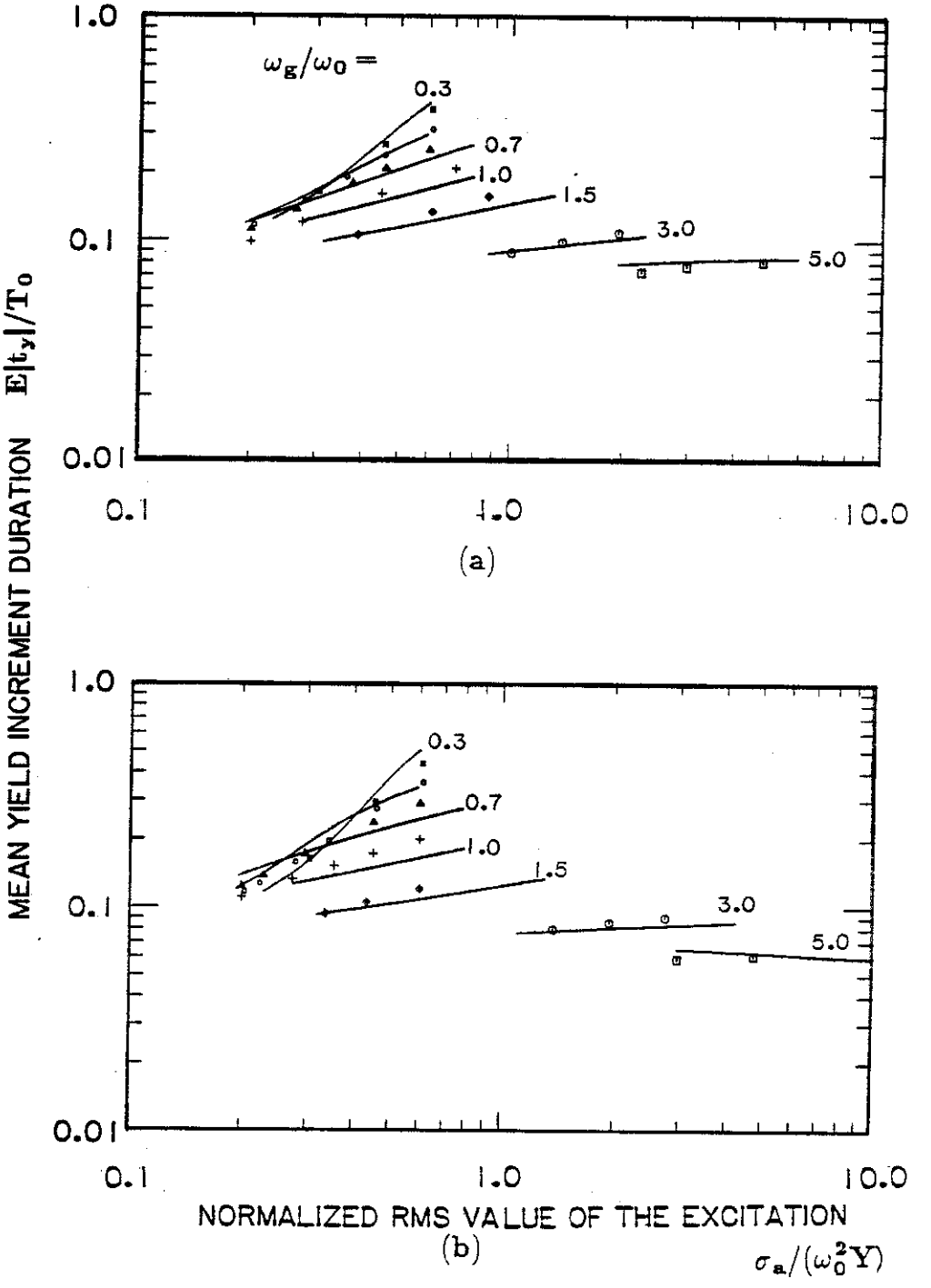

Figure 5.4
Stationary mean value of the yield duration, t_y, for bandwidth of excitation, (a) ς_g=0.50 (b) ς_g=0.25. Legend of simulation data given in Figure 4.0.

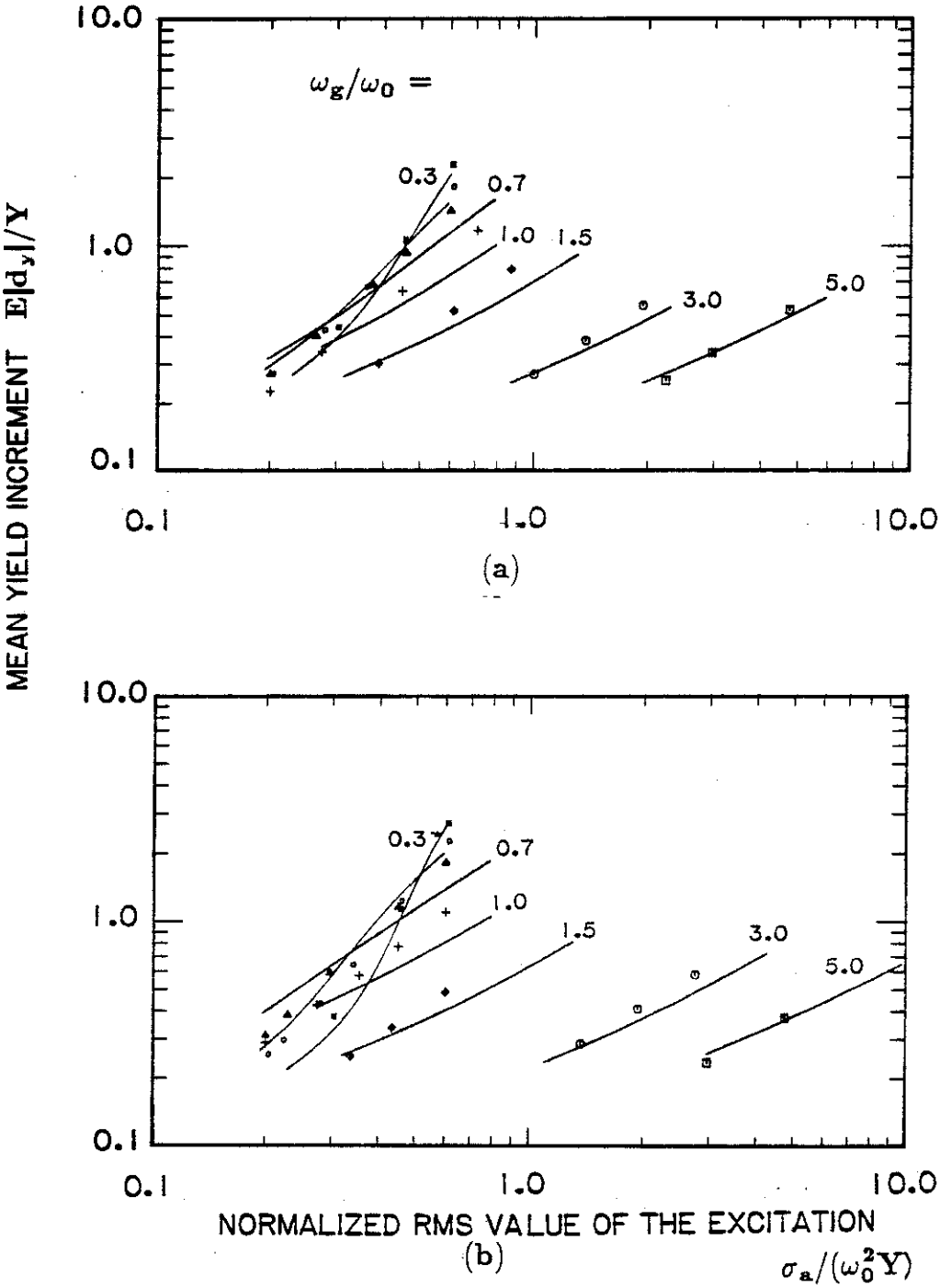

Figure 5.5
Stationary mean value of the yield increment, d_y, for bandwidth of excitation, (a) ζ_g=0.50 (b) ζ_g=0.25. Legend of simulation data given in Figure 4.0.

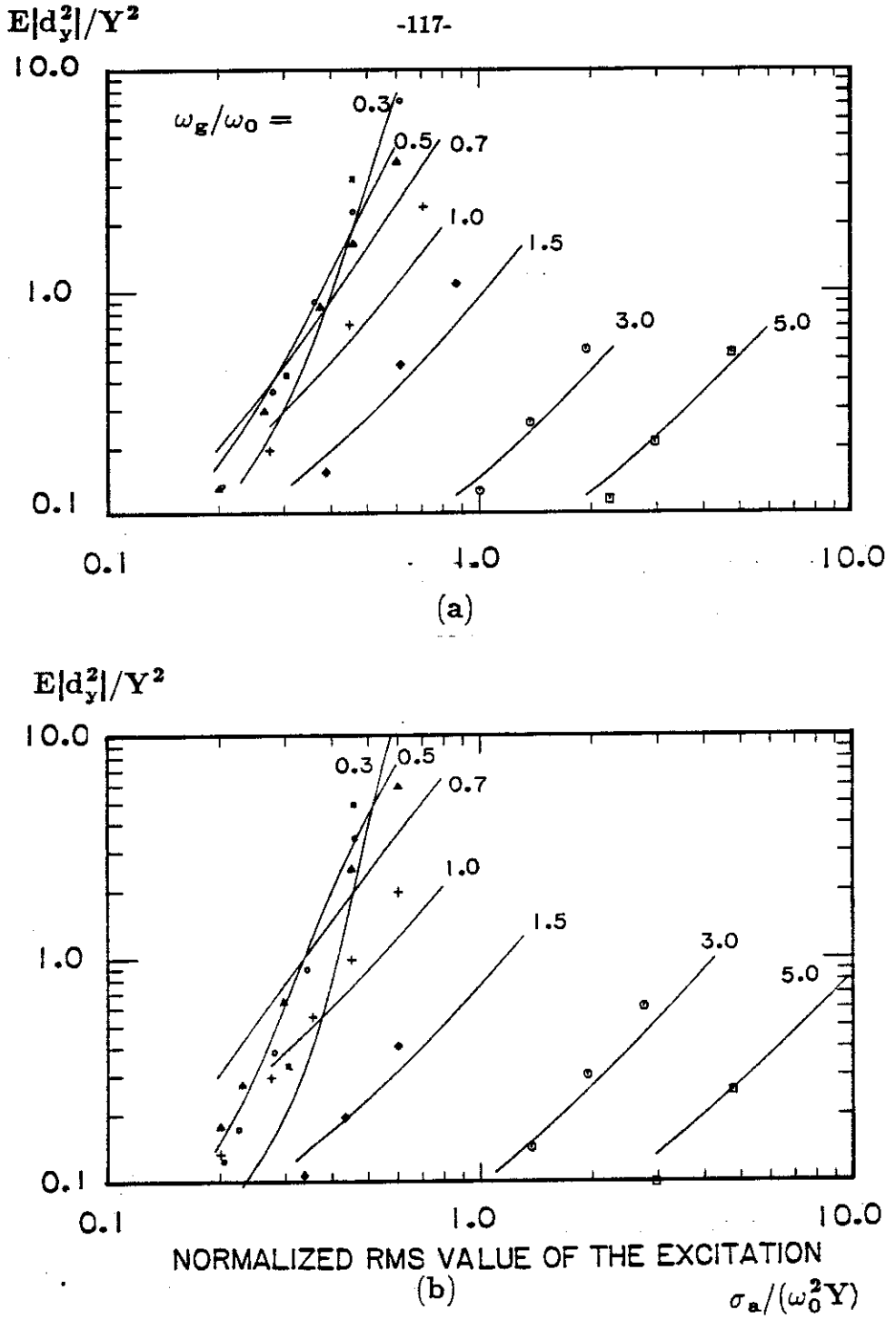

Figure 5.6
Stationary mean square value of the yield increment, d_y, for bandwidth of excitation, (a) ζ_g=0.50 (b) ζ_g=0.25. Legend of simulation data given in Figure 4.0.

Carlo simulations results, it is concluded that the solution scheme defined can be used in the prediction of the yield increment statistics, even for cases corresponding to large inelastic response.

5.2.3 Concluding remarks.

In Sections 5.2.1 and 5.2.2, an approximate solution scheme was developed for the calculation of the first order probability for the yield increment process. The method is based on the calculation of the stationary response statistics for the variables $\mathbf{u}^{\mathbf{T}} = \{\dot{x}, \phi, x_g, \dot{x}_g\}$ with the use of the equivalent linearization technique. The mean values for the processes d_y, t_y and v_y were calculated from the stationary solution of the equivalent linear system, with the use of the equations (4.33), (5.2) and (5.5)-(5.7). By assuming a constant value for the excitation during yielding, simple relations between d_y, t_y and v_y were established. It should be pointed out that relations (4.44) and (4.45) can be used not only for the calculation of mean values for the yield increment statistics, but also as a transformation for the associated probability density functions of the random variables d_y and t_y as shown in Figure 5.7.

The first order probability density of the yield increment process is approximately determined if a Rayleigh distribution is assumed for the v_y process. Then, by substituting equations (4.44) and (4.45) into equation (5.4b), and by appropriate change of variables, the approximate exponential and Rayleigh distribution for the random variables d_y, t_y is established. Based on simulation results, Vanmarcke (40) also suggested that the drift increment process has an exponential distribution, while Grossmayer (41) considered a Gaussian distribution for the yield increment duration t_y. The difference between the results obtained by Grossmayer and the results presented in this section, may be attributed to the stochastic excitation model. For the case of seismic excitation

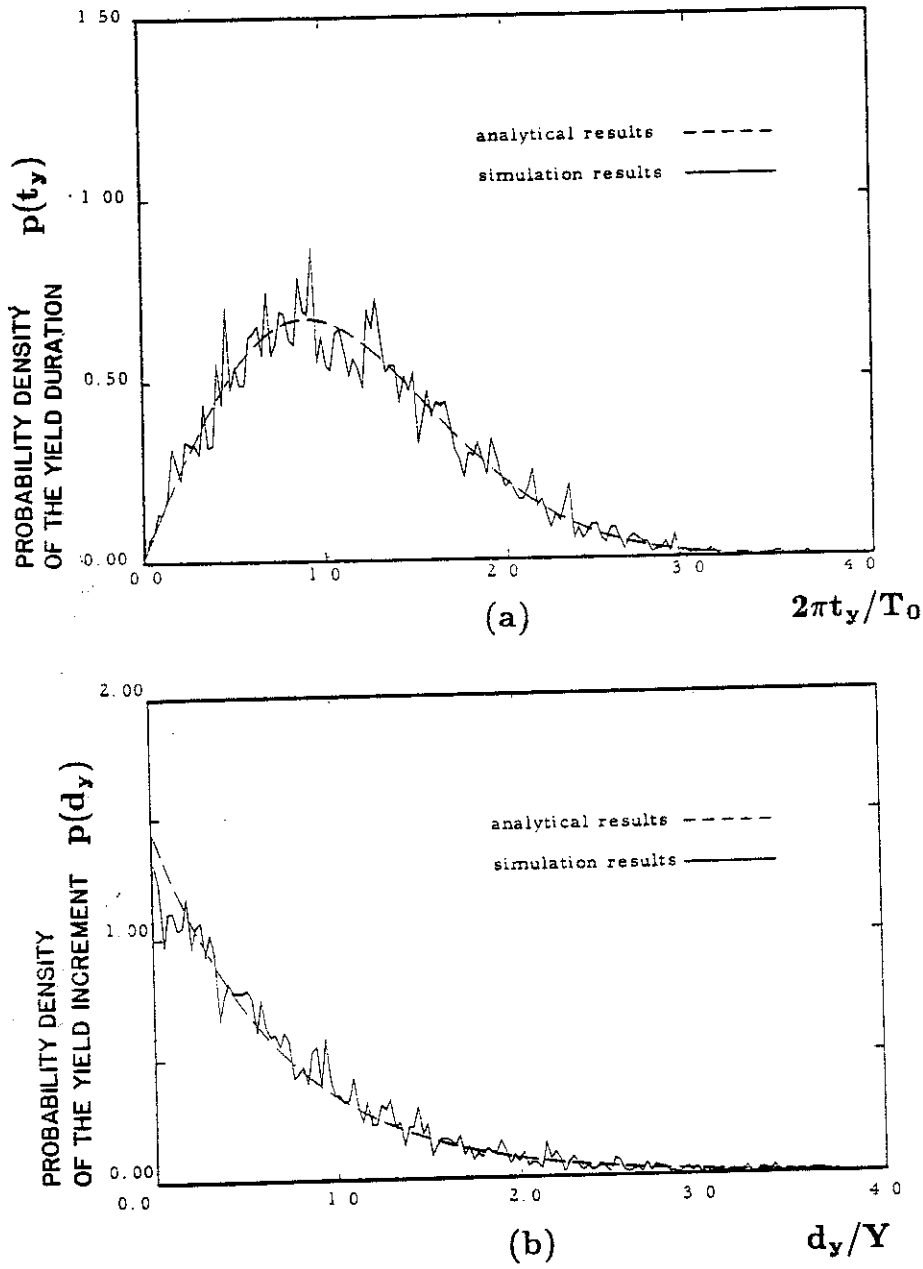

Figure 5.7
Probability density function of the (a) yield duration, t_y (b) yield increment, d_y, for parameter values S_0=0.40, ω_g/ω_0=0.70 and bandwidth of excitation, ζ_g=0.50.

with a characteristic frequency, ω_g, and no zero frequency content, the probability density p_{v_y} is approximately Rayleigh distributed. In contrast, for white noise excitation, irregular clumping of the yield level crossing by the process y, may occur. In this case, a complex structure for the probability density $p_{\dot{x}y}(\dot{x}, y)$ is observed, and the simplified transformations (4.44) and (4.45) can not be used for the calculation of first order probability density of the yield increment process.

5.3 Mean rate of yield occurence.

In previous analyses by Vanmarcke and Grossmayer, the mean rate of yield occurence ν_Y was calculated as the crossing rate of the inelastic barrier levels, $y = \pm 1$, divided by the mean clumsize of an associate linear system. An alternative approach is introduced in this section. The solution is based on the ergodicity of the elastic component of the response. For the ergodic process y, ν_Y is given by

$$\nu_Y = \frac{1}{E[t_y^{(i)}] + E[t_{el}^{(i)}]} = \frac{E[t_y^{(i)}]}{E[t_y^{(i)}] + E[t_{el}^{(i)}]} \frac{1}{E[t_y^{(i)}]}, \tag{5.11}$$

where $t_Y^{(i)}$ and $t_{el}^{(i)}$ are the durations of the i^{th} segment of inelastic and elastic response, respectively, or

$$t_y^{(i)} = t_e^{(i)} - t_b^{(i)} \tag{5.12a}$$

and

$$t_{el}^{(i)} = t_b^{(i+1)} - t_e^{(i)}. \tag{5.12b}$$

Because the segments of inelastic and elastic response alternate, the stationary yielding probability p_Y is given by

$$p_Y = \frac{E[t_y^{(i)}]}{E[t_y^{(i)}] + E[t_{el}^{(i)}]}. \tag{5.13}$$

But p_Y can be calculated from the the stationary probability distribution of the response variables $(\dot{x}, \phi)$, as

$$p_Y = \text{erfc}\left(\frac{1}{\sqrt{2Q_{\phi\phi}}}\right). \tag{5.14a}$$

From (5.11), (5.13) and (5.14a)

$$\nu_Y = \frac{p_Y}{E[t_y]}, \tag{5.14b}$$

or

$$\nu_Y = \frac{B^{(1)}}{B^{(2)}}\text{erfc}\left(\frac{1}{\sqrt{2Q_{\phi\phi}}}\right)(1 - m_0) \tag{5.14c}$$

where $Q_{\phi\phi}0$, m_0, $B^{(1)}$ and $B^{(2)}$ calculated in Section 5.2. In Figures (5.8a) and (5.8b) the analytical results for the mean rate of yield occurance, obtained from (5.14c) and for the cases ς_g=0.50 and 0.25, are illustrated. It will be noticed that there is a good overall agreement between the analytical results and the simulation data. The method is not so accurate for the cases ω_g/ω_0 =0.30 and 0.50 and for bandwidth of the excitation ς_g =0.25. The error, however, may be attributed to the less accurate results predicted by equivalent linearization for these parameter values.

From the analytical results, it can be deduced that in general there are less than two yield occurances per period of oscillation. The number of yield occurances per period is practically independent of the strength of the excitation for the case $\omega_g/\omega_0 \approx 1$. On the contrary, the number of yield occurances is strongly dependent on the excitation strength in the other cases. By comparing these results with the yield increment statistics shown in Figures 5.4, 5.5, 5.6, it can be noticed that for a small ratio of ω_g/ω_0, few increments of large magnitude are present. However, for $\omega_g/\omega_0 \approx 1$, the yield increments are more uniformly distributed in time. This suggests a strong dependence of the yield increment

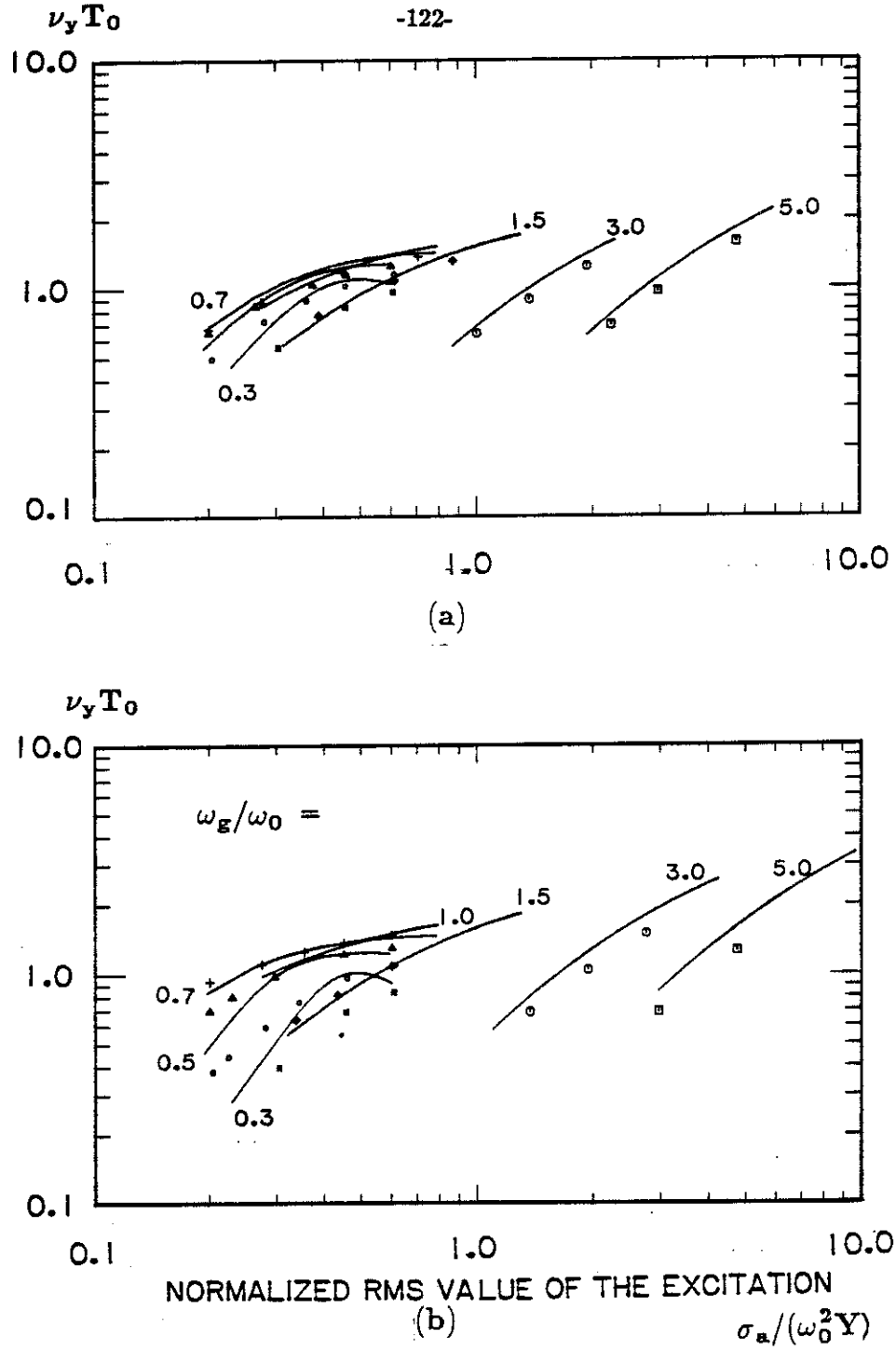

Figure 5.8
Stationary values for the mean rate of yield occurances, ν_y, for bandwidth of excitation, (a) ζ_g=0.50 (b) ζ_g=0.25. Legend of simulation data given in Figure 4.0.

statistics on the characteristic frequency of the excitation. On the other hand, the bandwidth of the excitation does not appear to play a very significant role in the yielding mechanism.

Finally, the simplicity of the solution scheme used in this analysis should be pointed out. Based on the ergodicity assumption, it was shown that the rate of yield occurance can be simply calculated from the stationary probability and mean duration of yielding.

5.4 Transition probabilities p^+ and p^-.

5.4.1 Formulation.

Without loss of generality, consider that the time t_e=0 corresponds to the end of a yield occurance in the positive direction, as illustrated in Figure 5.9. For $t \in (0, t_b)$, the elasto-plastic system behaves elastically, where t_b corresponds to the next crossing of the barrier levels $y = \pm 1$. The equation of motion is given by

$$\ddot{y} + 2\zeta\dot{y} + y = -\tilde{a}(t), \tag{5.15a}$$

with initial conditions

$$y(0) = 1 \tag{5.15b}$$

$$\dot{y}(o) = 0. \tag{5.15c}$$

The transition probabilities p^+ and p^- give the stationary probability for the direction of the next yield occurance, or

$$p^+ = \text{Prob}[y(t_b) = 1] \tag{5.16}$$

and

$$p^- = \text{Prob}[y(t_b) = -1]. \tag{5.17}$$

These can be calculated from the first passage probability of the corresponding barrier levels $y = \pm 1$.

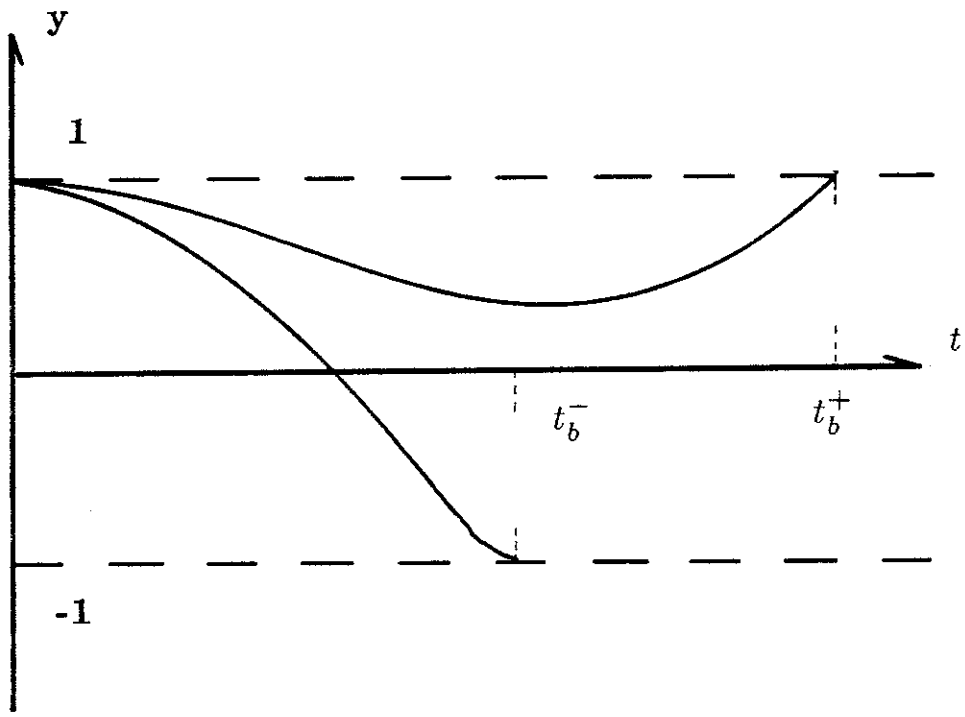

Figure 5.9
An illustration of the transition between the two inelastic states, corresponding to yielding in positive or negative direction.

Strictly speaking, the problem is ill posed because the initial condition lays on the boundary of the safe domain. For this reason, an exact solution can not be obtained. The approximate solution scheme proposed in this section is based on the relationship between the survival probability $W_b(t)$ and the conditional transition probability $q_b(y, \dot{y}, t)$, where

$$p_b(t) = -\frac{dW_b}{dt} = \int_0^\infty \dot{y} q_b(1, \dot{y}, t) d\dot{y} - \int_{-\infty}^0 \dot{y} q_b(-1, \dot{y}, t) d\dot{y}. \tag{5.18a}$$

It can be shown that

$$W_b(t) = \int_{-\infty}^\infty \int_{-1}^1 q_b(y, \dot{y}, t) dy d\dot{y}. \tag{5.18b}$$

From equation (5.18) it is implied that the transition probabilities p^+ and p^- are given by

$$p^+ = \int_0^\infty \int_0^\infty \dot{y} q_b(1, \dot{y}, t) d\dot{y} dt \tag{5.19a}$$

and

$$p^- = -\int_0^\infty \int_{-\infty}^0 \dot{y} q_b(-1, \dot{y}, t) d\dot{y} dt. \tag{5.19b}$$

Define

$$p_0^+(t) = \int_0^t \int_0^\infty \dot{y} q_b(1, \dot{y}, \tau) d\dot{y} d\tau \tag{5.20a}$$

$$p_0^-(t) = -\int_0^t \int_{-\infty}^0 \dot{y} q_b(-1, \dot{y}, \tau) d\dot{y} d\tau \tag{5.20b}$$

as the probabilities of leaving the safe domain $(-1, 1)$ at time $s \in (0, t)$, through the barrier levels $y = 1$ and $y = -1$, respectively.

Equation (5.18a) also can be written in the form

$$\frac{dW_b}{dt} = -W_b(t)(\alpha_+(t) + \alpha_-(t)), \tag{5.21a}$$

with

$$\alpha_+(t) = \frac{1}{W_b(t)} \int_0^\infty \dot{y} q_b(1, \dot{y}, t) d\dot{y} \tag{5.21b}$$

$$\alpha_-(t) = -\frac{1}{W_b(t)} \int_{-\infty}^{0} \dot{y} q_b(-1, \dot{y}, t) d\dot{y}. \tag{5.21c}$$

The solution for $W_b(t)$ satisfying (5.21a) is given by

$$W_b(t) = \exp\left[- \int_0^t (\alpha_+(\tau) + \alpha_-(\tau)) d\tau \right]. \tag{5.22}$$

But from equations (5.20) and (5.21), the following expressions are obtained:

$$p_0^+(t) = \int_0^t \alpha_+(\tau) W_b(\tau) d\tau \tag{5.23a}$$

$$p_0^-(t) = \int_0^t \alpha_-(\tau) W_b(\tau) d\tau. \tag{5.23b}$$

Equation (5.22) is often used for the calculation of the reliability function of a random process, and $\alpha_+(t)$ and $\alpha_-(t)$ are empirically calculated from the transition probability of the process. The derivation of equation (5.22) offers an alternative interpretation for the functions $\alpha_+(t)$ and $\alpha_-(t)$.

5.4.2 Transition probability density for elastic response.

For the excitation model used in this analysis, the ground motion acceleration is given by

$$-\ddot{a}(t) = 2\zeta_g \omega_g \dot{x}_g \tag{5.24a}$$

$$\ddot{x}_g + 2\zeta_g \omega_g \dot{x}_g + \omega_g^2 x_g = \xi(t), \tag{5.24b}$$

where $\xi(t)$ is a Gaussian white noise signal. This implies that the generalized response vector $\mathbf{v}^{\mathbf{T}} = \{y, \dot{y}, x_g, \dot{x}_g\}$ will satisfy the linear stochastic differential equations (5.15) and (5.24). While the initial conditions $(y, \dot{y})_{t=0}$ are given by (5.15), the initial conditions for the $(x_g, \dot{x}_g)$ process are obtained from the first passage problem associated with the inelastic response. Due to the complexity of this problem, an exact solution for the probability density function $p(x_g(0), \dot{x}_g(0))$ is practically impossible to obtain. The following solution scheme is proposed.

Consider that the time $t = -E[t_y]$ represents the starting time of an idealized yield occurance in the positive direction. Define m_{x_g} and $m_{\dot{x}_g}$, the expected values for the variables x_g and $\dot{x}_g$, conditional on yielding in positive direction. Following the procedure developed in Section 5.2.2, m_{x_g} and $m_{\dot{x}_g}$ can be calculated from equivalent linearization (see equation 5.10). It is assumed that for the idealized yield occurance, m_{x_g} and $m_{\dot{x}_g}$ represent the exact mean values for the variables $(x_g, \dot{x}_g)$ at time $T_Y = -\frac{1}{2}E[t_y]$. Because $(x_g, \dot{x}_g)$ is a solution of a linear stochastic differential equation, an approximate expression for $E[x_g(0)]$ and $E[\dot{x}_g(0)]$ is obtained as

$$E[x_g(0)] = e^{-\zeta_g \omega_g T_Y}\left(\frac{(\zeta_g \omega_g m_{x_g} + m_{\dot{x}_g})}{\omega_g\sqrt{1-\zeta_g^2}}\sin(\omega_{gd}T_Y) + m_{x_g}\cos(\omega_{gd}T_Y)\right) \quad (5.25a)$$

and

$$E[\dot{x}_g(0)] = e^{-\zeta_g \omega_g T_Y}\left(-\left(\frac{\omega_g}{\sqrt{1-\zeta_g^2}}m_{x_g} - \frac{\zeta_g}{\sqrt{1-\zeta_g^2}}m_{\dot{x}_g}\right)\sin(\omega_{gd}T_Y) + m_{\dot{x}_g}\cos(\omega_{gd}T_Y)\right), \quad (5.25b)$$

with ω_{gd} given by

$$\omega_{gd}^2 = \omega_g^2(1-\zeta_g^2). \quad (5.25c)$$

It will be assumed that $(x_g(0), \dot{x}_g(0))$ are Gaussian distributed, with mean values given by (5.25), and covariance approximately given by the stationary values

$$\sigma^2_{x_g(0)} = \frac{S_0}{4\zeta_g\omega_g^3} \quad (5.26a)$$

$$\sigma^2_{\dot{x}_g(0)} = \frac{S_0}{4\zeta_g\omega_g}. \quad (5.26b)$$

$$\sigma^2_{x_g(0)\dot{x}_g(0)} = 0 \quad (5.26c)$$

From equations (5.15b), (5.15c), (5.25) and (5.26), it is implied that the probability density function of the process $\mathbf{v}$ at time $t = 0$ is Gaussian distributed,

with mean $\mathbf{m^0}$ and covariance matrix $\mathbf{Q^0}$, such that

$$\begin{aligned} m_1^0 &= 1, \\ m_2^0 &= 0, \\ m_3^0 &= E[x_g(0)], \\ m_4^0 &= E[\dot{x}_g(0)] \end{aligned} \tag{5.27}$$

and

$$\mathbf{Q^0} = \begin{pmatrix} 0 & 0 & 0 & 0 \\ 0 & 0 & 0 & 0 \\ 0 & 0 & \sigma^2_{x_g(0)} & 0 \\ 0 & 0 & 0 & \sigma^2_{\dot{x}_g(0)} \end{pmatrix}. \tag{5.28}$$

But, $\mathbf{v}$ satisfies the linear stochastic differential equations (5.15) and (5.24) with initial conditions

$$p(y(0), \dot{y}(0), x_g(0), \dot{x}_g(0)) = \frac{1}{(2\pi)^2\sqrt{det|\mathbf{Q^0}|}} \exp(-\frac{1}{2}(\mathbf{v} - \mathbf{m^0})^T \mathbf{Q_0}^{-1}(\mathbf{v} - \mathbf{m^0})). \tag{5.29}$$

The transition probability density function of the process $\{y, \dot{y}\}$, $p_{y\dot{y}}(y, \dot{y}, t)$, is Gaussian distributed and is obtained from the solution of the mean and covariance equation associated with the linear stochastic equations (5.15) and (5.24).

5.4.3 Approximate solution for the first passage of the yielding levels.

It was previously shown that the conditional probabilities, p^+ and p^- can be expressed in terms of the crossing rates of the thresholds $y = 1$ and $y = -1$, $\alpha_+(t)$ and $\alpha_-(t)$, or

$$p^+ = \int_0^\infty \alpha_+(t) W_b(t) dt \tag{5.30a}$$

$$p^- = \int_0^\infty \alpha_-(t) W_b(t) dt, \tag{5.30b}$$

where $W_b(t)$, $\alpha_+(t)$, $\alpha_-(t)$ given by (5.21) and (5.22). Because an exact solution for the conditional transition probability density function $q_b(y, \dot{y}, t)$ cannot be

obtained, an approximate solution for the calculation of the crossing rates is proposed in this section. The solution scheme is based on the transition probability density function $p_{y\dot{y}}(y,\dot{y},t)$ calculated in the previous section.

Define $p^*(t)$ as

$$p^*(t) = \int_{-1}^{1}\int_{-\infty}^{\infty} p_{y\dot{y}}(y,\dot{y},t)d\dot{y}dy. \tag{5.31}$$

Then, $p^*(t)$ is the probability that the response at time t, belongs to the safe domain $(-1,1)$. A very important property of the reliability function $W_b(t)$ is that for all t, it should satisfy the following inequality:

$$W_b(t) \leq p^*(t) \quad \forall t. \tag{5.32}$$

Equation (5.32) is a consequence of the diffusion equations for the two probability functions. While all trajectories that at time t are in the safe domain $y \in (-1,1)$ contribute to $p^*(t)$, trajectories that crossed the safe domain boundary at times $\tau \in (0,t)$, are not accounted for the reliability function $W_b(t)$.

Consider $\alpha_+^{app}(t)$ and $\alpha_-^{app}(t)$, as approximate estimates for the rates of barrier crossings of the thresholds $y = \pm 1$. Then, a sufficient condition on $\alpha_+^{app}(t)$ and $\alpha_-^{app}(t)$ such that inequality (5.32) is satisfied is given by

$$\alpha_+^{app}(t) + \alpha_-^{app}(t) \geq \beta_+(t) + \beta_-(t), \tag{5.33a}$$

with

$$\beta_+(t) = \frac{1}{p^*(t)}\int_{-\infty}^{\infty} \dot{y}p(1,\dot{y},t)d\dot{y} \tag{5.33b}$$

$$\beta_-(t) = -\frac{1}{p^*(t)}\int_{-\infty}^{\infty} \dot{y}p(-1,\dot{y},t)d\dot{y}. \tag{5.33c}$$

This result may be shown by noting that from Section 5.4.1, $p^*(t)$ is given by

$$p^*(t) = \exp(-\int_0^{\infty} [\beta_+(\tau) + \beta_-(\tau)]d\tau). \tag{5.34}$$

From (5.22), (5.33a) and (5.34) it is implied that for $\alpha_+^{app}(t)$ and $\alpha_-^{app}(t)$, satisfying equation (5.33),

$$W_b(t) \leq p^*(t) \quad \forall t. \tag{5.32}$$

A consequence of this property is that the Poisson approximation for the crossing rates $\alpha_+(t)$ and $\alpha_-(t)$, may under certain circumstances violate the condition (5.32). Recall that, based on the Poisson approximation, the crossing rates, $\alpha_+(t)$ and $\alpha_-(t)$ are given by

$$\alpha_+(t) = \int_0^\infty \dot{y} p(1, \dot{y}, t) d\dot{y} \tag{5.35a}$$

$$\alpha_-(t) = -\int_{-\infty}^0 \dot{y} p(-1, \dot{y}, t) d\dot{y}. \tag{5.35b}$$

In particular, for the calculation of the conditional probabilities p^+ and p^-, the Poisson approximation produces a solution that violates relation (5.32), as illustrated in Figure 5.10. The poor performance of this approximate method may be attributed to the transient nature of the problem and the non zero mean of the response process $(y, \dot{y})$. In most problems of random vibration related to the first passage problem of type-D barrier by a zero mean process, the Poisson approximation gives conservative results for the reliability function. For this reason, it is suggested that the applicability of the method should be limited to these cases.

With respect to the transient nature of the problem, it should be pointed out that the crossing of the thresholds $y = \pm 1$ is expected to occur during the first period of oscillation of the linear system, as suggested from the results presented in Section 5.3. In the approximate solution scheme presented in this section, it is assumed that the crossing rates $\alpha_+(t)$ and $\alpha_-(t)$, are given by

$$\alpha_+(t) = \frac{\gamma}{p^*(t)} \int_0^\infty \dot{y} p(1, \dot{y}, t) d\dot{y} \tag{5.36a}$$

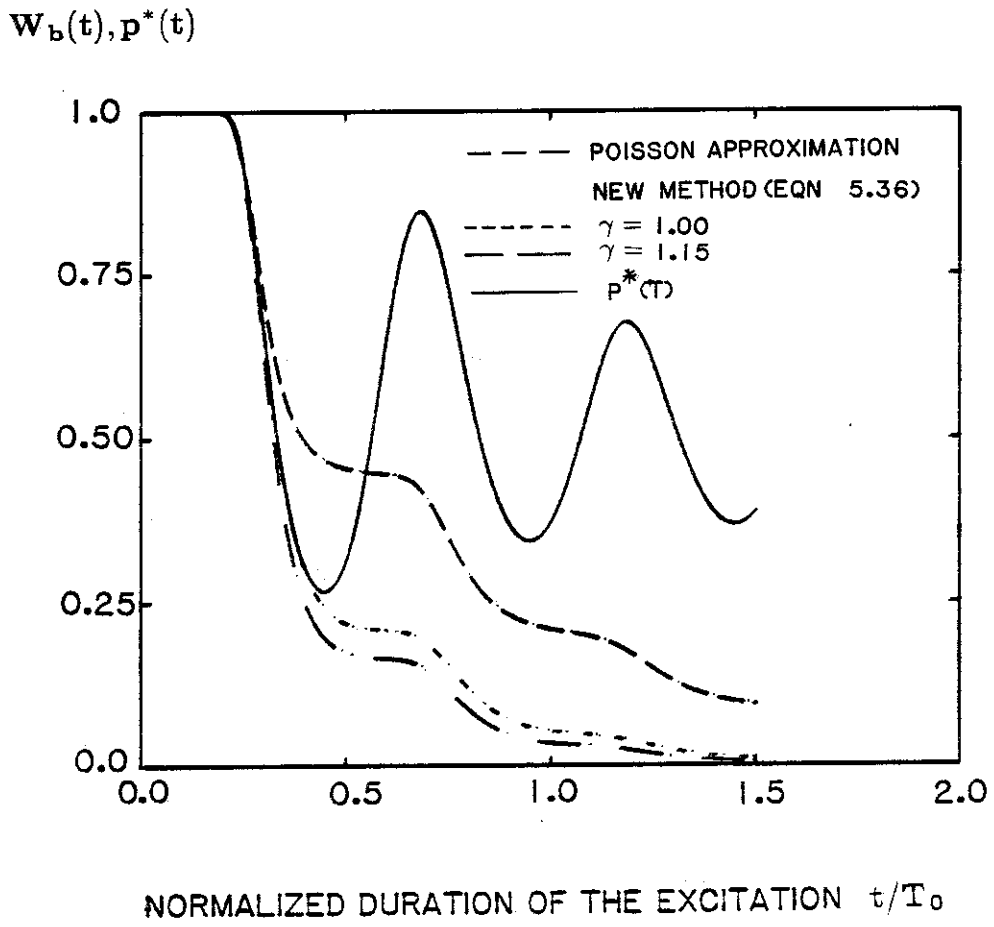

Figure 5.10
A comparison of different approximation techniques for the calculation of the reliability function, $W_b(t)$.

$$\alpha_-(t) = -\frac{\gamma}{p^*(t)} \int_{-\infty}^{0} \dot{y} p(-1, \dot{y}, t) d\dot{y}, \tag{5.36b}$$

with $\gamma \geq 1$. It can be shown that in this case, the condition (5.33) is satisfied. By substituting (5.36) in (5.30), the estimates for p^+ and p^- are obtained. Equation (5.30) is integrated numerically from $t = 0$ to $t = T^*$, where T^* is defined such that

$$p^+(T^*) + p^-(T^*) = .99. \tag{5.37}$$

In Figures 5.11a and 5.11b, the results produced by this approximate solution scheme are compared to numerical simulation results, for the cases ζ_g =0.50 and 0.25, respectively, and for $\gamma = 1.15$. Very good agreement between the results produced by the two methods can be noticed for most values of model parameters.

From the results illustrated in Figure 5.11, a strong dependence of p^+/p^- on both the characteristic frequency and strength of the excitation is observed for the case of a narrowbanded seismic excitation ($\zeta_g = 0.25$). For broadbanded excitation, a weaker dependence is noticed. A weaker dependence on the frequency content and strength of the excitation can be also observed for cases correponding to $\omega_g/\omega_0 > 1$.

Finally, the dependence of p^+/p^- on the probability density of the initial conditions, $x_g(0)$ and $\dot{x}_g(0)$, should be pointed out. From the results illustrated in Figure 5.12, it is noticed that by setting $E[x_g(0)]$ and $E[\dot{x}_g(0)]$ equal to zero, the approximate method produces very poor estimates for p^+ and p^-. It is suggested that even if the excitation is a zero mean process, the conditional mean values, $E[x_g(0)]$ and $E[\dot{x}_g(0)]$, are different than zero, and strongly dependent on the frequency content of the excitation.

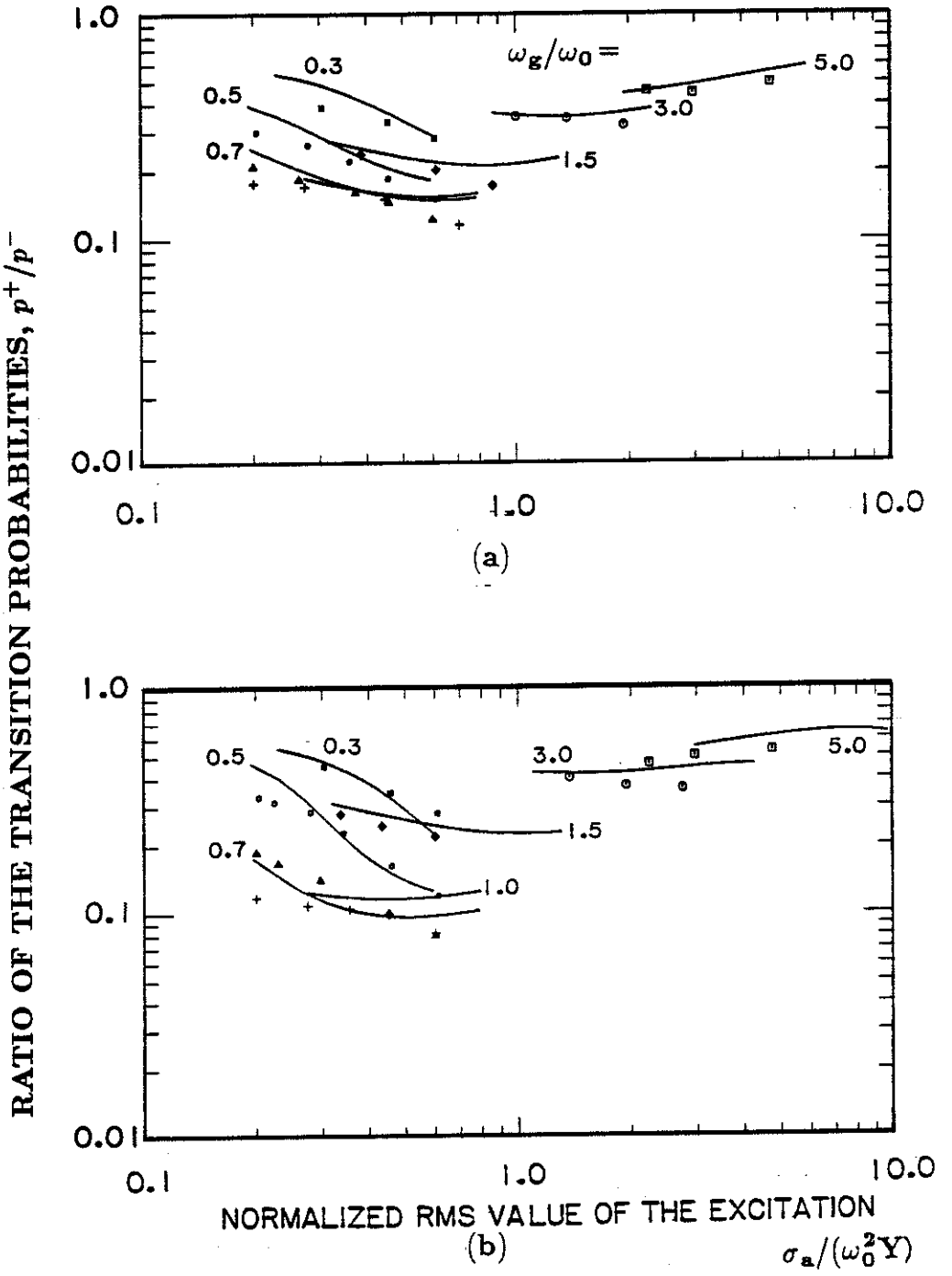

Figure 5.11
Comparison of the approximate results for the ratio of the transition probabilities, p^+/p^-, with numerical simulation data. (a) $\zeta_g = 0.50$ (b) $\zeta_g = 0.25$. Legend of simulation data given in Figure 4.0.

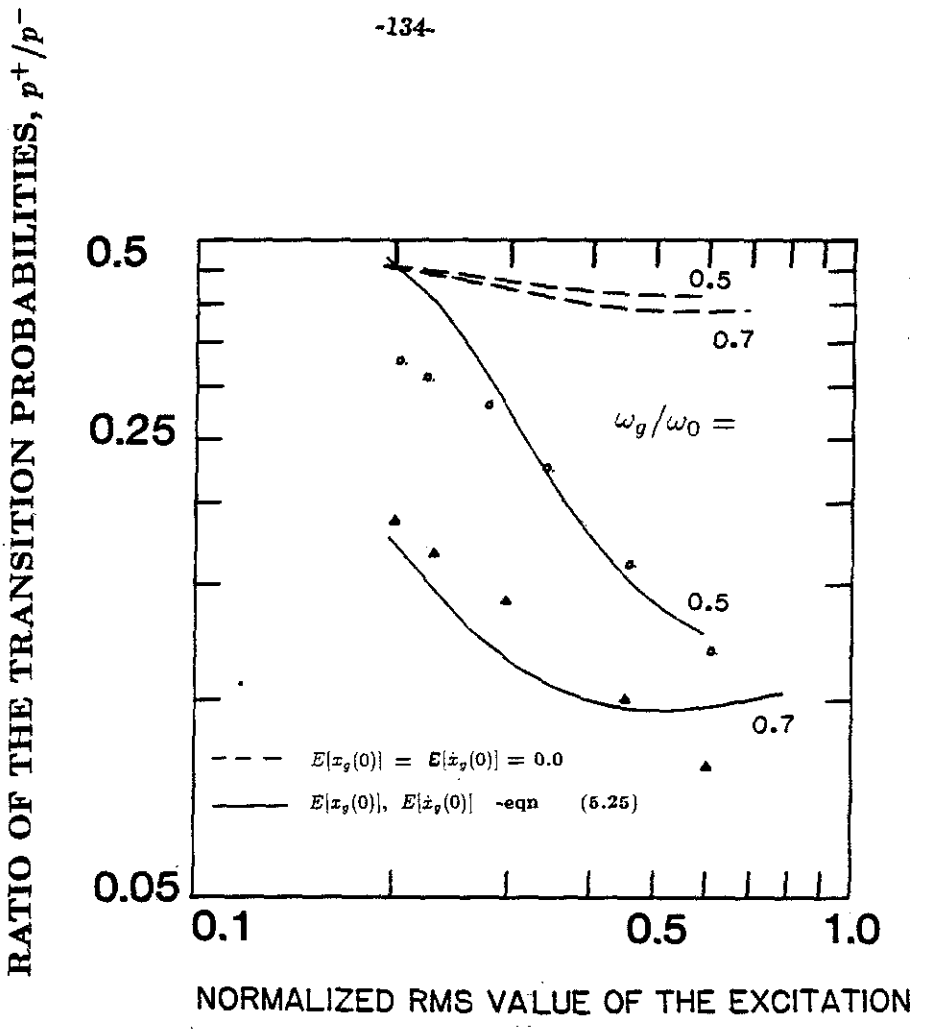

Figure 5.12
The significance of the mean values $E[x_g(0)]$ and $E[\dot{x}_g(0)]$, in the calculation of the transition probabilities, p^+ and p^-.

5.4.5 Numerical results for drift statistics.

As shown in Section 4.6.3, for $t \geq T_{ex}$, the mean square value of the drift is approximately given by

$$\sigma_z^2(t) \approx Q_0[0.5 + \nu_Y A(t - T_{ex})] \quad \text{for } t \geq T_{ex}. \tag{4.90a}$$

By considering the approximate expression for the correlation factor, given by (4.64a),

$$A \approx \frac{p^+}{p^-}, \tag{4.64a}$$

an expression for the mean square value drift increment per cycle, $\delta\sigma_z^2$, is obtained as

$$\delta\sigma_x^2 = \nu_Y \frac{p^+}{p^-} Q_0 T_0, \tag{5.38}$$

with ν_Y, Q_0, p^+ and p^- given by equations (5.14c), (5.7), (5.30) and (5.36).

The results for $\delta\sigma_z^2$, obtained by the approximate method introduced in this section are illustrated in Figure 5.13a and 5.13b, for bandwidth of the excitation $\zeta_g = 0.50$ and 0.25, respectively. Comparison with the corresponding numerical simulation results, indicates a good overall agreement between the two sets of results. It is observed that the approximate method gives a maximum error of 50% for the RMS value of the drift, in the case of small inelastic response or for values of $\omega_g/\omega_0 > 1$. These errors are attributed either to the equivalent linearization estimates for the velocity statistics, or to the simplified expression (equation 4.64a), for the correlation factor A. Nevertheless, the solution scheme presented in this section represents a first attempt to calculate transient drift statistics for the random reponse of an elasto-plastic system, and can be considered a good approximate solution for the problem.

The results illustrated in Figure 5.13 provide information regarding the influence of excitation parameters on the drift response. It is suggested that

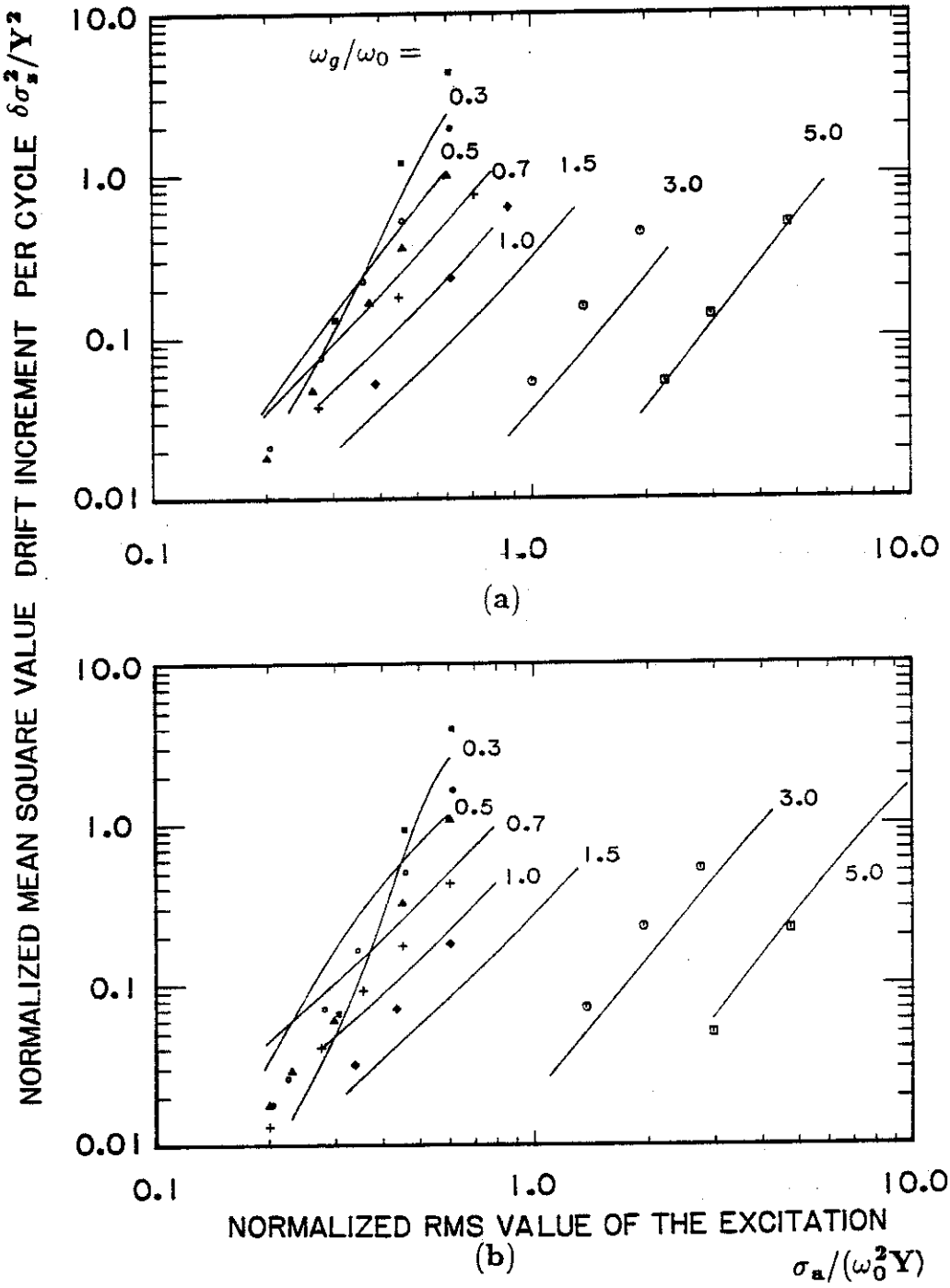

Figure 5.13
Normalized mean square value of the drift increment per cycle, $\delta\sigma_z^2$, for bandwidth of excitation (a) ζ_g=0.50 (b) ζ_g=0.25. Legend of simulation data given in Figure 4.0.

the mean square value of the drift depends primarly on the total energy of the excitation and on the characteristic frequency around which the energy is distributed. By contrast, the bandwidth of the excitation does not appear to play a very significant role. This can also be observed from Figure 5.14, in which the influence of the bandwidth of the excitation is examined, by comparison to the results for $\delta\sigma_x^2$ obtained for $\zeta_g = 0.25$ and 0.50. A dependence on ζ_g is observed only for large values of ω_g/ω_0.

Equation (4.90a) can be used for the calculation of the transient RMS value of the drift response. The expected time of first yield occurance, T_{ex}, is given by

$$T_{ex} = \int_0^\infty W_{ex}(t)dt, \tag{5.39a}$$

where W_{ex} is the reliability function associated with the first passage of a type-D barrier level at $|y| = 1$ by a linear oscillator initially at rest, and subjected to an excitation model given by equation (4.1). In this case, $(y, \dot{y})$ is a zero mean stochastic process, and as shown in the Figure 5.15, the results produced by the Poisson approximation are in very good agreement with the simulation data, and can be used as estimates of T_{ex}. In Figures 5.16a and 5.16b, two examples for the transient RMS value of the drift obtained by the solution scheme described in this section, are illustrated. The transient solutions are compared with the equivalent linearization results described in Section 4.3, and the corresponding simulation data. It can be concluded that for durations of excitation $T_s > T_{ex}$, the approximate solution scheme can be successfully used for the prediction of drift statistics, while for durations $T_s < T_{ex}$, the drift RMS value is accurately predicted by the equivalent linearization technique.

Of great interest for the damage analysis of hysteretic structural systems is the dissipated hysteretic energy, E_p. In the case of an elasto-plastic system, it can be shown that the normalized expected value for E_p is linearly divergent

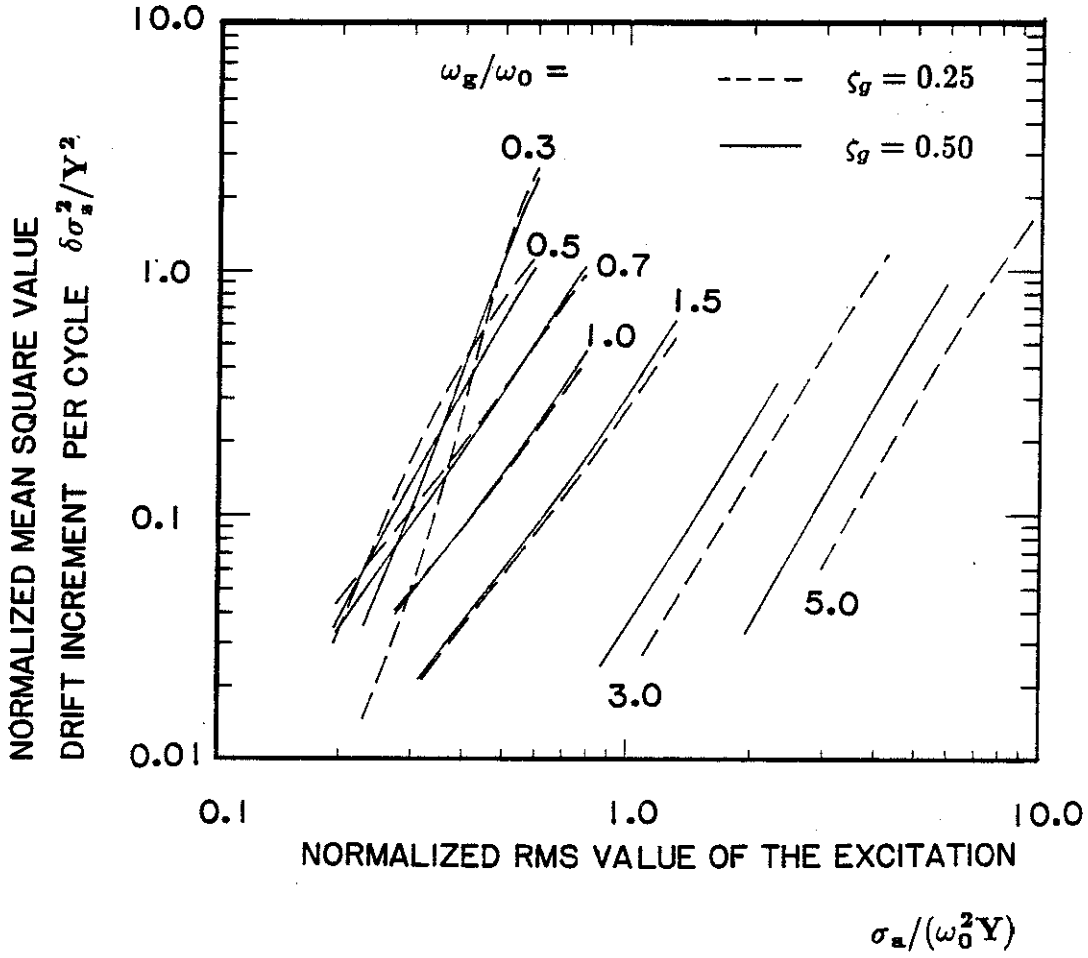

Figure 5.14
The influence of the bandwidth of excitation, ζ_g, on the mean square value of the drift increment per cycle.

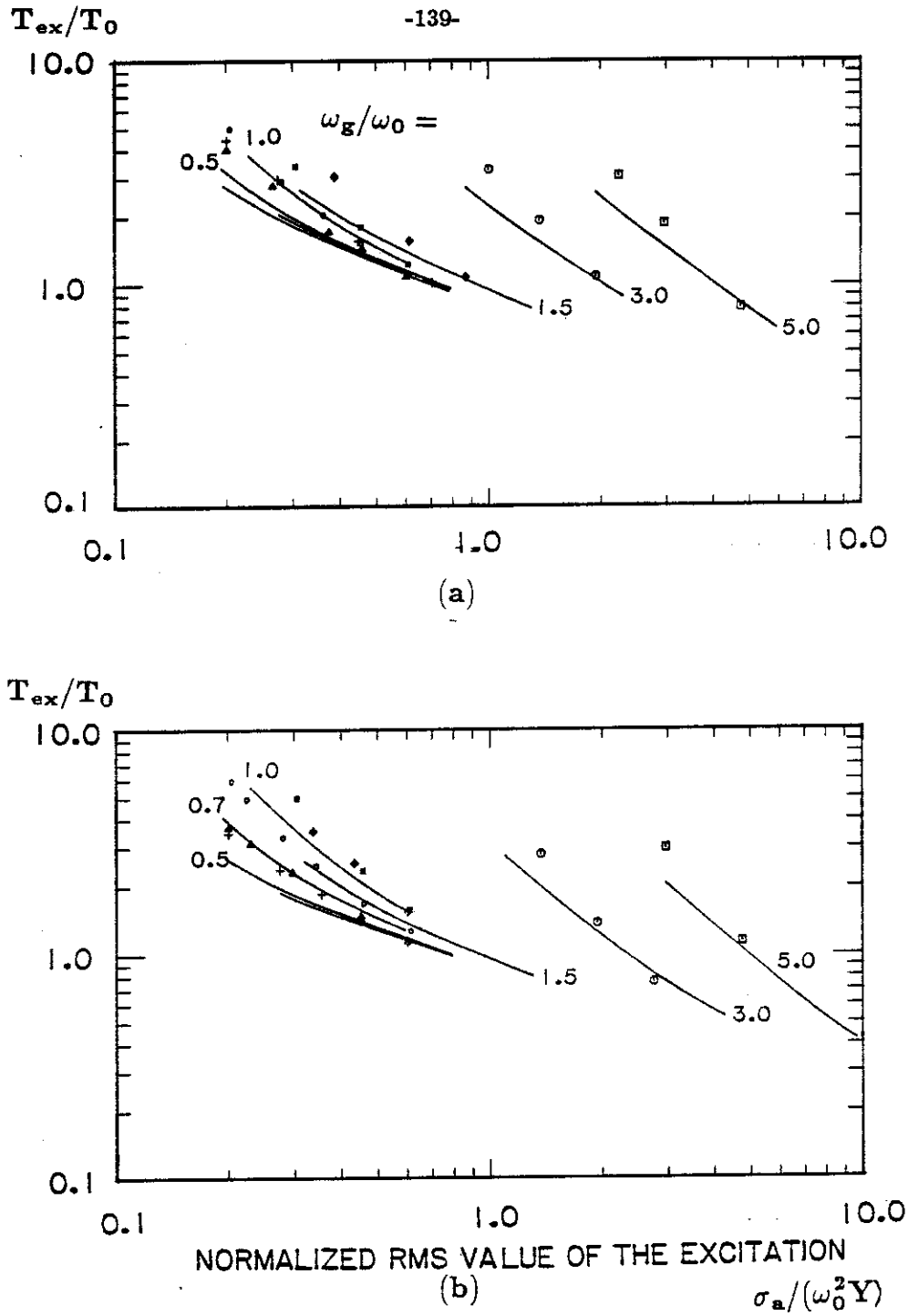

Figure 5.15
Expected time of first yield occurance, for the excitation model given by equation (2.27). Bandwidth of excitation (a) ζ_g=0.50 (b) ζ_g=0.25. Legend of simulation data given in Figure 4.0.

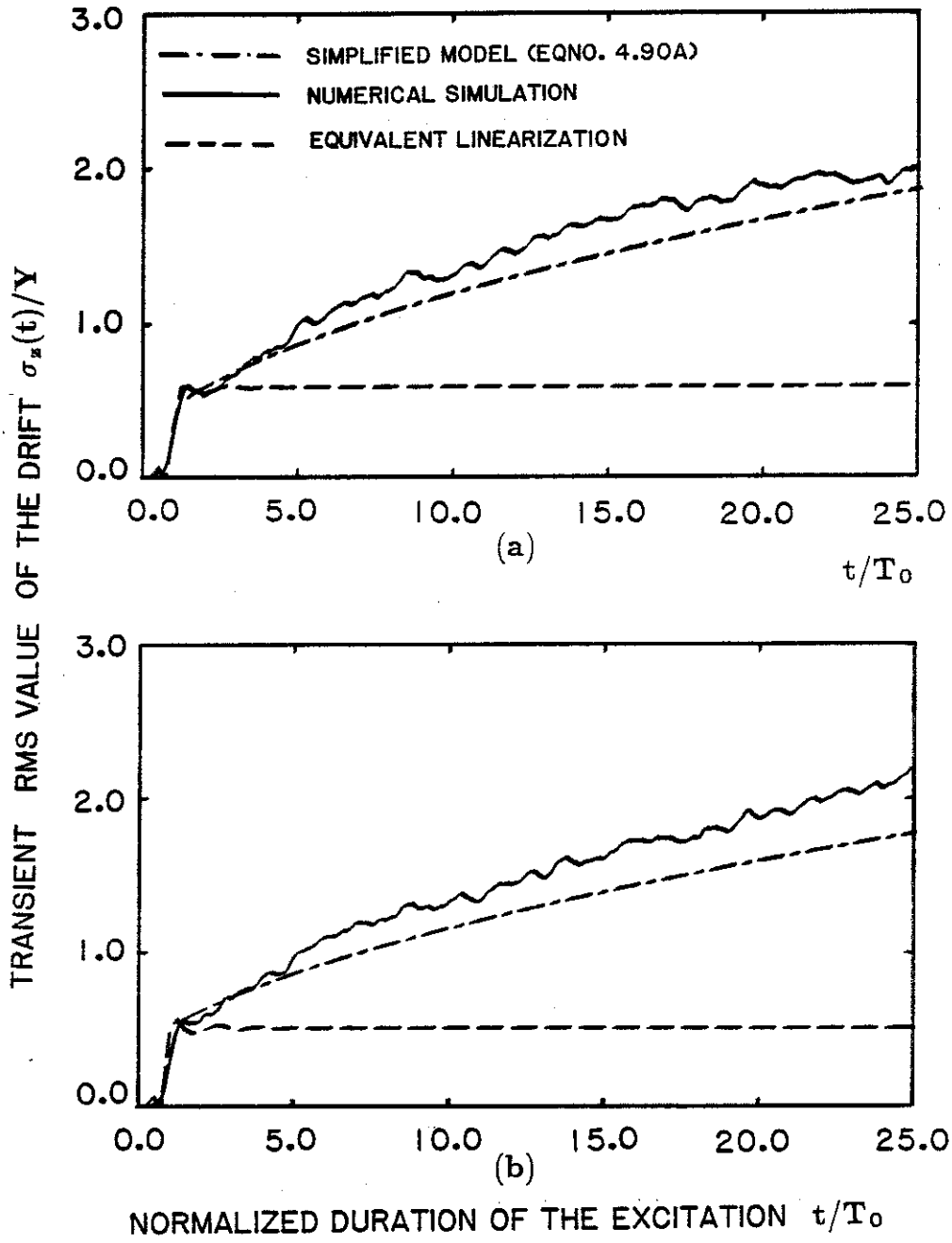

Figure 5.16
Transient RMS value of the drift response. S_0=0.40, ς_g=0.50 and ς=0.01. (a) ω_g/ω_0=0.70 (b) ω_g/ω_0=1.0.

with time, and is given by

$$E[E_p] = E_p^0 + \delta E_p \frac{t}{T_0}, \tag{5.40}$$

where δE_p is the normalized mean dissipated hysteretic energy per cycle, and is equal to

$$\delta E_p = \nu_Y E[d_Y] T_0. \tag{5.41}$$

In Figures 5.17a and 5.17b, the results for δE_p predicted by the approximate analytical solution, are illustrated for bandwidths of excitation $\varsigma_g = 0.50$ and 0.25, respectively.

5.5 Conclusion.

Based on the analytical results obtained in Chapter 4, an approximate solution for the random response of elasto-plastic systems has been presented. It has been shown that the probabilistic structure of the drift response is determined by the stationary probability density, $p_{\dot{x}y}(\dot{x}, y)$, of the velocity, $\dot{x}$, and of the elastic component of the displacement response, y. It is suggested that there is no need for the consideration of an associated linear system, as was previously done by Karnopp (39), Vanmarcke and Veneziano (40), Grossmayer (41) and Ditlevsen (42). By formulating the problem in terms of the variables x, $\dot{x}$ and y, very good estimates for $p_{\dot{x}y}(\dot{x}, y)$ are obtained by standard equivalent linearization.

By contrast with other available solutions, the method presented in this thesis is not limited to the calculation of yield increment statistics. By introducing the correlation factor, A, it is shown that the RMS value of the drift response can be calculated from the yield increment statistics. Because an analytical solution for A is practically impossible to obtain, an approximate relationship between A and the transition probabilities, p^+ and p^- has been established. The transition probabilities, p^+ and p^-, have been defined as the transition probability from

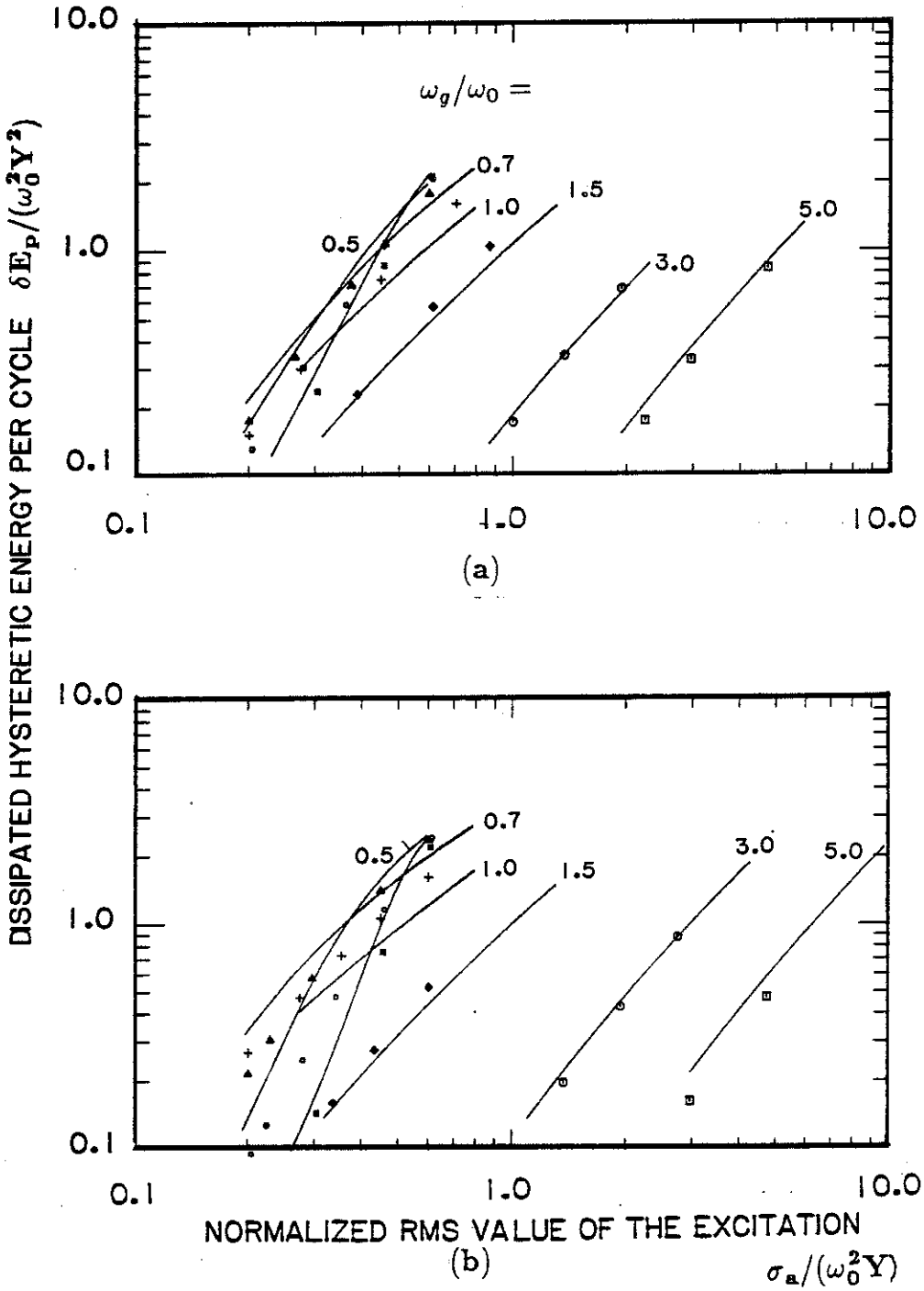

Figure 5.17
Expected value of the normalized dissipated hysteretic energy per cycle. (a) ζ_g=0.50 (b) ζ_g=0.25. Legend of simulation data given in Figure 4.0.

one inelastic state to another, and are calculated in Section 5.4 by an approximate solution of the related first passage problem. A new procedure for the evaluation of the mean rate of yield occurance, ν_Y, is also presented in Section 5.3.

Transient RMS values of the drift, predicted by the approximate solution introduced in this Chapter, are found to be in very good agreement with simulation results. It is suggested that, for small durations of the stochastic excitation, response statistics may also be calculated by equivalent linearization. By contrast, for long durations of the excitation, equivalent linearization fails to predict the linearly divergent behaviour of the mean square value of the drift.

Based on the seismic excitation model introduced in Section 2.3.4, it has been shown that the drift statistics are strongly dependent upon the total energy of the input and on the characteristic frequency around which the energy is distributed. The bandwidth of the excitation appears to influence the drift response statistics only for the case corresponding to large values of ω_g/ω_0.

Finally, the applicability of the approximate method for more complicated seismic excitation models, obtained by filtering a white noise excitation, is suggested. The stationary yield increment statistics are then obtained from equivalent linearization, following the procedure developed in this Chapter.

Chapter 6. SUMMARY AND CONCLUSIONS.

The objective of the analysis presented in this thesis is to determine the features of the hysteretic response of structural systems subjected to strong seismic excitation. The analysis is based on system and exitation models presented in Chapter 2. The nonlinear structural constitutive relation is modeled by a non-deteriorating multilinear hysteretic system. By formulating the restoring force in terms of additional state variables, a higher order and history independent equation of motion is obtained. In particular, for the case of a bilinear hysteretic system, such formulation enables the decomposition of the displacement response in terms of the elastic and inelastic components, while the additional state variable corresponds to the elastic deformation of the structural system.

Because of its influence on the drift response, consideration is given to the modeling of the excitation frequency content. It is shown that commonly used stochastic excitation models are not able to accurately represent the low frequency content of the earthquake spectrum. For this reason, a stochastic excitation model obtained by filtering a white noise signal through a second order linear filter is used in this thesis. The model is able to represent the low frequency content of the excitation, while the characteristic frequency, bandwidth, strength and duration of the seismic excitation are simply described in terms of four model parameters.

The following issues have been addressed in the body of this thesis: 1) the nature of hysteretic response behavior; 2) the influence of the structural system parameters on the response; 3) the influence of the frequency content of the excitation; and 4) the computational aspects of the problem.

In order to fully understand the hysteretic response behavior it is appropriate to express the displacement as the sum of the elastic component of the displacement and the drift of the structural system. In all of the cases examined,

the elastic component exhibits a narrowbanded response corresponding to oscillations at the natural frequency of the system. In contrast, the drift response depends upon the features of the hysteretic system. The bilinear hysteretic model is of particular interest and importance because it reveals the asymptotic properties of any nondeteriorating hysteretic system for the case of elastic and strong inelastic response. In the case of a bilinear hysteretic system, the nature of the drift response depends upon the parameter α_0, corresponding to the asymptotic stiffness of the system for large deflections. It is shown that in the case of stationary excitation, when $\alpha_0 > 0$, stationary solutions of the displacement and velocity response are obtained. Alternatively, for an elasto-plastic system, i.e., $\alpha_0 = 0$, the mean square value of the drift response is linearly divergent independent of the excitation frequency content. For this reason, the two classes of structural systems are treated separately.

In Chapter 3, the method of generalized equivalent linearization is used in the analysis of systems exhibiting hardening behavior and accurate estimates for the transient and stationary RMS values of the velocity and displacement response are obtained. It is shown that for an excitation with no zero frequency content, the low frequency content of the displacement response, cannot be predicted by equivalent linearization. As a consequence, the method fails to predict the linear divergent mean square value of the displacement and drift response in the case of an elasto-plastic system. It is important to note that equivalent linearization has a dual interpretation; 1) as a linearization of the equation of motion; or, 2) as a Gaussian closure of the associated F-P-K equation. In Chapter 4 it was shown that under stationary stochastic excitation, the drift response of an elasto-plastic system can be approximately considered as Brownian motion. As a consequence, the drift process is approximately Gaussian distributed, which suggest that accurate results obtained by equivalent linearization, even

for the case of a nearly elasto-plastic system, may be attributed to the Gaussian closure interpretation of the technique.

In Chapter 4, a new approach is followed in the analysis of the elasto-plastic system. The problem is formulated in terms of the drift, defined as the sum of yield increments associated with inelastic response. The analysis is based on the properties of discrete Markov process models of the yield increment process, while the yield increment statistics are expressed in terms of the probability density of the velocity and elastic component of the displacent response. Using this approach, an approximate exponential and Rayleigh distribution for the yield increment and yield duration, respectively, are established. It is suggested that, for duration of stationary seismic excitation of practical significance, the drift can be considered as a Brownian motion. Based on this observation, the approximate Gaussian distribution and the linearly divergent mean square value of the process, as well as an expression for the probability distribution of the peak drift response, are obtained. The validation of these results is accomplished by means of a Monte Carlo simulation study of the random response of an elasto-plastic system.

The analytical results presented in Chapter 4 also suggest that yield increment and drift statistics can be calculated from the probability density $p_{\dot{x}y}(\dot{x}, y)$, of the elastic deformation, y, and velocity response, $\dot{x}$. Based on these results, an approximate solution scheme for the calculation of the response statistics of an elasto-plastic system is introduced in Chapter 5. It is suggested that there is no need for the consideration of an associated linear system, as was previously done by Karnopp and Scharton (39), Vanmarcke and Veneziano (40), Grossmayer (41) and Ditlevsen (42). By formulating the problem in terms of the additional state variable, corresponding to the elastic component of the displacement, good estimates for $p_{\dot{x}y}(\dot{x}, y)$ are obtained by standard equivalent linearization. Sta-

tionary response statistics for the yield duration, yield increment, rate of yield occurance, dissipated hysteretic energy and RMS value of the drift are then obtained, and found to be in very good agreement with the simulation results. It is shown that the drift response statistics are strongly dependent on the normalized characteristic frequency and strength of the excitation, while a weaker dependence on the bandwidth of excitation is noted.

Based on these results, it is suggested that transient equivalent linearization and the approximate solution scheme introduced in Chapter 5 can be used in the analysis of a large class of hysteretic systems. Finally, it is concluded that the understanding of the behaviour of the yield increment process is crucial for the understanding of hysteretic response behavior.

References

[1] Rice, S. O., 'Mathematical Analysis of Random Noise.' in Selected Papers of Noise and Stochastic Processes, Nelson Wax, ed., New York: Dover Publications, Inc., (1954).

[2] Ito, K., ' On Stochastic Differential Equations.' Memoirs Amer. Math. Soc., No. 4, (1951).

[3] Stratonovitch, R.L.,'Topics in the Theory of Random Noise.' Vol. 1, Gordon and Breach, (1963).

[4] Stratonovitch, R.L.,'Topics in the Theory of Random Noise.' Vol. 2, Gordon and Breach, (1967).

[5] Krylov, N. and Bogoliubov, N., ' Intoduction a la Mechanique Nonlineaire: les Methodes Approachees et Asymptotiques.' Ukr. Akad. Nauk. Inst. de la Mecanique, Chaire de Phys. Math. Ann (1937). Translated by S. Lefshetz in Ann. Math. Studies, No 11, Princeton, NJ, (1947).

[6] Caughey, T. K. ' Nonlinear Theory of Random Vibrations.' Adv. Appl. Mech., (11), (1971).

[7] Lin, Y.K., 'Probabilistic Theory of Structural Dynamics., New York: McGraw Hill, (1967).

[8] Crandall, S., and Mark, W. 'Random Vibration in Mechanical Systems.' New York: Academic Press, (1963).

[9] Feller, W., 'An Introduction to Probability Theory and its Applications.' New York: John Wiley and Sons, Inc., (1971).

[10] Simon, B. ' Functional Integration and Quantum Physics.', Academic Press, (1979).

[11] Knight, F. B. 'Essentials of Brownian Motion and Diffusion.' Mathematical Surveys No. 18, (1981).

[12] Roberts, J. B. ' Response of Nonlinear Mechanical Systems to Random Excitation PART 1: Markov Methods.' Shock and Vibration Digest, (1979).

[13] Roberts, J. B. ' Response of Nonlinear Mechanical Systems to Random Excitation PART 2: Equivalent Linearization and Other Methods.' Shock and Vibration Digest, (1979).

[14] Caughey, T. K. ' Equivalent Linearization Techniques.' The Journal of the Acoustical Society of America, Vol. 35, No 11, (1963).

[15] Booton, R. C. ' The Analysis of Nonlinear Control Systems with Random Inputs.' IRE Trans. Circuit Theory, Vol. 1, (1954).

[16] Iwan, W. D. and Yang, I. M., 'Statistical Linearisation for Nonlinear Structures.' ASCE J. Eng. Mech. Div., Vol. 97, (1971).

[17] Atalik, T. S. and Utku, S. ' Stochastic Linearization of Multi-Degree-of-Freedom Non-Linear Systems.' Earthquake Engineering and Structural Dynamics, Vol 4, (1976).

[18] Iwan, W. D. and Mason A. B. 'Equivalent Linearization for Systems Subjected to Non-Stationary Random Excitation.' Int. J. Non-Linear Mechanics, Vol. 15, (1980).

[19] Spanos, P-T. D. and Iwan, W. D. ' On the Existence and Uniqueness of Solutions Generated by Equivalent Linearization.' Int. J. Non-Linear Mechanics, Vol 13, (1978).

[20] Sancho, N. G. F. ' Technique for Finding the Moment Equations of a Nonlinear Stochastic System.' J. of Math. Physics, Vol. 11, No. 3, (1970).

[21] Bover D.C.C. ' Moment Equation Methods for Nonlinear Stochastic Systems.' J. of Math. Analysis and Applications, Vol. 65, (1978).

[22] Shinozuka, M., ' Monte Carlo Solution of Structural Dynamics.' Intl. J. Computers Struc., Vol. 2, (1972).

[23] Shinozuka, M. and Jan, C. M., 'Digital Simulation of Random Processes and Its Applications.' J. Sound Vib., Vol. 25, (1972).

[24] Hall, J. F. ' An FFT Algorithm for Structural Dynamics.' Earthquake Eng. and Structural Dynamics, Vol. 10, (1982).

[25] Housner, G. W. ' Characteristics of Strong-Motion Earthquakes.' Bulletin of the Seismological Society of America, Vol. 37, No. 1, (1947).

[26] Kanai, K. 'Semi-empirical Formula for the Seismic Characteristics of the Ground.' Bulletin of the Earthquake Research Institute, (1957).

[27] Kanai, K. ' An Empirical Formula for the Spectrum of Strong Earthquake Motions.' Bulletin of the Eartquake Research Institute, Vol 39, (1961).

[28] Tajimi, H., ' A Statistical Method of Determining the Maximum Response of a Building Structure During an Earthquake.' Proceedings of the Seconf World Conference on Earthquake Engineering, Tokyo and Kyoto, Japan, Vol. II, (1960).

[29] Kameda H. ' Stochastic Process Models of Strong Earthquake Motions for Inelastic Structural Response.' U.S.- Southeast Asia Synposium on Engineering for Natural Hazards Protection, Manila, (1977).

[30] Boore, D. M. ' Stochastic Simulation of High-Frequency Ground Motions Based on Seismological Models of the Radiated Spectra'. Bulletin of the Seismological Society of America, Vol 76, No. 6, (1983).

[31] Nau, R. F., Oliver, R. M., and Pister, K. S. 'Simulating and Analyzing Artificial Nonstationary Eartquake Ground Motions.' Bulletin of the Seismological Society of America, Vol 72, No. 2, (1982).

[32] Luco J. E., ' On Strong Ground Motion Estimates Based On Models of the Radiated Spectrum.' Bulletin of the Seismological Sociaty of America, Vol. 75, No. 3, (1985).

[33] Jennings, P. C., Housner, G.W., and Tsai, N.C., 'Simulated Earthquake Motions.' Earthquake Engineering Research Laboratory, California Institute of Technology, Pasadena, California, (1968).

[34] Shinozuka, M., and Sato, Y. ' Simulation of Nonstationary Random Process.' J. Eng. Mechanics Division, (1967).

[35] Saragoni, R. and Hart, G. C., ' Simulation of Artificial Earthquakes.' Eartquake Eng. and Structural Dynamics, Vol. 2, (1974).

[36] Vanmarcke, E. H. and Lai, S-S. P. 'Strong- Motion Duration and RMS Amplitude of Earthquake Records.' Bulletin of the Seismological Society of America, Vol. 70, No. 4, (1980).

[37] Iwan, W. D. ' A Distributed-Element Model for Hysteresis and Its Steady-State Dynamic Response.' J. of Applied Mechanics, Vol. 33, (1966).

[38] Bouc. R., ' Forced Vibration of Mechanical System with Hysteresis.' Proc. 4th Conf. Nonlin. Oscill., Prague, Czechoslovakia, (1967).

[39] Karnopp, D. and Scharton, T. D. ' Plastic Deformation in Random Vibration.' The Journal of Acoustical Society of America., Vol 39, No. 6, (1966).

[40] Vanmarcke, E. H. and Veneziano, D. ' Probabilistic Seismic Response of Simple Inelastic Systems.' Third World Conference on Earthquake Engineering, (1973).

[41] Grossmayer, R. L., ' Stochastic Analysis of Elasto-Plastic Systems.' Journal of the Engineering Mechanics Division, Vol. 107, (1981).

[42] Ditlevsen, O. 'Elasto- Plastic Oscillator with Gaussian Excitation.' Journal of Engineering Mechanics, Vo. 112, No. 4, (1986).

[43] Caughey, T. K. ' Random Excitation of a System With Bilinear Hysteresis.' Journal of Applied Mechanics, Vol. 27, (1960).

[44] Iwan, W. D. and Lutes, L.D. ' Responce of the Bilinear Hysteretic System to Stationary Random Excitation.' The Journal of the Acoustical Society of America, Vol. 43, No. 3, (1968).

[45] Crandall, S. H., Lee, S. S. and Williams, J.H., Jr ' Accumulated Slip of a Friction-Controlled Mass Excited by Earthquake Motions.' Journal of Applied Mechanics, Vol. 41, (1974).

[46] Kobori, T., Minai, R. and Suzuki, Y. ' Statistical Linearization Techniques of Hysteretic Structures to Eartquake Excitations.' Bull. Disas. Prev. Res. Inst., Kyoto Univ., Vol. 23, Parts 3-4, (1973).

[47] Kobori, T., Minai, R. and Suzuki, Y. ' Stochastic Seismic Response of Hysteretic Structures.' Bull. Disas. Prev. Res. Inst., Kyoto Univ., Vol. 26, Part 1, (1976).

[48] Asano, K. and Iwan, W. D. ' An Alternative Approach to the Random Response of Bilinear Hysteretic Systems.' Eartquake Enginearing and Structural Dynamics, Vol. 12, (1984).

[49] Asano, K. and Suzuki, S. 'Hysteretic Structural Earthquake Response.' 4th International Conference on Structural Safety and Reliability, Tokyo, (1984).

[50] Suzuki, Y. and Minai R. 'Seismic Reliability Analysis of Hysteretic Structures Based on Stochastic Differential Equations.' 4th International Conference on Structural Safety and Reliability, Tokyo, (1984).

[51] Kimura, K., Yagasaki, K. and Sakata M. ' Non- Statonary Responses of a System With Bilinear Hysteresis Subjected to Non-White Random Excitation.' Journal of Sound and Vibration, Vol. 91(2), (1983).

[52] Lutes, L. D., ' Approximate Technique for Treating Random Vibration of Hysteretic Systems.' The Journal of the Acoustical Society of America (1969).

[53] Grossmayer, R. L., ' Elastic-plastic Oscillators Under Random Excitation.' Journal of Sound and Vibration, Vol. 65(3), (1979).

[54] Spanos, P-T. D. ' Hysteretic Structural Vibrations under Random Load.' J. Acoust. Soc. Am., Vol. 65(2), (1979).

[55] Wen, Y. K. 'Approximate Method for Nonlinear Random Vibration.' Journal of the Engineering Mechanics Division, Vol. 101, (1975).

[56] Wen, Y. K. 'Method for Random Vibration of Hysteretic Systems.' Journal of the Engineering Mechanics Division, Vol. 102, (1976).

[57] Wen, Y. K. ' Equivalent Linearization for Hysteretic Systems Under Random Excitation.' Journal of Applied Mechanics, Vol. 47, (1980).

[58] Wen, Y. K. ' Stochastic Response and Damage Analysis of Inelastic Structures.' Probabilistic Engineering Mechanics, Vol. 1, No. 1, (1986).

[59] Mason, A. B. ' Some observations on the Random Response of Linear and Nonlinear Dynamical Systems.' Earthquake Engineering Research Laboratory, Re. No. (79-01), (1979).

[60] Smith, S. K. ' Stochastic Analysis of the Seismic Response of Secondary Systems.' Eartquake Engineering Research Laboratory, Re. No. (85-01), (1985).

[61] Hanks, T. C. and McGuire, R. K. 'The character of high frequency strong ground motion.' Bull. Seism. Soc. Am., Vol. 71, (1981).

Appendix A. APPROXIMATE EXPRESSION FOR THE SPECTRAL DENSITY FUNCTION OF A MULTILINEAR HYSTERETIC SYSTEM SUBJECTED TO FILTERED WHITE NOISE EXCITATION. SOLUTION BY EQUIVALENT LINEARIZATION.

Consider the equivalent linear system associated with the hysteretic model analyzed in Chapter 3. For a duration of excitation $T_s \to \infty$ and if a stationary solution of the covariance equation (3.8) exists, an expression for the spectral density function of the displacement response x, can be derived of the form

$$\Phi_{xx}(\omega) = \Phi_{aa}|H_x(i\omega)|^2, \tag{A.1}$$

where $H_x(i\omega)$ is the transfer function for the variable x, and Φ_{aa} is the spectral density function of the stationary stochastic excitation $\ddot{a}(t)$ corresponding to the case $T_s \to \infty$. For the seismic excitation model corresponding to stationary solution of the equations (3.1d)-(3.1f), $\ddot{a}(t)$ is defined by

$$-\ddot{a}(t) = 2\zeta_g\omega_g\dot{x}_g b_1 + \omega_g^2 x_g b_2 \tag{A.2a}$$

$$\ddot{x}_g + 2\zeta_g\omega_g\dot{x}_g + \omega_g^2 x_g = \xi(t), \tag{A.2b}$$

where $\xi(t)$ is a zero mean Gaussian white noise signal with spectral density function $S_0/(2\pi)$. This is a special case of the model described by the equation (2.17), corresponding to $n_1 = 1$, $n_2 = 2$ and

$$M[x_g(t)] = 2\zeta_g\omega_g\dot{x}_g b_1 + \omega_g^2 x_g b_2, \tag{A.3a}$$

$$L[x_g(t)] = \ddot{x}_g + 2\zeta_g\omega_g\dot{x}_g + \omega_g^2 x_g. \tag{A.3b}$$

The corresponding transfer functions are given by

$$H_M(i\omega) = \frac{1}{\omega_g^2 b_2 + (i\omega)2\zeta_g\omega_g b_1}, \tag{A.4a}$$

$$H_L(i\omega) = \frac{1}{(\omega_g^2 - \omega^2) + (i\omega)2\zeta_g\omega_g}. \qquad (A.4b)$$

Using equation (2.19), the spectral density function of the excitation, $\Phi_{aa}(\omega)$ is given by

$$\Phi_{aa}(\omega) = \frac{4\zeta_g^2\omega_g^2 b_1^2\omega^2 + \omega_g^4 b_2^2}{(\omega_g^2 - \omega^2)^2 + 4\zeta_g^2\omega_g^2\omega^2}\frac{S_0}{(2\pi)}. \qquad (A.5)$$

For the equivalent linear system governed by the equations (3.4) and (3.10), the equation of motion is given by

$$\ddot{x} + \alpha_0\omega_0^2 x + B_0\dot{x} + \omega_0^2\sum_{i=1}^{n}\alpha_i C_{2i}\phi_i = -\ddot{a}(t), \qquad (A.6a)$$

and

$$\dot{\phi}_i = C_{4i}\dot{x} + C_{3i}\phi_i \quad \text{for} \quad i = 1, ..., n. \qquad (A.6b)$$

The transfer function of the response variable x can be obtained in the form

$$\frac{1}{H_{xx}(i\omega)} = (\alpha_0\omega_0^2 - \omega^2) + (i\omega)B_0 + \omega_0^2\sum_{i=1}^{n}(i\omega)\frac{\alpha_i C_{2i}C_{4i}}{i\omega - C_{3i}}, \qquad (A.7)$$

or

$$\frac{1}{H_{xx}(i\omega)} = R_x + iI_x, \qquad (A.8a)$$

where

$$R_x = (\alpha_0 - \omega^2) + \omega^2\omega_0^2\sum_{i=1}^{n}\frac{\alpha_i C_{2i}C_{4i}}{\omega^2 + C_{3i}^2}, \qquad (A.8b)$$

$$I_x = \omega\left[B_0 - \omega_0^2\sum_{i=1}^{n}\frac{\alpha_i C_{2i}C_{3i}C_{4i}}{\omega^2 + C_{3i}^2}\right]. \qquad (A.8c)$$

Following (A.1), (A.5) and (A.8), the expression for the spectral density function of the stationary response variable x is obtained as

$$\Phi_{xx}(\omega) = \frac{S_0}{(2\pi)}\frac{4\zeta_g^2\omega_g^2 b_1^2\omega^2 + \omega_g^4 b_2^2}{(\omega_g^2 - \omega^2)^2 + 4\zeta_g^2\omega_g^2\omega^2}\frac{1}{(R_x^2 + I_x^2)}. \qquad (A.9)$$

Appendix B. DIMENSIONLESS GROUPS FOR THE RANDOM VIBRATION OF A MULTILINEAR HYSTERETIC SYSTEM.

Consider the equation of motion for the general multilinear hysteretic system governed by equation (3.1):

$$\ddot{x} + 2\zeta\omega_0\dot{x} + \alpha_0\omega_0^2 x + \omega_0^2 \sum_{i=1}^{n} \alpha_i g_1(\phi_i, \dot{x}, x_{y_i}) = 2\zeta_g\omega_g\dot{x}_g b_1 + \omega_g^2 x_g b_2, \quad (B.1a)$$

$$\dot{\phi} = g_2(\phi_i, \dot{x}, x_{y_i}) \quad i = 1, ..., n, \quad (B.1b)$$

$$\ddot{x}_g + 2\zeta_g\omega_g\dot{x}_g + \omega_g^2 x_g = e(t)\xi(t), \quad (B1.c)$$

$$\dot{x}_g(0) = x_g(0) = 0 \quad (B.1d)$$

and

$$\sum_{i=1}^{n} \alpha_i = 1. \quad (B.1e)$$

Consider also the following transformations

$$\tau = \omega_0 t, \quad (B.2a)$$

and for $Y > 0$

$$x'_g = \frac{x_g}{Y}, \quad (B.2b)$$

$$x' = \frac{x}{Y}, \quad (B.2c)$$

$$\phi'_i = \frac{\phi}{Y}, \quad (B.2d)$$

$$x'_{y_i} = \frac{x_{y_i}}{Y} \quad \text{for} \quad i = 1, ..., n. \quad (B.2e)$$

Define

$$(...)' = \frac{d}{d\tau}(...), \quad (B.3a)$$

corresponding to differentiation with respect to τ of the quantity in parenthesis. By applying (B.2a), the following relation is derived:

$$\frac{d}{dt}(...) = \omega_0 \frac{d}{d\tau}(...). \quad (B.3b)$$

From (2.6c), (2.6d), (B.2) and (B.3)

$$g_1(\phi_i, \dot{x}, x_{y_i}) = Y g_1(\phi_i', (x')', x_{y_i}'), \tag{B.4a}$$

$$g_2(\phi_i, \dot{x}, x_{y_i}) = \omega Y g_2(\phi_i', (x')', x_{y_i}'). \tag{B.4b}$$

Substituting (B.2), (B.3) and (B.4) into (B.1), the equation of motion for x', x_g' is derived as

$$(x')'' + 2\zeta(x') + \alpha_0 x' + \sum_{i=1}^{n} \alpha_i g_1(\phi_i', (x')', x_{y_i}') = 2\zeta_g \left(\frac{\omega_g}{\omega_0}\right)(x_g')' b_1 + \left(\frac{\omega_g}{\omega_0}\right)^2 x_g' b_2. \tag{B.5a}$$

$$(\phi')' = g_2(\phi_i', (x')', x_{y_i}') \quad i = 1, ..., n, \tag{B.5b}$$

$$(x_g')'' + 2\zeta_g \left(\frac{\omega_g}{\omega_0}\right)(x_g')' + \left(\frac{\omega_g}{\omega_0}\right)^2 x_g' = e'(\tau)\,\xi'(\tau), \tag{B5.c}$$

$$(x_g')'_{(\tau=0)} = (x_g')_{(\tau=0)} = 0, \tag{B.5d}$$

where $e'(\tau)$ defined as

$$e'(\tau) = \begin{cases} 1, & \text{if } \tau \leq \omega_0 T_s; \\ 0, & \text{if } \tau > \omega_0 T_s \end{cases}, \tag{B.5e}$$

and $\xi'(\tau)$ is a zero mean Gaussian white noise process, with spectral density $S_0/(\omega_0^3 Y^2)$. Based on equation (B.5), it is concluded that the following dimensionless groups

$$(\omega_0 t), \qquad \left(\frac{\omega_g}{\omega_0}\right), \qquad \left(\frac{S_0}{\omega_0^3 Y^2}\right), \qquad \left(\frac{x}{Y}\right) \tag{B.6}$$

can be defined for the problem of a multilinear hysteretic system subjected to the stochastic excitation model defined by (2.27). This excitation model corresponds to the filtering of modulated white noise excitation through a second order linear filter.

Appendix C. SURVIVING PROBABILITY FOR A CONDITIONAL RANDOM WALK WITH EXPONENTIALLY DISTRIBUTED INCREMENTS.

Consider a two-state Markov process F, corresponding to $F = \pm 1$ and with transition matrix

$$\mathbf{p} = \begin{pmatrix} p^+ & p^- \\ p^- & p^+ \end{pmatrix} \qquad p^- > p^+, \tag{C1}$$

where p^+ and p^- are defined as

$$p^+ = P(F^{(i)} = 1 | F^{(i-1)} = 1) = P(F^{(i)} = -1 | F^{(i-1)} = -1), \tag{C.2a}$$

$$p^- = P(F^{(i)} = 1 | F^{(i-1)} = -1) = P(F^{(i)} = -1 | F^{(i-1)} = 1). \tag{C.2b}$$

Define $z^{(n)}$ as a conditional random walk, such that

$$z^{(n)} = \sum_{i=1}^{n} d^{(i)} F^{(i)}, \tag{C.3}$$

where $(d^{(i)};\ i = 1, ..., n)$ are exponentially distributed and mutually independent increments, or

$$p(d^{(i+1)}; F^{(i+1)} | d^{(i)}; F^{(i)}) = p(d^{(i+1)}) p(F^{(i+1)} | F^{(i)}), \tag{C.4a}$$

$$p_d(d^{(i)}) = e^{-d^{(i)}} h(d^{(i)}), \tag{C.4b}$$

and $h(...)$ the unit step function. For the case of zero start, symmetric with respect to F, initial conditions

$$p^{(0)}(z^{(0)}) = \delta(0), \tag{C.5a}$$

$$p^{(1)}(z^{(1)}) = e^{-|z^{(1)}|}, \tag{C.5b}$$

and

$$p(F^{(1)} = 1) = p(F^{(1)} = -1) = \frac{1}{2}. \tag{C.5c}$$

The survival probability of the process $z^{(n)}$, $W_b^{(n)}$, for crossing of the type-D barrier at $|z| = b$, is defined as

$$W_b^{(n)} = \text{Prob}(|z^{(i)}| \leq b \text{ for } 0 \leq i \leq n). \tag{C.6}$$

The conditional transition probability density functions $p^{(i)}$ can be expressed as

$$p^{(i)}(z) = p_1^{(i)}(z) + p_2^{(i)}(z), \tag{C.7a}$$

where $p_1^{(i)}(z)$ and $p_2^{(i)}(z)$ correspond to $F^{(i)} = 1$ and $F^{(i)} = -1$, respectively. By applying (C.2), (C.3) and (C.4), $p_1^{(i)}(z)$, $p_2^{(i)}(z)$ will satisfy the following diffussion equations

$$p_1^{(i+1)}(z) = \int_{-b}^{z} e^{-(z-x)}[p^+ p_1^{(i)}(x) + p^- p_2^{(i)}(x)]dx \tag{C.7b}$$

and

$$p_2^{(i+1)}(z) = \int_{z}^{b} e^{-(x-z)}[p^+ p_2^{(i)}(x) + p^- p_1^{(i)}(x)]dx, \tag{C.7c}$$

with boundary conditions

$$p_1^{(i)}(-b) = p_2^{(i)}(b) = 0, \tag{C.7d}$$

and initial conditions

$$p^{(0)}(z) = \delta(0) \tag{C.7e}$$

$$p_1^{(1)}(z) = \frac{1}{2}e^{-z}h(z) \tag{C.7f}$$

$$p_2^{(1)}(z) = \frac{1}{2}e^{z}h(-z). \tag{C.7g}$$

The survival probability is then given by

$$W_b^{(i)} = \int_{-b}^{b} p^{(i)}(x)dx. \tag{C.8}$$

The solution of equation (C.7) is expressed in terms of an eigenfunction expansion, as follows.

Consider α, $p_1(z)$ and $p_2(z)$ an eigenvalue and the corresponding eigenfunctions associated with equation (C.7). Because of the nature of the problem, (C.7) is asymptotically stable, or $|\alpha| < 1$, and p_1 and p_2 satisfy the following integral equations

$$\alpha p_1(z) = \int_{-b}^{z} e^{-(z-x)}[p^+ p_1(x) + p^- p_2(x)]dx \qquad (C.9a)$$

and

$$\alpha p_2(z) = \int_{z}^{b} e^{-(x-z)}[p^+ p_2(x) + p^- p_1(x)]dx, \qquad (C.9b)$$

with boundary conditions

$$p_1(-b) = p_2(b) = 0. \qquad (C.9c)$$

By differentiating (C.9) with respect to z, it can be shown that p_1 and p_2 satisfy the following differential equations

$$\alpha \frac{dp_1}{dz} = (p^+ - \alpha)p_1 + p^- p_2, \qquad (C.10a)$$

$$\alpha \frac{dp_2}{dz} = -p^- p_1 + (\alpha - p^+)p_2, \qquad (C.10b)$$

or by differentiating one more time with respect to z

$$\frac{d^2 p_1}{dz^2} + \beta^2 p_1 = 0, \qquad (C.11a)$$

$$\frac{d^2 p_2}{dz^2} + \beta^2 p_2 = 0, \qquad (C.11b)$$

where

$$\beta^2 = \frac{p^{-2} - (\alpha - p^+)^2}{\alpha^2} = \frac{(1-\alpha)(p^- + \alpha - p^+)}{\alpha^2} > 0. \qquad (C.11c)$$

The general expressions for the solutions of equation (C.11) are

$$p_1(z) = A_1\sin(\beta z) + A_2\cos(\beta z), \qquad (C.12a)$$

$$p_2(z) = C_1\sin(\beta z) + C_2\cos(\beta z). \qquad (C.12b)$$

From (C.7),

$$p(z) = (A_1 + C_1)\sin(\beta z) + (A_2 + C_2)\cos(\beta z). \qquad (C.12c)$$

From (C.12a), (C.12b) and (C.10a)

$$C_1 = -\frac{\alpha\beta A_2 - (\alpha - p^+)A_1}{p^-}, \qquad (C.13a)$$

$$C_2 = \frac{\alpha\beta A_1 + (\alpha - p^+)A_2}{p^-}, \qquad (C.13b)$$

while from the boundary condition (C.9),

$$\frac{A_2}{A_1} = \tan(\beta b), \qquad (C.14a)$$

$$\frac{C_2}{C_1} = -\tan(\beta b). \qquad (C.14b)$$

By substituting (C.13) into (C.14)

$$\frac{\alpha\beta\frac{A_1}{A_2} + \alpha - p^+}{\alpha\beta\frac{A_2}{A_1} - (\alpha - p^-)} = 1. \qquad (C.15)$$

From (C.15)

$$\alpha\beta\left(\tan(\beta b) - \frac{1}{\tan(\beta b)}\right) = 2(\alpha - p^+). \qquad (C.16)$$

But (C.16) is a second-order equation in $(\tan(\beta b))$ and for $\tan(\beta b) \neq 0$,

$$\alpha\beta(\tan(\beta b))^2 - 2(\alpha - p^+)\tan(\beta b) - \alpha\beta = 0, \qquad (C.17)$$

or,

$$(\tan(\beta b))_{1,2} = \frac{\alpha - p^+ \pm \sqrt{(\alpha - p^+)^2 + \alpha^2\beta^2}}{\alpha\beta}. \qquad (C.18a)$$

Substituting β^2 from (C.11c) yields

$$(\tan(\beta b))_{1,2} = \frac{\alpha - p^+ \pm p^-}{\alpha\beta} = -\frac{\alpha\beta}{\alpha - p^+ \mp p^-}. \qquad (C.18b)$$

Equation (C.18.b) gives two families of eigenvalues, satisfying the following equations

$$\tan(\beta_1 b) = \beta_1 b \frac{\alpha_1}{b(1-\alpha_1)}, \qquad (C.19a)$$

or

$$\tan(\beta_2 b) = -\beta_2 b \frac{\alpha_2}{b(\alpha_2 + p^- - p^+)}, \qquad (C.19b)$$

respectively.

Both families will also satisfy the following equation:

$$\tan(2\beta_{1,2} b) = -2\beta_{1,2} b \frac{\alpha_{1,2}}{2b(\alpha_{1,2} + p^- - p^+)}. \qquad (C.20)$$

For α, satisfying equation (C.20), the following relations for the coefficients A_1, A_2, C_1, C_2 are derived

$$A_1 + C_1 = \frac{A_1}{p^-}[\alpha + p^- - p^+ - \alpha\beta\tan(\beta b)] = \frac{A_2}{p^-}\left[\frac{\alpha + p^- - p^+}{\tan(\beta b)} - \alpha\beta\right] \qquad (C.21a)$$

and

$$A_2 + C_2 = \frac{A_1}{p^-}[(\alpha + p^- - p^+)\tan(\beta b) + \alpha\beta] = \frac{A_2}{p^-}\left[\alpha + p^- - p^+ + \frac{\alpha\beta}{\tan(\beta b)}\right]. \qquad (C.21b)$$

From (C.21) it can be seen that for α_1, β_1 satisfying (C.19a),

$$A_1^{(1)} + C_1^{(1)} = 0 \quad \text{and} \quad A_2^{(1)} + C_2^{(1)} = D_1 \neq 0 \qquad (C.22a)$$

and

$$p(z) = D_1 \cos(\beta_1 z), \qquad (C.22b)$$

while for α_2, β_2 satisfying (C.19b),

$$A_2^{(2)} + C_2^{(2)} = 0 \quad \text{and} \quad A_1^{(2)} + C_1^{(2)} = D_2 \neq 0 \tag{C.22c}$$

and

$$p(z) = D_2 \sin(\beta_1 z). \tag{C.22d}$$

It can be seen from the equation (C.22) that the family of eigenvalues satisfying (C.19a) corresponds to even eigenfunctions, while the family satisfying (C.19b), corresponds to odd eigenfunctions.

A solution for (C.19a) and (C.19b) can not be obtained in the general case. In the analysis that follows, it will be considered that n is large, or that $n \to \infty$. In Section 4.5.2 it was shown that

$$\sigma_z^{(n)} \asymp \frac{n}{2p^-} E[d^2] = \frac{n}{p^-} \quad \text{as } n \to \infty. \tag{C.23}$$

For barrier level b, such that

$$b = \gamma \sigma_z^{(n)}, \tag{C.24}$$

and for $\gamma \sim O(1)$, a solution for the survival probability will be derived using the eigenvalue expansion. Recall that

$$W_b^{(n)} = \sum_{i=1}^{\infty} \alpha_i^n \delta_i, \tag{C.25}$$

where α_i are the corresponding eigenvalues satisfying (C.20). Consider the first k such eigenvalues that are significant in the series expansion (C.25). Because for $i = 1, ...k$, $\alpha_i^n \sim O(1)$, it is implied that as $n \to \infty$, $\alpha_i \to 1$. But from (C.11c) it can be shown that for $i = 1, ..., k$, $\beta_i \to 0$. Recall that

$$\beta_i^2 = \frac{p^{-2} - (\alpha_i - p^+)^2}{\alpha_i^2}. \tag{C.11c}$$

Solving for α_i,

$$\alpha_i^2(1+\beta_i^2) - 2\alpha_i p^+ - (p^{-2} - p^{+2}) = 0, \qquad (C.26)$$

or, for $\alpha_i \to 1$,

$$\alpha_i = \frac{p^+ + p^- \sqrt{1 + \beta_i^2 \frac{(p^- - p^+)}{p^{-2}}}}{1+\beta_i^2}. \qquad (C.27)$$

For $\beta_i \ll 1$, after performing the calculations in (C.27), the following expression for α_i is obtained:

$$\alpha_i = 1 - \frac{\beta_i^2}{2p^-} + O(\beta^4). \qquad (C.27b)$$

But α_i, β_i satisfy (C.20), or

$$tg(2\beta_{1,2}b) = -2\beta_{1,2}b \frac{\alpha_{1,2}}{2b(\alpha_{1,2} + p^- - p^+)}. \qquad (C.20)$$

and for $\sigma_z^{(n)} \to \infty$ and for $\gamma \sim O(1)$, $b \to \infty$ and the solution of (C.20) is approximately given by

$$tg(2\beta b) \approx 0 \qquad (C.28a)$$

or

$$\beta_i \approx \frac{i\pi}{2b}. \qquad (C.28b)$$

By substituting (C.28b) into (C.27b)

$$\alpha_i \approx 1 - \frac{i^2\pi^2}{8b^2p^-}, \qquad (C.29a)$$

and for b given by (C.23) and (C.24)

$$\alpha_i \approx 1 - \frac{i^2\pi^2}{8\gamma^2 n}, \qquad (C.29b)$$

and as $n \to \infty$

$$\alpha_i^n \approx e^{-\frac{i^2\pi^2}{8\gamma^2}}. \qquad (C.30)$$

Equation (C.30) implies that for the first k significant eigenvalues(α_i, $i = 1,...,k$), α_i^n becomes independent on n and p^-, while depends only on i and γ. The reliability function is given by

$$W_b^{(n)} = \sum_{i=1}^{\infty} \alpha_i^n \delta_i. \qquad (C.25)$$

Consider an approximate expression for $W_b^{(n)}$, obtained as a finite sum truncation of (C.25)

$$W_b^{(n)} \approx \sum_{i=1}^{k} \alpha_i^n \delta_i \qquad (C.31)$$

and δ_i are calculated from the initial conditions. The eigenfunctions

$$p^{(2j+1)} = D_{2j+1} \cos \frac{(2j+1)\pi}{2b} z \qquad (C.32a)$$

and

$$p^{(2j)} = D_{2j} \sin \frac{2j\pi}{2b} z \qquad (C.32b)$$

are orthogonal on $(-b, b)$, and for symmetric initial conditions, it is implied that

$$D_{2j} = 0. \qquad (C.33)$$

For zero initial conditions and after performing the calculations, the coefficients D_{2j+1} are given by

$$D_{2j+1} = \frac{4}{\pi} \frac{(-1)^{2j+1}}{2j+1}. \qquad (C.34)$$

Substituting (C.33) and (C.34) into (C.31) the approximate expression for $W_b^{(n)}$ is obtained

$$W_b^{(n)} \approx \frac{4}{\pi} \sum_{j=1}^{k} \frac{(-1)^{2j+1}}{2j+1} e^{-\frac{j^2\pi^2}{8\gamma^2}}. \qquad (C.35)$$

Although (C.35) was obtained as a truncation of the related infinite series expansion, it can be considered that for large n, or for $n \to \infty$, the approximate expression (C.35) will converge to the limit, or

$$W_b^{(n)} \approx \frac{4}{\pi} \sum_{j=1}^{\infty} \frac{(-1)^{2j+1}}{2j+1} e^{-\frac{j^2\pi^2}{8\gamma^2}}. \qquad (C.36)$$

Appendix D. MOMENTS OF A WINDOWED GAUSSIAN DISTRIBUTION.

Define $B^{(k)}$ as

$$B^{(k)} = \int_0^\infty x^k \exp(-\frac{(x-m)^2}{2s^2})dx. \qquad (D.1)$$

Now,

$$B^{(k)} = \int_0^\infty x^{k-1}(x-m)\exp(-\frac{(x-m)^2}{2s^2})dx + m\int_0^\infty x^{k-1}\exp(-\frac{(x-m)^2}{2s^2})dx. \qquad (D.2)$$

By performing integration by parts in equation (D.2), it is implied that

$$B^{(k)} = s^2 x^{k-1}\exp(-\frac{(x-m)^2}{2s^2})|_{x=0} + s^2(k-1)B^{(k-2)} + mB^{(k-1)}, \qquad (D.3)$$

or

$$B^{(k)} = mB^{(k-1)} + (k-1)s^2 B^{(k-2)} \quad for\ k \geq 2, \qquad (D.4a)$$

with

$$B^{(0)} = \sqrt{\frac{\pi}{2}}s[1 + \mathrm{erf}(\frac{m}{\sqrt{2}s})] \qquad (D.4c)$$

$$B^{(1)} = s^2\exp(-\frac{(x-m)^2}{2s^2}) + m\sqrt{\frac{\pi}{2}}s[1 + \mathrm{erf}(\frac{m}{\sqrt{2}s})]. \qquad (D.4d)$$

Equation (D.4) gives a reccurant algorithm for the derivation of the moments, $B^{(k)}$. As mentioned in Section 5.2., the yield increment statistics can be calculated as a function of $B^{(k)}$.

CALIFORNIA INSTITUTE OF TECHNOLOGY

Reports Published

by

Earthquake Engineering Research Laboratory*
Dynamic Laboratory
Disaster Research Center

Note: Numbers in parenthesis are Accession Numbers assigned by the National Technical Information Service; these reports may be ordered from the National Technical Information Service, 5285 Port Royal Road, Springfield, Virginia, 22161. Accession Numbers should be quoted on orders for reports (PB --- ---). Reports without this information either have not been submitted to NTIS or the information was not available at the time of printing. An N/A in parenthesis indicates that the report is no longer available at Caltech.

1. Alford, J.L., G.W. Housner and R.R. Martel, "Spectrum Analysis of Strong-Motion Earthquake," 1951. (Revised August 1964). (N/A)

2. Housner, G.W., "Intensity of Ground Motion During Strong Earthquakes," 1952. (N/A)

3. Hudson, D.E., J.L. Alford and G.W. Housner, "Response of a Structure to an Explosive Generated Ground Shock," 1952. (N/A)

4. Housner, G.W., "Analysis of the Taft Accelerogram of the Earthquake of 21 July 1952." (N/A)

5. Housner, G.W., "A Dislocation Theory of Earthquakes," 1953. (N/A)

6. Caughey, T.K., and D.E. Hudson, "An Electric Analog Type Response Spectrum," 1954. (N/A)

7. Hudson, D.E., and G.W. Housner, "Vibration Tests of a Steel-Frame Building," 1954. (N/A)

8. Housner, G.W., "Earthquake Pressures on Fluid Containers," 1954. (N/A)

9. Hudson, D.E., "The Wilmot Survey Type Strong-Motion Earthquake Recorder," 1958. (N/A)

10. Hudson, D.E., and W.D. Iwan, "The Wilmot Survey Type Strong-Motion Earthquake Recorder, Part II," 1960. (N/A)

* To order directly by phone the number is 703-487-4650.

11. Caughey, T.K., D.E. Hudson, and R.V. Powell, "The CIT Mark II Electric Analog Type Response Spectrum Analyzer for Earthquake Excitation Studies," 1960. (N/A)

12. Keightley, W.O., G.W. Housner and D.E. Hudson, "Vibration Tests of the Encino Dam Intake Tower," 1961. (N/A)

13. Merchant, Howard Carl, "Mode Superposition Methods Applied to Linear Mechanical Systems Under Earthquake Type Excitation," 1961. (N/A)

14. Iwan, Wilfred D., "The Dynamic Response of Bilinear Hysteretic Systems," 1961. (N/A)

15. Hudson, D.E., "A New Vibration Exciter for Dynamic Test of Full-Scale Structures," 1961. (N/A)

16. Hudson, D.E., "Synchronized Vibration Generators for Dynamic Tests of Full-Scale Structures," 1962. (N/A)

17. Jennings, Paul C., "Velocity Spectra of the Mexican Earthquakes of 11 May and 19 May 1962," 1962. (N/A)

18. Jennings, Paul C., "Response of Simple Yielding Structures to Earthquake Excitation," 1963. (N/A)

19. Keightley, Willard O., "Vibration Tests of Structures," 1963. (N/A)

20. Caughey, T.K., and M.E.J. O'Kelly, "General Theory of Vibration of Damped Linear Dynamic Systems," 1963. (N/A)

21. O'Kelly, M.E.J., "Vibration of Viscously Damped Linear Dynamic Systems," 1964. (N/A)

22. Nielsen, N. Norby, "Dynamic Response of Miltistory Buildings," 1964. (N/A)

23. Tso, Wai Keung, "Dynamics of Thin-Walled Beams of Open Section," 1964. (N/A)

24. Keightley, Willard O., "A Dynamic Investigation of Bouquet Canyon Dam," 1964. (N/A)

25. Malhotra, R.K., "Free and Forced Oscillations of a Class of Self-Excited Oscillators," 1964.

26. Hanson, Robert D., "Post-Elastic Response of Mild Steel Structures," 1965.

27. Masri, Sami F., "Analytical and Experimental Studies of Impact Dampers," 1965.

28. Hanson, Robert D., "Static and Dynamic Tests of a Full-Scale Steel-Frame Structures," 1965.

29. Cronin, Donald L., "Response of Linear, Viscous Damped Systems to Excitations Having Time-Varying Frequecy," 1965.

30. Hu, Paul Yu-fei, "Analytical and Experimental Studies of Random Vibration," 1965.

31. Crede, Charles E., "Research on Failure of Equipment when Subject to Vibration," 1965.

32. Lutes, Loren D., "Numerical Response Characteristics of a Uniform Beam Carrying One Discrete Load," 1965. (N/A)

33. Rocke, Richard D., "Transmission Matrices and Lumped Parameter Models for Continuous Systems," 1966. (N/A)

34. Brady, Arthur Gerald, "Studies of Response to Earthquake Ground Motion," 1966. (N/A)

35. Atkinson, John D., "Spectral Density of First Order Piecewise Linear Systems Excited by White Noise," 1967. (N/A)

36. Dickerson, John R., "Stability of Parametrically Excited Differential Equations," 1967. (N/A)

37. Giberson, Melbourne F., "The Response of Nonlinear Multi-Story Structures Subjected to Earthquake Excitation," 1967. (N/A)

38. Hallanger, Lawrence W., "The Dynamic Stability of an Unbalanced Mass Exciter," 1967.

39. Husid, Raul, "Gravity Effects on the Earthquake Response of Yielding Structures," 1967. (N/A)

40. Kuroiwa, Julio H., "Vibration Test of a Multistory Building," 1967. (N/A)

41. Lutes, Loren Daniel, "Stationary Random Response of Bilinear Hysteretic Systems," 1967.

42. Nigam, Navin C., "Inelastic Interactions in the Dynamic Response of Structures," 1967.

43. Nigam, Navin C. and Paul C. Jennings, "Digital Calculation of Response Spectra from Strong-Motion Earthquake Records," 1968.

44. Spencer, Richard A., "The Nonlinear Response of Some Multistory Reinforced and Prestressed Concrete Structures Subjected to Earthquake Excitation," 1968. (N/A)

45. Jennings, P.C., G.W. Housner and N.C. Tsai, "Simulated Earthquake Motions," 1968.

46. "Strong-Motion Instrumental Data on the Borrego Mountain Earthquake of 9 April 1968," (USGS and EERL Joint Report), 1968.

47. Peters, Rex B., "Strong Motion Accelerograph Evaluation," 1969.

48. Heitner, Kenneth L., "A Mathematical Model for Callculation of the Run-Up of Tsunamis," 1969.

49. Trifunac, Mihailo D., "Investigation of Strong Earthquake Ground Motion," 1969. (N/A)

50. Tsai, Nien Chien, "Influence of Local Geology on Earthquake Ground Motion," 1969. (N/A)

51. Trifunac, Mihailo D., "Wind and Microtremor Induced Vibrations of a Twenty-Two Steel Frame Building," EERL 70-01, 1970.

52. Yang, I-Min, "Stationary Random Response of Multidegree-of-Freedom Systems," DYNL-100, June 1970. (N/A)

53. Patula, Edward John, "Equivalent Differential Equations for Nonlinear Dynamic Systems," DYNL-101, June 1970.

54. Prelewicz, Daniel Adam, "Range of Validity of the Method of Averaging," DYNL-102, 1970.

55 Trifunac, M.D., "On the Statistics and Possible Triggering Mechanism of Earthquakes in Southern California," EERL 70-03, July 1970.

56. Heitner, Kenneth Leon, "Additional Investigations on a Mathematical Model for Calculation of Run-Up of Tsunamis," July 1970.

57. Trifunac, Mihailo D., "Ambient Vibration Tests of a Thirty-Nine Story Steel Frame Building," EERL 70-02, July 1970.

58. Trifunac, Mihailo D. and D.E. Hudson, "Laboratory Evaluations and Instrument Corrections of Strong-Motion Accelerographs," EERL 70-04, August 1970. (N/A)

59. Trifunac, Mihailo D., "Response Envelope Spectrum and Interpretation of Strong Earthquake Groun Motion," EERL 70-06, August 1970.

60. Keightley, W.O., "A Strong-Motion Accelerograph Array with Telephone Line Interconnections," EERL 70-05, September 1970.

61. Trifunac, Mihailo D., "Low Frequency Digitization Errors and a New Method for Zero Baseline Correction of Strong-Motion Accelerograms," EERL 70-07, September 1970.

62. Vijayaraghavan, A., "Free and Forced Oscillations in a Class of Piecewise-Linear Dynamic Systems," DYNL-103, January 1971.

63. Jennings, Paul C., R.B. Mathiesen and J. Brent Hoerner, "Forced Vibrations of a 22-Story Steel Frame Building," EERL 71-01, February 1971. (N/A) (PB 205 161)

64. Jennings, Paul C., "Engineering Features of the San Fernando Earthquake of February 9, 1971," EERL 71-02, June 1971. (PB 202 550)

65. Bielak, Jacobo, "Earthquake Response of Building-Foundation Systems," EERL 71-04, June 1971. (N/A) (PB 205 305)

66. Adu, Randolph Ademola, "Response and Failure of Structures Under Stationary Random Excitation," EERL 71-03, June 1971. (N/A) (PB 205 304)

67. Skattum, Knut Sverre, "Dynamic Analysis of Coupled Shear Walls and Sandwich Beams," EERL 71-06, June 1971. (N/A) (PB 205 267)

68. Hoerner, John Brent, "Model Coupling and Earthquake Response of Tall Buildings," EERL 71-07, June 1971. (N/A) (PB 207 635)

69. Stahl, Karl John, "Dynamic Response of Circular Plates Subjected to Moving Massive Loads," DYNL-104, June 1971. (N/A)

70. Trifunac, M.D., F.E. Udwadia and A.G. Brady, "High Frequency Errors and Instrument Corrections of Strong-Motion Accelerograms," EERL 71-05, 1971. (PB 205 369)

71. Furuike, D.M., "Dynamic Response of Hysteretic Systems With Application to a System Containing Limited Slip," DYNL-105, September 1971. (N/A)

72. Hudson, D.E. (Editor), "Strong-Motion Instrumental Data on the San Fernando Earthquake of February 9, 1971," (Seismological Field Survey, NOAA, C.I.T. Joint Report), September 1971. (PB 204 198)

73. Jennings, Paul C. and Jacobo Bielak, "Dynamics of Building-Soil Interaction," EERL 72-01, April 1972. (PB 209 666)

74. Kim, Byung-Koo, "Piesewise Linear Dynamic Systems with Time Delays," DYNL-106, April 1972.

75. Viano, David Charles, "Wave Propagation in a Symmetrically Layered Elastic Plate," DYNL-107, May 1972.

76. Whitney, Albert W., "On Insurance Settlements Incident to the 1906 San Francisco Fire," DRC 72-01, August 1972. (PB 213 256)

77. Udwadia, F.E., "Investigation of Earthquake and Microtremor Ground Motions," EERL 72-02, September 1972. (PB 212 853)

78. Wood, John H., "Analysis of the Earthquake Response of a Nine-Story Steel Frame Building During the San Fernando Earthquake," EERL 72-04, October 1972. (PB 215 823)

79. Jennings, Paul C., "Rapid Calculation of Selected Fourier Spectrum Ordinates," EERL 72-05, November 1972.

80. "Research Papers Submitted to Fifth World Conference on Earthquake Engineering, Rome, Italy, 25-29 June 1973," EERL 73-02, March 1973. (PB 220 431)

81. Udwadia, F.E., and M.D. Trifunac, "The Fourier Transform, Response Spectra and Their Relationship Through the Statistics of Oscillator Response," EERL 73-01, April 1973. (PB 220 458)

82. Housner, George W., "Earthquake-Resistant Design of High-Rise Buildings," DRC 73-01, July 1973. (N/A)

83. "Earthquake and Insurance," Earthquake Research Affiliates Conference, 2-3 April, 1973, DRC 73-02, July 1973. (PB 223 033)

84. Wood, John H., "Earthquake-Induced Soil Pressures on Structures," EERL 73-05, August 1973. (N/A)

85. Crouse, Charles B., "Engineering Studies of the San Fernando Earthquake," EERL 73-04, March 1973. (N/A)

86. Irvine, H.Max, "The Veracruz Earthquake of 28 August 1973," EERL 73-06, October 1973.

87. Iemura, H. and P.C. Jennings, "Hysteretic Response of a Nine-Story Reinforced Concrete Building During the San Fernando Earthquake," EERL 73-07, October 1973.

88. Trifunac, M.D. and V. Lee, "Routine Computer Processing of Strong-Motion Accelerograms," EERL 73-03, October 1973. (N/A) (PB 226 047/AS)

89. Moeller, Thomas Lee, "The Dynamics of a Spinning Elastic Disk with Massive Load," DYNL 73-01, October 1973.

90. Blevins, Robert D., "Flow Induced Vibration of Bluff Structures," DYNL 74-01, February 1974.

91. Irvine, H. Max, "Studies in the Statics and Dynamics of Simple Cable Systems," DYNL-108, January 1974.

92. Jephcott, D.K. and D.E. Hudson, "The Performance of Public School Plants During the San Fernando Earthquake," EERL 74-01, September 1974. (PB 240 000/AS)

93. Wong, Hung Leung, "Dynamic Soil-Structure Interaction," EERL 75-01, May 1975. (N/A) (PB 247 233/AS)

94. Foutch, D.A., G.W. Housner, and P.C. Jennings, "Dynamic Responses of Six Multistory Buildings During the San Fernando Earthquake," EERL 75-02, October 1975. (PB 248 144/AS)

95. Miller, Richard Keith, "The Steady-State Response of Multidegree-of-Freedom Systems with a Spatially Localized Nonlinearity," EERL 75-03, October 1975. (PB 252 459/AS)

96. Abdel-Ghaffar, Ahmed Mansour, "Dynamic Analyses of Suspension Bridge Structures," EERL 76-01, May 1976. (PB 258 744/AS)

97. Foutch, Douglas A., "A Study of the Vibrational Characteristics of Two Multistory Buildings," EERL 76-03, September 1976. (PB 260 874/AS)

98. "Strong Motion Earthquake Accelerograms Index Volume," Earthquake Engineering Research Laboratory, EERL 76-02, August 1976. (PB 260 929/AS)

99. Spanos, P-T.D., "Linearization Techniques for Non-Linear Dynamical Systems," EERL 76-04, September 1976. (PB 266 083/AS)

100. Edwards, Dean Barton, "Time Domain Analysis of Switching Regulators," DYNL 77-01, March 1977.

101. Abdel-Ghaffar, Ahmed Mansour, "Studies of the Effect of Differential Motions of Two Foundations upon the Response of the Superstructure of a Bridge," EERL 77-02, January 1977. (PB 271 095/AS)

102. Gates, Nathan C., "The Earthquake Response of Deteriorating Systems," EERL 77-03, March 1977. (PB 271 090/AS)

103. Daly, W., W. Judd and R. Meade, "Evaluation of Seismicity at U.S. Reservoirs," USCOLD, Committee on Earthquakes, May 1977. (PB 270 036/AS)

104. Abdel-Ghaffer, A.M. and G.W. Housner, "An Analysis of the Dynamic Characteristics of a Suspension Bridge by Ambient Vibration Measurements," EERL 77-01, January 1977. (PB 275 063/AS)

105. Housner, G.W. and P.C. Jennings, "Earthquake Design Criteria for Structures," EERL 77-06, November 1977. (PB 276 502/AS)

106. Morrison, P., R. Maley, G. Brady, R. Porcella, "Earthquake Recordings on or Near Dams," USCOLD, Committee on Earthquakes, November 1977. (PB 285 867/AS)

107. Abdel-Ghaffar, A.M., "Engineering Data and Analyses of the Whittier, California Earthquake of January 1, 1976," EERL 77-05, November 1977. (PB 283 750/AS)

108. Beck, James L., "Determining Models of Structures from Earthquake Records," EERL 78-01, June 1978. (PB 288 806/AS)

109. Psycharis, Ioannis, "The Salonica(Thessaloniki) Earthquake of June 20, 1978," EERL 78-03, October 1978. (PB 290 120/AS)

110. Abdel-Ghaffar, A.M. and R.F. Scott, "An Investigation of the Dynamic Characteristics of an Earth Dam," EERL 78-02, August 1978. (PB 288 878/AS)

111. Mason, Alfred B., Jr., "Some Observations on the Random Response of Linear and Nonlinear Dynamical Systems," EERL 79-01, January 1979. (PB 290 808/AS)

112. Helmberger, D.V. and P.C. Jennings (Organizers), "Strong Ground Motion: N.S.F. Seminar-Workshop," SL-EERL 79-02, February 1978.

113. Lee, David M., Paul C. Jennings and George W. Housner, "A Selection of Important Strong Motion Earthquake Records," EERL 80-01, January 1980. (PB 80 169196)

114. McVerry, Graeme H., "Frequency Domain Identification of Structural Models from Earthquake Records," EERL 79-02, October 1979. (PB-80-194301)

115. Abdel-Ghaffar A.M., R.F.Scott and M.J.Craig, "Full-Scall Experimental Investigation of a Modern Earth Dam," EERL 80-02, February 1980. (PB-81-123788)

116. Rutenberg, Avigdor, Paul C. Jennings and George W. Housner, "The Response of Veterans Hospital Building 41 in the San Fernando Earthquake," EERL 80-03, May 1980. (PB-82-201377)

117. Haroun, Medhat Ahmed, "Dynamic Analyses of Liquid Storage Tanks," EERL 80-04, February 1980. (PB-81-123275)

118. Liu, Wing Kam, "Development of Finite Element Procedures for Fluid-Structure Interaction," EERL 80-06, August 1980. (PB 184078)

119. Yoder, Paul Jerome, "A Strain-Space Plasticity Theory and Numerical Implementation," EERL 80-07, August 1980. (PB-82-201682)

120. Krousgrill, Charles Morton, Jr., "A Linearization Technique for the Dynamic Response of Nonlinear Continua," EERL 80-08, September 1980. (PB-82-201823)

121. Cohen, Martin, "Silent Boundary Methods for Transient Wave Analysis," EERL 80-09, September 1980. (PB-82-201831)

122. Hall, Shawn A., "Vortex-Induced Vibrations of Structures," EERL 81-01, January 1981. (PB-82-201849)

123. Psycharis, Ioannis N., "Dynamic Behavior of Rocking Structures Allowed to Uplift," EERL 81-02, August 1981. (PB-82-212945)

124. Shih, Choon-Foo, "Failure of Liquid Storage Tanks Due to Earthquake Excitation," EERL 81-04, May 1981. (PB-82-215013)

125. Lin, Albert Niu, "Experimental Observations of the Effect of Foundation Embedment on Structural Response," EERL 82-01, May 1982. (PB-84-163252)

126. Botelho, Dirceau L.R., "An Empirical Model for Vortex-Induced Vibrations," EERL 82-02, August 1982. (PB-84-161157)

127. Ortiz, L. Alexander, "Dynamic Centrifuge Testing of Cantilever Retaining Walls," SML 82-02, August 1982. (PB-84-162312)

128. Iwan, W.D., Editor, "Proceedings of the U.S. National Workshop on Strong-Motion Earthquake Instrumentation, April 12-14, 1981, Santa Barbara, California," California Institute of Technology, Pasadena, California, 1981.

129. Rashed, Ahmed, "Dynamic Analysis of Fluid-Structure Systems," EERL 82-03, July 1982. (PB-84-162916)

130. National Academy Press, "Earthquake Engineering Research-1982."

131. National Academy Press, "Earthquake Engineering Research-1982, Overview and Recommendations."

132. Jain, Sudhir Kumar, "Analytical Models for the Dynamics of Buildings," EERL 83-02, May 1983. (PB-84-161009)

133. Huang, Moh-Jiann, "Investigation of Local Geology Effects on Strong Earthquake Ground Motions," EERL 83-03, July 1983. (PB-84-161488)

134. Mcverry, G.H. and J.L. Beck, "Structural Identification of JPL Building 180 Using Optimally Synchronized Earthquake Records." EERL 83-01, August 1983. (PB-84-162833)

135. Bardet, J.P., "Application of Plasticity Theory to Soil Behavior: A New Sand Model," SML 83-01, September 1983. (PB-84-162304)

136. Wilson, John C., "Analysis of the Observed Earthquake Response of a Multiple Span Bridge," EERL 84-01, May 1984. (PB-85-240505/AS)

137. Hushmand, Behnam, "Experimental Studies of Dynamic Response of Foundations," SML 83-02, November 1983. (PB-86-115383/A)

138. Cifuentes, Arturo O., "System Identification of Hysteretic Structures," EERL 84-04, 1984. (PB-240489/AS14)

139. Smith, Kenneth Scott, "Stochastic Analysis of the Seismic Response of Secondary Systems," EERL 85-01, November 1984. (PB-85-240497/AS)

140. Maragakis, Emmanuel, "A Model for the Rigid Body Motions of Skew Bridges," EERL 85-02, December 1984. (PB-85-248433/AS)

141. Jeong, Garrett Duane, "Cumulative Damage of Structures Subjected to Response Spectrum Consistent Random Process," EERL 85-03, January 1985. (PB-86-100809)

142. Chelvakumar, Kasivisvanathan, "A Simple Strain-Space Plasticity Model for Clays," EERL 85-05, 1985. PB-

143. Pak, Ronald Y.S., "Dynamic Response of a Patially Embedded Bar Under Transverse Excitations," EERL 85-04, May 1985. PB-

144. Tan, Thiam-Soon, "Two Phase Soil Study: A. Finite Strain Consolidation, B. Centrifuge Scaling Considerations," SML 85-01, August 1985. PB-

145. Iwan, Wilfred D., Michael A. Moser and Chia-Yen Peng, "Strong-Motion Earthquake Measurement Using a Digital Accelerograph," EERL 84-02, April 1984.

146. Beck, R.T. and J.L. Beck, "Comparison Between Transfer Function and Modal Minimization Methods for System Identification," EERL 85-06, April 1984.

147. Jones, Nicholas Patrick, "Flow-Induced Vibration of Long Structures," DYNL 86-01, May 1986. PB-

148. Peek, Ralf, "Analysis of Unanchored Liquid Storage Tanks Under Seismic Loads," EERL 86-01, April 1986. PB-

Strong-Motion Earthquake Accelerograms
Digitized and Plotted Data

Uncorrected Accelerograms

Volume I

Part	Report No.	NTIS Accession No.
A	EERL 70-20	PB 287 847
B	EERL 70-21	PB 196 823
C	EERL 71-20	PB 204 364
D	EERL 71-21	PB 208 529
E	EERL 71-22	PB 209 749
F	EERL 71-23	PB 210 619
G	EERL 72-20	PB 211 357
H	EERL 72-21	PB 211 781
I	EERL 72-22	PB 213 422
J	EERL 72-23	PB 213 423
K	EERL 72-24	PB 213 424
L	EERL 72-25	PB 215 639
M	EERL 72-26	PB 220 554
N	EERL 72-27	PB 223 023
O	EERL 73-20	PB 222 417
P	EERL 73-21	PB 227 481/AS
Q	EERL 73-22	PB 232 315/AS
R	EERL 73-23	PB 239 585/AS
S	EERL 73-24	PB 241 551/AS
T	EERL 73-25	PB 241 943/AS
U	EERL 73-26	PB 242 262/AS
V	EERL 73-27	PB 243 483/AS
W	EERL 73-28	PB 243 497/AS
X	EERL 73-29	PB 243 594/AS
Y	EERL 73-30	PB 242 947/AS

Strong-Motion Earthquake Accelerograms
Digitized and Plotted Data

Corrected Accelerograms and Integrated
Ground Velocity and Displacement Curves

Volume II

Part	Report No.	NTIS Accession No.
A	EERL 71-50	PB 208 283
B	EERL 72-50	PB 220 161
C	EERL 72-51	PB 220 162
D	EERL 72-52	PB 220 836
E	EERL 73-50	PB 223 024
F	EERL 73-51	PB 224 977/9AS
G	EERL 73-52	PB 229 239/AS
H	EERL 74-50	PB 231 225/AS
I	EERL 74-51	PB 232 316/AS
J,K	EERL 74-52	PB 233 257/AS
L,M	EERL 74-53	PB 237 174/AS
N	EERL 74-54	PB 236 399/AS
O,P	EERL 74-55	PB 239 586/AS
Q,R	EERL 74-56	PB 239 587/AS
S	EERL 74-57	PB 241 552/AS
T	EERL 75-50	PB 242 433/AS
U	EERL 75-51	PB 242 949/AS
V	EERL 75-52	PB 242 948/AS
W,Y	EERL 75-53	PB 243 719

Analyses of Strong-Motion Earthquake Accelerograms
Response Spectra

Volume III

Part	Report No.	NTIS Accession No.
A	EERL 72-80	PB 212 602
B	EERL 73-80	PB 221 256
C	EERL 73-81	PB 223 025
D	EERL 73-82	PB 227 469/AS
E	EERL 73-83	PB 227 470/AS
F	EERL 73-84	PB 227 471/AS
G	EERL 73-85	PB 231 223/AS
H	EERL 74-80	PB 231 319/AS
I	EERL 74-81	PB 232 326/AS
J,K,L	EERL 74-82	PB 236 110/AS
M,N	EERL 74-83	PB 236 400/AS
O,P	EERL 74-84	PB 238 102/AS
Q,R	EERL 74-85	PB 240 688/AS
S	EERL 74-86	PB 241 553/AS
T	EERL 75-80	PB 243 698/AS
U	EERL 75-81	PB 242 950/AS
V	EERL 75-82	PB 242 951/AS
W,Y	EERL 75-83	PB 243 492/AS

Analyses of Strong-Motion Earthquake Accelerograms
Fourier Amplitude Spectra

Volume IV

Part	Report No.	NTIS Accession No.
A	EERL 72-100	PB 212 603
B	EERL 73-100	PB 220 837
C	EERL 73-101	PB 222 514
D	EERL 73-102	PB 222 969/AS
E	EERL 73-103	PB 229 240/AS
F	EERL 73-104	PB 229 241/AS
G	EERL 73-105	PB 231 224/AS
H	EERL 74-100	PB 232 327/AS
I	EERL 74-101	PB 232 328/AS
J,K,L,M	EERL 74-102	PB 236 111/AS
N,O,P	EERL 74-103	PB 238 447/AS
Q,R,S	EERL 74-104	PB 241 554/AS
T,U	EERL 75-100	PB 243 493/AS
V,W,Y	EERL 75-101	PB 243 494/AS
Index Volume	EERL 76-02	PB 260 929/AS